

Petrography and Facies of the Al- Mahruqah Formation in the Murzuq Basin, SW Libya.

Dissertation
zur Erlangung des Doktorgrades
der Naturwissenschaften im Department
Geowissenschaften
der Universität Hamburg

Vorgelegt von
Mustafa Abdullah
aus
Sabha-Libyen

Hamburg
2010

Als Dissertation angenommen vom Department Geowissenschaften der Universität
Hamburg

Aufgrund der Gutachten von
und
Prof. Dr. Christian Betzler
Prof. Dr. Friedhelm Thiedig

Hamburg, den 06. Juli. 2010

Prof. Dr. Jürgen Oßenbrügge
Leiter des Departments Geowissenschaften

SUMMARY

The target of this work is to characterize the superficial carbonate beds in the Murzuq Basin, which were defined as Al Mahruqah Formation. The working area is situated at the northern flank of the northern Murzuq Basin SW Libya. In recent studies, Al Mahruqah Formation was interpreted as Middle Pleistocene lacustrine deposits and subdivided into four separated members: Antalkhata, Brak, Bi'r az Zallaf, and Aqar member respectively. This interpretation and subdivision gave rise to the notion of "Megalake Fezzan" which was proposed to have covered about 150.000 km² and to have periodically existed in the Murzuq Basin.

Facies analysis, XRD, ²³⁰Th/U and OSL dating were performed to reconstruct the components, sedimentary facies, mineralogy, absolute age and the depositional environment of Brak, Bi'r az Zallaf, and Aqar members separately in order to determine if different limestones members of Al Mahruqah Formation are reliable tracers for the occurrence of large lakes (previously described as "Megalake Fezzan") in the northern Sahara during the Pleistocene.

The Antalkhata Mb. was not investigated in this study because of its poor and limited exposures.

Based on textural and compositional characteristics, the limestones of Brak Mb. are interpreted as calcrete deposits (i.e. groundwater calcrites) and are not lacustrine sediments as reported in published literature. The member has been subdivided into four lithologic intervals: transitional siliciclastic/carbonate, conglomerate, evaporite-carbonate and massive limestone interval.

²³⁰Th/U results of the sampled calcrites from the Brak Mb. ranged from 364±12 ka to 398±60 ka (conglomerate components) and 334±10 ka to 349±14 ka (micritic matrix). Our interpretation for these unexpected age discrepancies is that, the ²³⁰Th/U dating significantly underestimates the age of the calcrites and thus is unsuitable for providing reliable ages for the calcrites owing to diagenetic alteration of the

calcretes, as evidenced in thin slices. It is proposed that the Brak Mb. is much older than the age reported by Thiedig et al. (2000).

Bi'r az Zallaf Mb., comprises a complex alternation of green weakly consolidated sandstones and thin laminated carbonate beds. This sequence is subdivided into two lithostratigraphic facies: The sands facies is classified and interpreted as fluvial-aeolian sediments. The carbonate facies occurs as thin bedded dolomitic limestone, intercalated with thin green salty sandstones laminae, which are interpreted as playa lake deposits. Rare to frequent fossiliferous components such as ostracodes, pelecypods, gastropods and charophyte debris were observed in these carbonate sediments. The carbonate facies of Bi'r az Zallaf Mb. consist of dolomite (80%) and 10-20 % of calcite. OSL analysis of the upper sand interval (sample ZaS4) yielded an absolute age of (410± 50 ka), indicating that the lower sand intervals are older than Middle Pleistocene. OSL results suggest that the Bi'r az Zallaf deposits are clearly older than the uranium-series estimated Quaternary ages of 240-260 ka, which were published in former geological studies.

Aqar Mb. occupied the lower portions of Wadi ash Shati depression. It consists mainly of abundant *Cerastoderma glaucum* shells, ostracods, gastropods, rare foraminifera and abundant admixture of clastic material composed of mud, silt and sand grain with abundant pebbles and boulders of sandstones. Filed studies show that these coquina deposits of Aqar Mb. are similar in all outcrops in the study area. Using outcrop data and facies description and interpretation, Aqar Mb. sediments in Wadi as Shati area are identified and attributed to one sedimentary facies "Cerastoderma facies", which is interpreted as recent wadi deposits.

The analysed data reveal that the Wadi ash Shati endorhic depression previously contained several small palaeolakes, indicating that the climate in the past was more humid. It also suggests that climate and topography were the main factors that controlled the distribution of this facies in the study area.

This new data and resulting interpretation contradicts previous interpretations of the Al Mahruqah Formation as a lacustrine limestone. The results of the $^{230}\text{Th}/\text{U}$ and OSL dating show that the Al Mahruqah Formation is actually older than previously published.

The new data presented in this study definitely conflicts with the notion of the middle Pleistocene Megalake Fezzan. All of the above mentioned facts should be taken into

account for further reconstructions of the palaeohydrological regime in the northern Sahara.

The results of this study disprove the assumption that a pronounced phase of humidity occurred north of the central Saharan watershed during the Pleistocene interglacial periods.

ZUSAMMENFASSUNG

Nach vielen Jahren von Forschung in Murzuq Becken im Südwest Libyen besteht immer noch Unklarheit über die Herkunft, Ablagerungsbedingungen und das Alter von jüngeren nicht marinen Karbonatablagerungen im Murzuq Becken.

Zuletzt wurden diese karbonatischen Sedimente als "Al Mahruqah Formation" benannt und als quartäre lakustrine Ablagerungen klassifiziert. Man hat sie in vier verschiedene und getrennte Member unterteilt, weil sie innerhalb des Murzuq Beckens in verschiedenen topographischen Höhen vorkommen und unterschiedliche $^{230}\text{Th}/\text{U}$ -Altersdaten liefern haben. Entsprechend isotopischer Altersdatierungen ($^{230}\text{Th}/\text{U}$) wurden die Member in der Reihenfolge (älter-jünger) benannt:

- 1.) Das Antalkhata Member,
- 2.) Das Brak Member,
- 3.) Das Bi`r az Zallaf Member
- 4.) Das Aqr Member.

Wegen der großen Verbreitung der als lakustrine Ablagerungen angesehenen Karbonate entstand der Begriff „Megalake Fezzan“, der indem abflusslosen Murzuq Becken zeitweise bestand.

Ziel der Arbeit ist die Charakterisierung pleistozäner Karbonatablagerungen der Al Mahruqah Fm. der Zentralsahara (nördliches Murzuq Becken). Basierend auf geologischen Geländearbeiten, Laborarbeiten (XRD, $^{230}\text{Th}/\text{U}$, und OSL-Datierung) und Dünnschliffanalysen konnten für die einzelnen karbonatischen Einheiten der Al Mahruqah Fm. fazielle-, stratigraphische-, und Altersmodelle angefertigt werden. Altersdatierungen dienten zur Überprüfung der „Megalake-Fezzan“-Theorie, wonach die karbonatischen Einheiten als lakustrin Sedimente klassifiziert wurden.

Die Antalkhata Member wurde in dieser Studie wegen seiner geringen und begrenzten Vorkommen in dem Arbeitsgebiet nicht untersucht.

Bei den Ablagerungen der Brak-Einheit handelt es sich, nach Untersuchungen im Arbeitsgebiet im Wadi ash Shati im nördlichen Rand des Murzuq Beckens, um bis zu 12 m mächtige Grundwasser calcrete Sedimente, die von Kalk-Matrix unterstützten Sandsteinkonglomerate, Pisoide, Peloide, und intraklasten als auch Extraktlasten bestehen

Anhand der Fazies erfolgte eine Unterteilung des Brak Member in vier Sub-Member. $^{230}\text{Th}/\text{U}$ -Datierungen belegen für das Brak Member Altersdiskrepanzen von 364 bis $398 \pm 12\text{ ka} \pm 60\text{ ka}$ anhand von Konglomeraten und $334 \pm 10\text{ ka}$ bis $349 \pm 14\text{ ka}$ anhand der mikritischen Matrix. Als Ursache für die Diskrepanzen sind hauptsächlich diagenetische Veränderungen verantwortlich. Dies verdeutlicht, dass $^{230}\text{Th}/\text{U}$ -Altersdatierungen an diagenetisch überprägten Calcreten keine zuverlässigen Daten hervorbringen. Daher wird vom Altersmodell nach Thiedig et al., (2000) Abstand genommen und vorgeschlagen, die Brak-Einheit stratigraphisch älter einzuordnen.

Die Bir az Zallaf-Einheit umfasst eine Wechsellagerung von siliziklastischen Ablagerungen mit dünnbankigen Karbonathorizonten. Zwei unterschiedliche Fazies wurden erfasst.

- 1) Grünliche Sande wurden als fluvial-äolische Sedimente interpretiert.
- 2) Die karbonatischen Zwischenlagen, welche fein laminierte Dolomitbänke (Dolomitgehalt bis zu 80 %) von den grünlichen Sandsteinbänken trennen, bestehen hauptsächlich aus Peloiden und schlecht sortiertem siliziklastischem Detritus.

Als biogene Bestandteile der karbonatischen Fazies sind Ostrakoden, Pelecypoden, Gastropoden und Charophyten zu erwähnen. Aufgrund der anzutreffenden Lithologie und der Karbonatfazies wird die Bir az Zallaf-Einheit als Playa-See Ablagerungsraum interpretiert. OSL-Datierungen an siliziklastischen Proben (oberes Sandintervall, Probe ZaS4) ergaben ein absolutes Alter von $410 \pm 50\text{ ka}$, wonach entgegengesetzt zu früheren Studien ($^{230}\text{Th}/\text{U}$ -Datierung nach Thiedig et al., 2000; Geyh and Thiedig, 2008), die Bir az Zallaf-Einheit in das Mittlere Pleistozän zu stellen ist.

Sedimente der Agar-Einheit sind ausschließlich in den morphologischen Senken des Wadis ash Schati aufgeschlossen. Aufgrund des massenhaften Auftretens der Pelecypode *Cerastoderma glaucum* werden die karbonatischen Ablagerungen zur

Cerastoderma-Fazies zusammengefasst. Neben biogenen Komponenten, wie Ostrakoden, Gastropoden und vereinzelt Foraminiferen ist vornehmlich siliziklastisches Material (Ton bis Geröll-Fraktion) innerhalb der Fazies anzutreffen. Die im gesamten Untersuchungsgebiet homogen auftretende Fazies baut grossmaßstäbliche Schrägschichtungskörper auf, welche in Form kleiner Wadi-Fächer zu beobachten sind und als Paläodeltageometrien interpretiert wurden.

Der aufgenommene sedimentologische Datensatz zeugt von der Existenz von Paläo-Seen innerhalb, der abflusslosen Wadi ash Shati-Senke. Die aufgestellten Fazies der Agar-Einheit deuten auf ein humideres Klima als gegenwärtig hin. Als Kontrollmechanismen des Sedimentationsraumes sind klimatische Aspekte sowie die Paläotopographie zu nennen.

Die vorliegende Arbeit verdeutlicht, dass entgegengesetzt früheren Interpretationen über die Al Mahruqah Fm., kein vollständig lakustriner Ablagerungsraum anzunehmen ist.

Den bisherigen Vorstellungen, dass das Murzuq Becken während des mittleren Pleistozäns von einem „Megalake“ bedeckt wurde kann nicht gefolgt werden. Durchgeführte $^{230}\text{Th}/\text{U}$ und OSL-Altersdatierungen belegen eine höhere Alterseinstufung für die Al Mahruqah Fm.

ACKNOWLEDGMENT

On December 2005 a meeting between Prof. Christian Betzler, Prof. Friedhelm Thiedig and I took place in Geological Palaeontological institute (GPI) in University of Hamburg. In this meeting we discussed various issues concerning the geology, Hydrology and the Palaeo-climate in Murzuq Basin, especially the notion of Megalake Fezzan, which was introduced by several authors and published recently in numerous scientific articles. The Megalake Fezzan occurred in several stages and covered large areas of Murzuq Basin during the humid Middle Pleistocene period.

The presence of isolated discontinuous carbonate deposits, elevation of these carbonate deposits, the existence of great quantity of fossil groundwater and topography of Basin were taken as clear evidence of the existence of these ancient giant lakes in the past.

In order to confirm or to deny the existence of these ancient lakes, Prof. Christian Betzler, Prof. Friedhelm Thiedig decided to carry out this study. They offered me a position in the geological institute in the University of Hamburg to write my PhD thesis about this interesting theme.

My deepest thanks go to both of them allowing me to benefit this opportunity and carry out this study. I am deeply grateful to Prof. Christian Betzler for all time and effort that he spent, such as in the pleasant field trips to Spain, Murzuq Basin in Libya and to Germany, correcting and revising the texts and figures of this study several times. Very special thanks go also to Prof. Friedhelm Thiedig, for his support at all times for offering his competent knowledge about Libyan geology and specific geology of the study area, and not least, for making me feel at home in Hamburg. My great thanks go to all his family members especially his wife Elke, who supported me and my family all time through out studies in Hamburg.

My sincere thanks go to Prof. M. El Chair, my Libyan teacher, who taught me the fundamentals of Geology and introduced me to the geology of the province of Fezzan, and guided me during the field investigations in the an extensive study area. I owe him thanks for his financial and logistical support. He was always ready to consult me concerning the different aspects of this study.

I also want to express my thanks to Prof. M. Frechen and his division in Leibniz Institute for Applied Geophysics in Hanover- Germany, especially to Frau Dr. Melania Sirralta for her significant assistance by performing and carrying out the $^{230}\text{Th}/\text{U}$ and OSL age determination on several carbonate and sandstone samples from study area.

I would like to thank all my friends and colleagues in the Basin Analysis research group: Sebastian Lindhorst, Hamphery Ajonina, Sebastian Ceaser, Mohammed Mahsoub, Gunnar Ries, Kay Menckhoff, Katharina Peterknecht and Frau Anna Marie Gerhard. Special thanks also go to the rest of the staff of the 9th floor in our institute Building.

I will be eternally grateful to my wife, **Radia Khalil Ahmad**, and I specially appreciated her great support. She has made possible all this work with her unwavering help and her unlimited support.

Table of contents

| | |
|-----------------------|-----|
| Summary | iii |
| Zusammenfassung | vi |
| Acknowledgment | ix |

1 Introduction..... 1

| | |
|-----------------------------|---|
| 1.1 Study area | 4 |
| 1.2 Aims of the study | 5 |
| 1.3 Outline of thesis..... | 5 |

2 Geological Setting 6

| | |
|--|----|
| 2.1 Geomorphology of the Murzuq Basin | 6 |
| 2.1.1 External margin | 6 |
| 2.1.2 Internal margins | 8 |
| 2.2 Geological history of the Murzuq Basin | 9 |
| 2.3 Basin Stratigraphy | 11 |
| 2.4 Tectonic structure of the Murzuq Basin | 13 |
| 2.4.1 The Basement..... | 13 |
| 2.4.2 The Caledonian structural stage | 13 |
| 2.4.3 Hercynian structural stage | 14 |
| 2.4.4 Middle Cretaceous to Early Tertiary tectonics..... | 15 |
| 2.4.5 Upper Cretaceous/ Eocene structural stage | 15 |
| 2.5. Current Climate of the Murzuq Basin | 15 |
| 2.5.1 Rainfall in the Murzuq Basin..... | 16 |
| 2.5.2 Relative humidity..... | 17 |
| 2.5.3 Temperture | 18 |
| 2.5.4 Evaporation..... | 18 |
| 2.5.5 Dominant wind directions in the Murzuq Basin..... | 19 |

3 Brak Member..... 21

| | |
|--|----|
| ABSTRACT | 21 |
| 3.1 Introduction..... | 22 |
| 3.2 Methods..... | 24 |
| 3.3 Results | 28 |
| 3.3.1 Transition Interval | 28 |
| 3.3.2 Conglomerate interval..... | 28 |
| 3.3.3 Evaporite-carbonate interval | 29 |
| 3.3.4 Massive limestone interval | 31 |
| 3.3.5 Carbonate mineralogy | 33 |
| 3.3.5 $^{230}\text{Th}/\text{U}$ Dating..... | 33 |
| 3.4 Interpretation | 34 |
| 3.4 Discussion and Conclusion | 36 |

4 Bi'r az Zallaf Member..... 39

| | |
|--|----|
| ABSTRACT | 39 |
| 4.1 Introduction..... | 40 |
| 4.2 Geological setting | 42 |
| 4.3 Methods..... | 43 |
| 4.4 Results | 45 |
| 4.4.1 Lithology and sedimentary facies | 45 |
| 4.4.1.1 Sand facies | 45 |
| 4.4.1.2 Carbonate facies | 47 |
| 4.4.1.2.1 Lower carbonate interval | 47 |
| 4.4.1.2.2 Middle carbonate interval | 49 |
| 4.4.1.2.3 Upper carbonate interval | 50 |
| 4.4.1.2.4 Uppermost carbonate interval | 51 |
| 4.4.2 Fossil content..... | 53 |
| 4.4.3 Carbonate mineralogy..... | 54 |
| 4.4.4 OSL age Determinations | 55 |
| 4.5 Interpretation | 57 |

| | |
|----------------------------------|----|
| 4.5.1 Facies interpretation..... | 57 |
| 4.5.1.1 Sand facies | 57 |
| 4.5.1.2 Carbonate facies | 57 |
| 4.5.2 Depositional model..... | 58 |
| 4.5.2.1 Alluvial stages | 59 |
| 4.5.2.2 Lacustrine stages | 59 |
| 4.6 Discussion | 60 |
| 4.7 Conclusion..... | 64 |

5 Aqar Member.....65

| | |
|-------------------------------|----|
| ABSTRACT | 65 |
| 5.1 Introduction..... | 66 |
| 5.2 Geological setting | 68 |
| 5.3 Methods..... | 69 |
| 5.4 Results | 70 |
| 5.4.1 Palaeontology | 70 |
| 5.4.1.1 Bivalves..... | 70 |
| 5.4.1.2 Gastropods..... | 71 |
| 5.4.1.3 Ostracods..... | 72 |
| 5.4.1.4 Charophytes..... | 72 |
| 5.4.2 Depositional model..... | 74 |
| 5.5 Interpretation | 77 |
| 5.6 Discussion | 80 |
| 5.7 Conclusion..... | 85 |

6 General conclusions and outlook.....86

| | |
|----------------------|----|
| 6.1 Conclusions..... | 87 |
| 6.2 Outlook | 87 |

References

88

1

INTRODUCTION

The roughly triangular Murzuq Basin in SW Libya is located between 21° - 29° N and 10° - 17° E (Fig. 1). It is one of the several endorheic Basins of the North African platform, and covers an area over 350 000 km² (Davidson et al., 2000). The borders of the basin are the Gargaf Uplift to the North, the Tassili Plateau to the west, the Haruj and Tibesti Uplifts to the East. To the South the basin extends into the Djado Basin in Niger. The shape of the basin reflects a Variscan and Mesozoic overprint on an older structural relief (Klitzsch, 2000).

Strata on the basin flanks generally dip towards the basin center, exposing Cambrian to Quaternary rock units in a concentric pattern. The sediments in the central part of the basin have a thickness of about 3500 m, comprised of Palaeozoic and Mesozoic sediments, which are mainly sandstones and shales. The oldest Palaeozoic rocks outcrop at the external margins of the Basin, whereas Triassic, Jurassic and Cretaceous sediments form an escarpment in the middle part of the basin. Late Tertiary and Quaternary sand dunes of Awbari and Murzuq Sand Sea together with lacustrine and alluvial deposits as well as calcretes occupy the deep depressions in the basin centre.

The geology of Murzuq Basin was established through the regional geological mapping programme in Southwest Libya carried out by the Industrial Research Centre of Libya with the publication of maps on the scale 1:250.000 and accompanying reports (Seidl and Röhlich, 1984; Korab, 1984; Pařízek et al., 1984;

Berendeyev, 1985; Woller, 1978, 1984; Štefek and Röhlich, 1984; Rončević, 1984; Mrazek, 1984; Grubić et al., 1991).

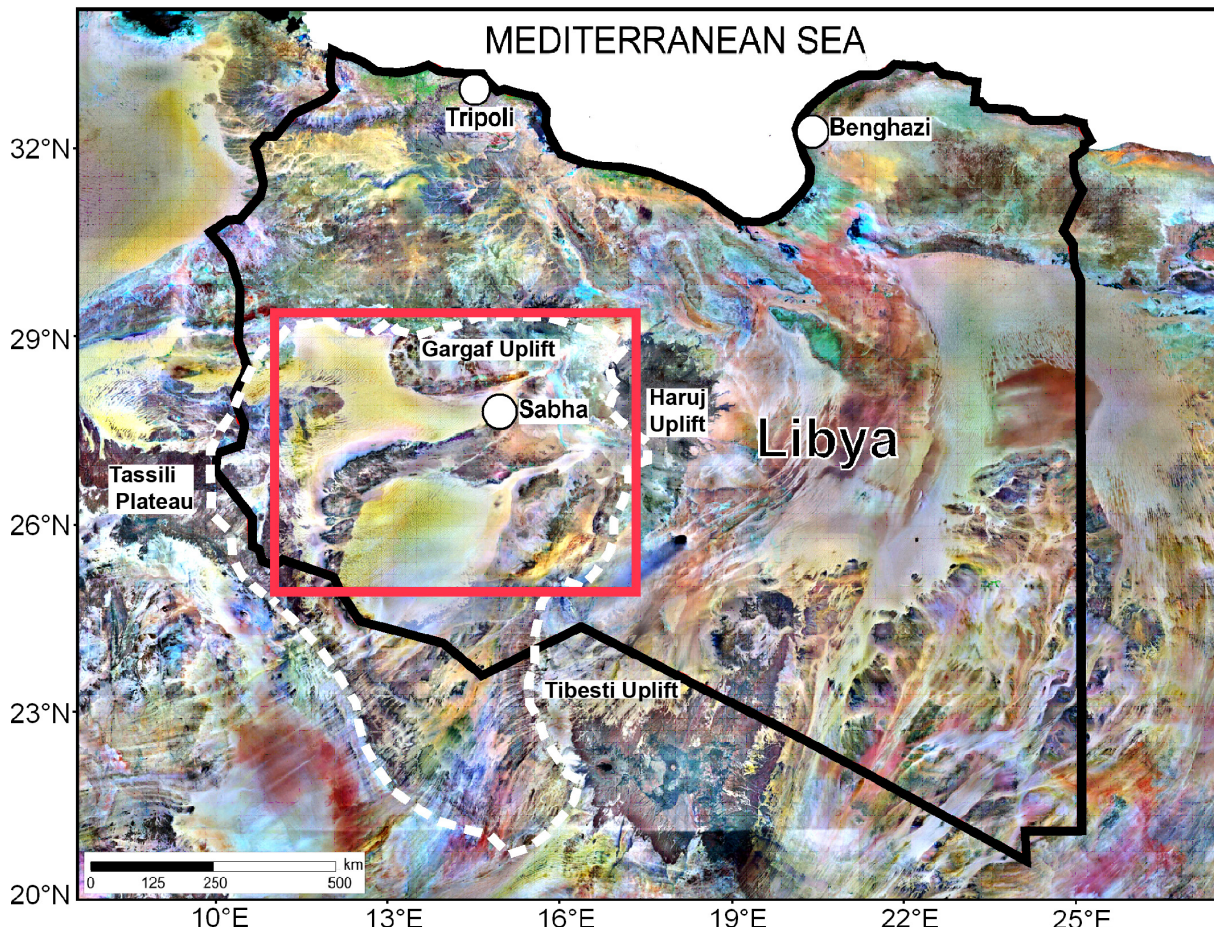


Figure 1. Regional overview showing the outline (dashed white line) and location of Murzuq Basin and study area (red box) in SW Libya

According to Klitzsch (2000), subsidence in the basin increased progressively from the Early Palaeozoic to Mesozoic, while the basin was continuously being filled, mainly with continental siliciclastics and minor Palaeozoic marine limestones. The Mesozoic sediments are represented by the continental Nubian Sandstone, and by remnants of marine Maastrichtian sandy limestone that are present in the N and to E of Wadi ash Shati (Seidl and Röhlich, 1984; Berendeyev, 1985). Cenozoic sediments consist of about 100 m thick Palaeocene marine limestone, dolomite and marl, which are preserved only on the northern and north-eastern margin of the Murzuq Basin. Quaternary deposits are widely distributed in the Murzuq Basin and they were classified according to their genetic criteria and morphological position into several

types: lacustrine (Al Mahruqah Formation), slope, sabkha, old wadi, recent wadi, fluvioeolian, and eolian deposits (Seidl and Röhlich, 1984).

Many geological studies have been carried out on Al Mahruqah Formation. However, there is no agreement among researchers concerning the depositional environment and the age of this formation (Desio, 1936; Pangi, 1938; Bellair, 1944, 1947, 1953; Lelubre 1946a, 1946b, 1952; Collomb, 1962; Goudarzi, 1970; Klitzsch, 1974; Panerjee, 1980; Petit-Marie et al. 1980; Gaven, 1981, 1982; Seidl and Röhlich, 1984).

Thiedig et al. (2000); Thiedig and Geyh (2004); Geyh and Thiedig (2008) expanded the Al Mahruqah Fm. to include all isolated superficial carbonate deposits in the Murzuq Basin. They interpreted these limestones as Quaternary lacustrine deposits and subdivided them into four units: the Antalkhata, the Brak, the Bi'r az Zallaf, and the Aqar members. This interpretation and subdivision gave rise to the notion of "Megalake Fezzan" (Thiedig et al., 2000, Thiedig and Geyh, 2004; Pachur and Altmann, 2006; Geyh and Thiedig, 2008).

These controversies on the age and environment of deposition among researchers are readily attributed to the lack of detail information on the facies architecture of the the Al Mahruqah Formation.

This study integrates stratigraphic, sedimentologic, petrographic and chronologic data from the Al Mahruqah Formation in order to clarify origin, depositional environment and the age of this Formation and to better understanding of the geology and palaeogeography of the Murzuq Basin and central Sahara region during the Tertiary and Quaternary periods.

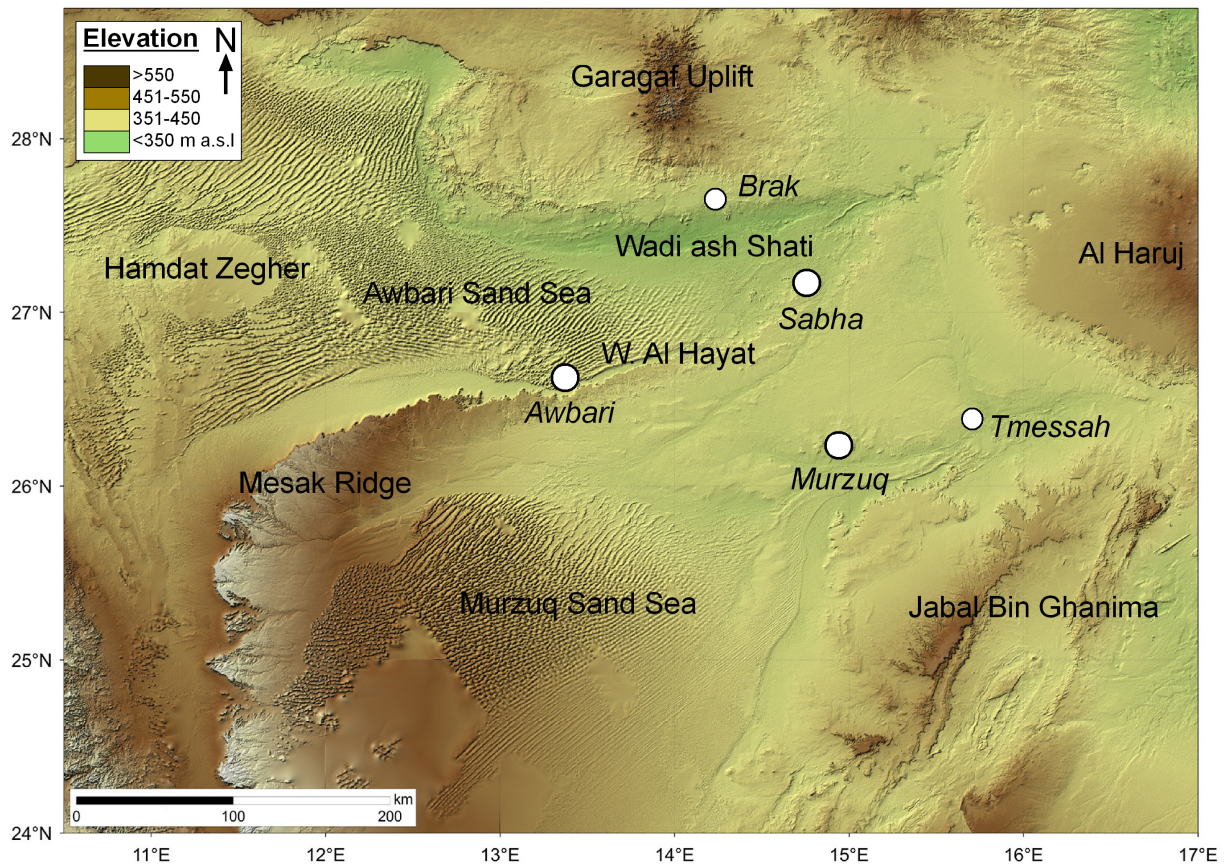


Figure 2. A radar photo of the study area showing the main morphological and topographical features in central part of Murzuq Basin.

1.1 Study area

The study area is situated on the southern flank of the Gargaf uplift, in the northern part of the Murzuq Basin, which is located in the SW Libya between 21° to 28° N, and 10° to 17° E (Fig. 1 and 2).

The focus area is located in Wadi ash Shati and Wadi Zallaf depressions (Fig. 2). The investigated sediments belong to the Al Mahruqah Formation, consisting of Brak, Bi'r az Zallaf and Aqar members, which are well exposed at the Wadi ash Shati and Wadi za Zallaf areas. It is within this area that the lithology, geometry of the individual member and their relationships has been established. To a lesser degree, this study also includes the Hamadat Zegeher area, which is located at the western central part of the Murzuq Basin.

1.2 Aims of the study

This work focuses on the three members of the Al Mahruqah Formation (Brak, Bi'r az Zallaf and Aqar members). It will investigate these three members separately by using a comprehensive facies analysis to determine their components, mineralogy, fossil content, sedimentary facies and depositional environments, in order to reconstruct the different stages of "Megalake Fezzan" concept.

This concept was suggested by numerous geologists in the last decades to explain the distribution as well as the different nature, age and thickness of the deposits.

Based on the obtained data and resulted interpretation thereof, we determined, described, and interpreted the components, mineralogy, sedimentary structures as well as the geometry of these members for the first time. Additionally, we proposed sedimentary models for each member, which could serve as a key to recognize the sedimentary facies and depositional environment of each member of Al Mahruqah Formation in the study area.

$^{230}\text{Th}/\text{U}$ and OSL age dating analysis provide another evidence to support the interpretation concerning the age assignments, origin, and depositional environment of the investigated deposits.

1.3 Outline of thesis

The thesis of this study is presented in six chapters. The first chapter introduces the study. The second chapter, "Geological Setting", gives brief information concerning the geomorphology, geology and climate of Murzuq Basin. The third chapter, "Brak Member", focuses on the Brak member deposits. The fourth Chapter, "Bi'r az Zallaf Member" defines criteria for the identification, description and interpretation of the examined deposits and their geological and palaeogeographical significance of study area. The fourth chapter deals with Bi'r az Zallaf member, with special attention given to the thin bedded to laminate carbonate beds, for the purpose of identifying and clarifying their components, mineralogy, origin and sedimentary environment. In the fifth chapter, "Aqar Member", fossil contents, geometry and two simplified sedimentary models for the Aqar member coquina are documented and discussed in detail. Finally the sixth chapter is a general conclusions and outlook.

2

GEOLOGICAL SETTING

2.1 Geomorphology of the Murzuq Basin

Morphologically, the Murzuq Basin is one of the principal features of the central Sahara, and can be described as an enormous, flat dish of approximately 1000 km long and 600 km wide, surrounded by an outward-turned cuesta landscape. Strata on the flanks dip gently towards the basin centre, exposing all rock units around the flanks in a concentric pattern (Fig. 3). According to Thiedig et al. (2000), the present shape of the continental endorheic Murzuq Basin was formed during the Tertiary, by deflation and fluvial erosion during humid intervals. These processes carved out the Mesak Ridge between the present large sand Sea areas. The main morphological units of this basin consist of plateaus, bench lands (cuestas), planation, wadis and sand dunes cover. On the basis of morphological features, the Murzuq Basin can be subdivided into external and internal margins. These basin margins are separated from each other by low lands covered mostly by gravelly sand and sand dunes (Fig. 3).

2.1.1 External margin

The most prominent feature in the northern margin of the Murzuq Basin is the Gargaf Uplift (Jabal al Hasawnah). This Uplift extends approximately 330 km east-west and is more than 760 m above sea level in its central part. The Jabal Hasawnah is made up of monotonous outcrops of the sandstones of the Hasawnah Formation and remnants of Tertiary volcanic domes (El Chair, 1984).

Few outcrops of Precambrian basement rocks occur in the higher central part of the Jabal al Hasawnah Mountain (Gargaf Uplift). These mountains are characterized by sharp, deeply incised canyon-like wadis, which flow to the south to Wadi ash Shati and Wadi Al Arial, and further south into the Awbari Sand Sea area.

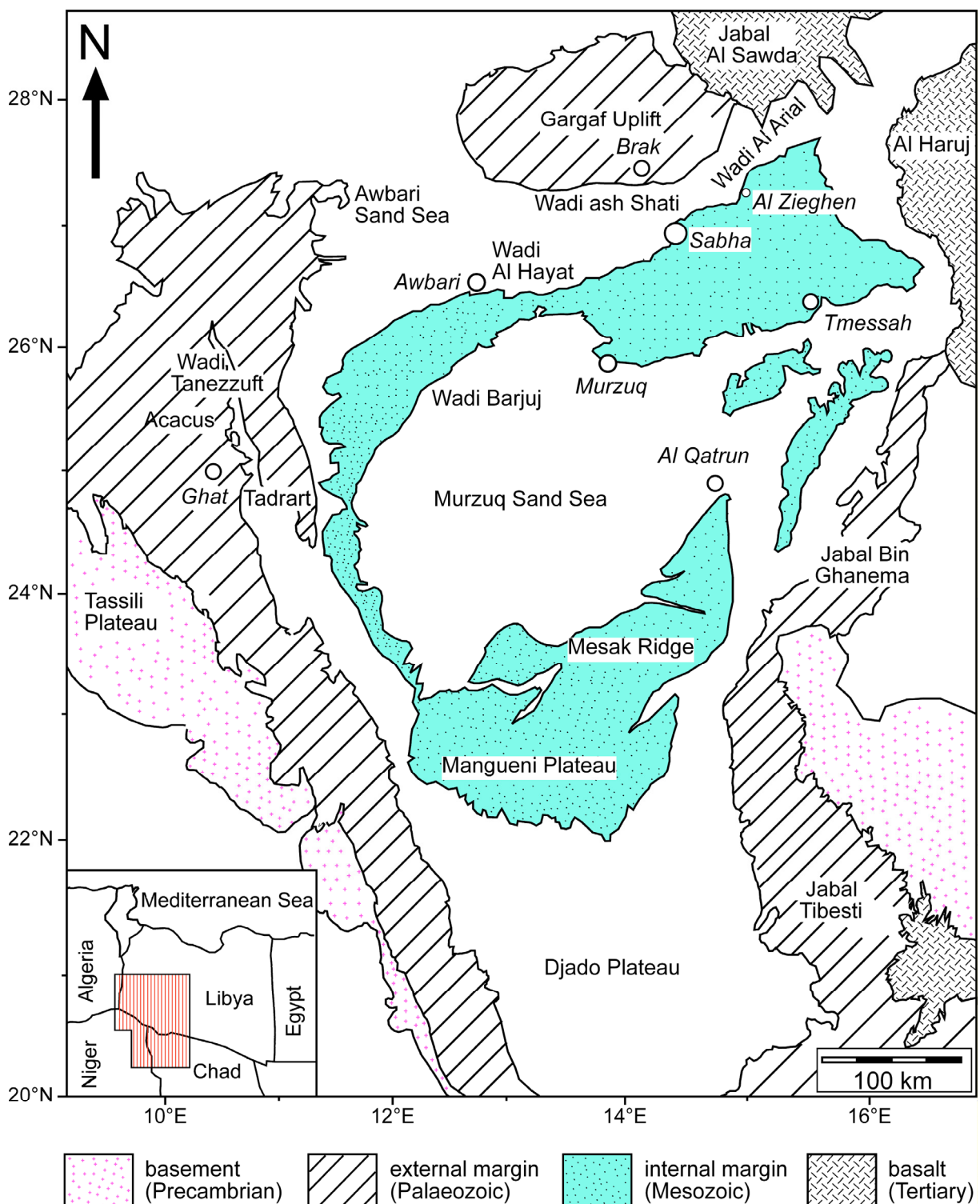


Figure 3 Sketch map showing the regional extension of Murzuq Basin and its main morphological features. Modified after El Chair (1984).

Tassili and Djado Plateaus form in the south and south-western outer margins of the Murzuq Basin (Fig. 3). These plateaus are located in the bordering countries of Algeria and Niger. The Acacus and Tadrart Mountains, which consist mainly of Paleozoic sandstone and claystone formations, form another prominent mountain range, which stretch from north to south and are separated from each other by Wadi Tanezzuft. The trench of this Wadi at Acacus Mountains produces a remarkable rock wall, which has a peak that than 1400 m above sea level, whereas the maximum height of Tadrart Mountains is about 1250 m (El Chair, 1984). These mountains are characterized by steep, deep Wadis, which drain into large plains and closed depressions located to the east in Awbari and Murzuq Sand Sea areas. Today those large plains and depressions are covered entirely by sand dunes (Fig. 2 and 3). A gap exists only in the northeastern external margin of the Murzuq Basin, where it gradually transitions into the foreland of the Jabal Haruj basaltic Mountain (Fig. 3). The south-eastern part of Murzuq Basin is represented by Jabal Bin Ghanema Mountain. This mountain is made of Paleozoic sandstones and lies between Tibesti Mountains and Jabal Al Haruj (Fig. 3).

2.1.2 Internal margins

The inner margin of the Murzuq Basin is a cuesta. It starts from the northern part of Sabha- Al Zieghen and it extends to the south along the Wadi Al Hayat to build the prominent Mesak Mountains, which continue further to the south and southeast of the Mangueni Plateau, and adjoin the northeastern part of Jabal Bin Ghanema (Fig. 3).

The top of the internal margin of the Murzuq Basin is frequently incised by Wadi drainage systems. These wadis are relative smaller in comparison with external margin drainage wadis. These wadis terminate at the rims of the Murzuq Sand Sea cover and build very large depressions to the west of Murzuq town (Fig. 2 and 3).

The central part of the basin has been filled by Paleozoic to Quaternary sedimentary rocks. These sedimentary rocks are arranged in a concentric pattern around the middle core of the basin, with recent deposits in deepest parts and in the central part surrounding by older ones. The Paleozoic deposits in the central part of the basin are covered by Middle to Late Tertiary and Quaternary sand dunes measuring about 300 km long and 300 km wide.

2.2 Geological history of the Murzuq Basin

The geology of the Murzuq Basin, referred to in this study, is from the works of Klitzsch (1963, 1970, 1974, 2000); Conant and Goudarzi (1964); Fürst and Klitzsch (1963); Seidl and Röhlich (1984); Koràb (1984); El Chair (1984); Domáci et al. (1991); Aziz (2000). A comprehensive and detailed geological map of Murzuq Basin is provided in (Fig. 4).

Current knowledge of the geology of the Murzuq Basin, together with the important information obtained by mapping project of large areas of Murzuq Basin allows us to outline its geological history as follows: In the Palaeozoic periods, large repeated NW-SE sea transgressions took place in the central Sahara. These transgressions occurred in different stages and reached different points in the south of the recent Sahara. Because of the variations in the range and duration of the transgressions in the Sahara, thick marine sedimentary successions were formed in the northern part of Sahara, which gradually decrease in thickness towards the southern part of the Sahara.

During the Late Cambrian, the highly weathered Pan-African Basement was gradually covered by a shallow sea. The next and largest transgression in the Murzuq Basin was in the Ordovician, which was intense enough to reach as far south as the location of present-day Lake Chad (Grunert, 1983). It left fine-grained marine sandstones and claystones, which usually cover the coarse-grained fluvial sandstones from the Middle to Late Cambrian (Hasawnah Formation). These Cambro-Ordovician Formations form the outer edge of the Murzuq Basin (Figs. 3 and 5). The third largest sea transgression occurred during the Silurian; it also reached the southern central Sahara and again resulted in the deposition of clay and sandstones the claystones generally represent the flooding phase (transgression), whereas the sandstones are assigned to the regression phase. These deposits are the marine graptolite-bearing Tanezzuft Formation and the younger Acacus Formation, which are overlain by the Tadrart Formation of Lower Devonian age (Fig. 5). After a temporary retreat in the Early Devonian, the sea over flooded the central Sahara again in the Middle Devonian time and reached as far south as latitude 15° N, whereby it submerged Acacus and Tadrart mountains and deposited the Ounkasa Formation (Fig. 5), which consists of marine sandstones and minor clay, siltstones.

The enormous transgressions of Silurian and Middle Devonian Sea into the area of today's central Sahara was possible only due to large NW-SE trending troughs and uplifts structures, whose formation probably started in the Cambrian age, and reached its maximum range in the Upper Devonian/Lower Carboniferous periods (Fig. 6). The Murzuq Basin was situated on the axis of the broad Murzuq-Djado Trough at that time, which can be followed to the present latitude 18° N in Republic of Chad (Klitzsch, 2000). It was bordered by the Tihemboka Uplift in the West, and by Tripoli-Tibesti Uplift in the East (Fig. 6). The evidence for formation of uplifts and trough structures can be deduced from the presence of unconformity surfaces and variations in the thickness of different sediments (Fig. 5). For instance, in case of the Tihemboka Uplift at the northwest edge of the Murzuq Basin, where Carboniferous sediments directly superimpose the Cambro-Ordovician formations, their Silurian and Devonian sediment covers were entirely weathered due to elevation during a tectonic uplift (Klitzsch, 2000). On the other hand, the sediments in the center of the trough have a much greater thickness of more than 1000 m in the deep protected areas. Even in the western margin of the Murzuq-Djado Trough, for example in the Acacus Mountains, the Silurian and Devonian deposits reach about 1200 m in thickness (El Chair, 1984). According to Klitzsch (1970) the structural orientation gradually changed in the Lower Carboniferous from NW-SE direction to NE-SW direction caused by the Hercynian orogeny (Fig. 7). Hence, in the Lower Carboniferous, the sea transgression overflowed the Al Hamada Basin in the North and extended southward to approximately latitude 20° N in the middle Sahara (Fig. 6). The Gargaf Uplift prevented the later transgressions into Murzuq Basin (Seidl and Röhlich, 1984). Therefore, the continental conditions prevailed in the Murzuq Basin and have continued until present time. The east edge of the Murzuq Basin was occupied by a shallow sea in the Upper Cretaceous /Lower Tertiary period, which originated from the Sirte Basin and extended to the northern edge of the Tibesti Mountains (Fürst and Klitzsch, 1963).

Subsidence in the basin increased progressively from the Late Palaeozoic to Mesozoic, while the basin was continuously being filled with continental sediments (clay-, silt- and sandstones). During the Late Tertiary and Quaternary, sand dunes were developed under arid climate conditions, which continued with short interruptions during the middle Miocene and Pleistocene periods, when the dry desert climate changed to a humid climate with heavy rainfall, which led to the

creation of several freshwater lakes in many locations in the Central Sahara (Pachur and Altmann, 2006; Thiedig et al., 2000). The occurrence of lake deposits in the Murzuq Basin is clear evidence for Miocene and Pleistocene humid periods in the Central Sahara.

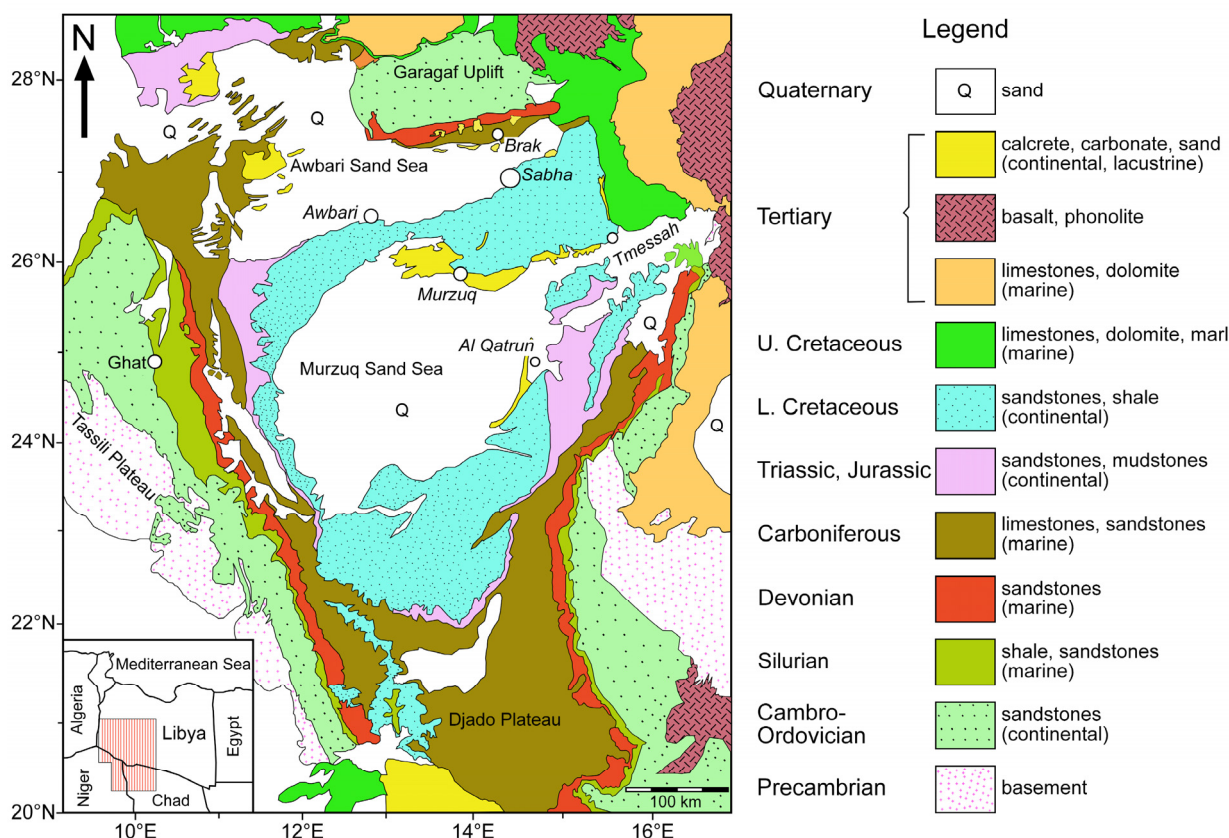


Figure 4. Geological map of the Murzuq Basin showing the main stratigraphical units. Modified after El Chair (1984).

2.3 Basin Stratigraphy

A stratigraphic column for the Murzuq Basin is depicted in (Fig. 5). The sedimentary deposits in the basin range from the Cambrian to the Quaternary in age, and can be subdivided into different sedimentary units (Mamgain, 1980; Bellini and Massa 1980; Abugares and Ramaekers, 1993). The stratigraphic schemes established by these authors have been slightly modified in order to incorporate additional information derived from the surface and subsurface of the present basin center (Fig. 5).

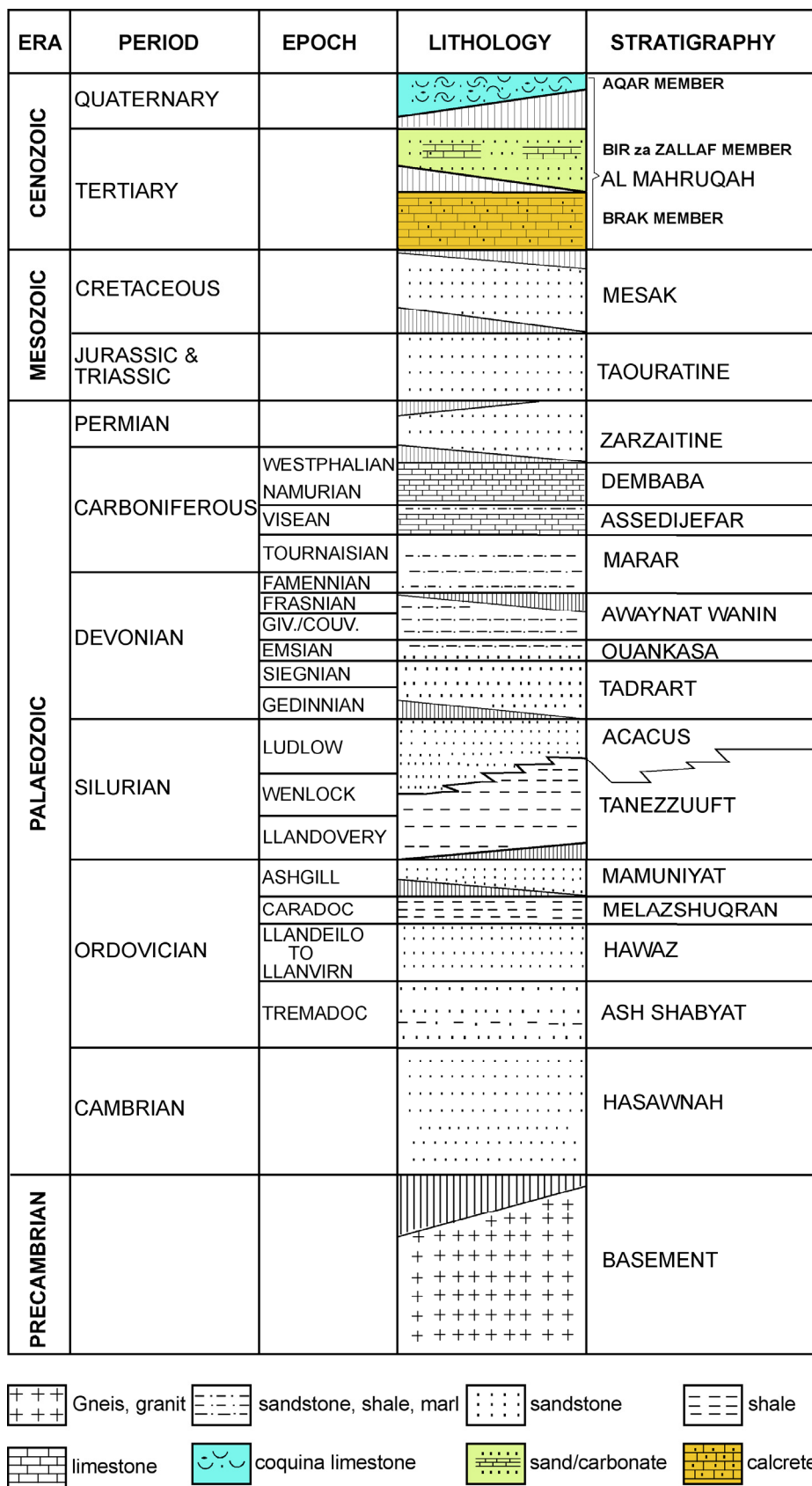


Figure 5. Stratigraphy column of the Wadi ash Shati area in the northern margin of the Murzuq Basin, constructed from several wells and from diagrams of various literature.

2.4 Tectonic structure of Murzuq Basin

The Tibesti-Haruj, Tassili and Gargaf Uplifts on the eastern, western and northern flanks respectively constitute the present-day tectonic elements delimiting the Murzuq Basin. To the south, the Basin narrows and terminates at the Djado Basin in the northern part of the Republic of Niger (Fig. 3).

2.4.1 The Basement

According to Aziz (2000), the basement rocks exposed along the Basin margins are generally divided into two groups:

- (1) A high-grade metamorphic suite comprising mica-schist, gneiss and amphibolites associated with granite and granodiorite.
- (2) A low-grade metamorphic suite of quartzite and schist, including locally preserved metamorphosed rocks of the so-called Mourizidie Formation (Jacqué, 1962; Aziz, 2000). This formation overlies the Precambrian with distinct angular unconformity and is itself discordantly overlain by basal conglomerate of the Cambrian Hasawnah Formation. The deposits exposed in the study area belong to the following structural stages and substages.

2.4.2 The Caledonian structural stage

This stage is confined to the northern part of the study area. On the basis of regional unconformity, it can be subdivided into two substages:

- A) Lower substage (Cambrian-Hasawnah Formation) which is the lowermost lithostratigraphic unit overlying the basement rocks in the Murzuq Basin (Fig. 5).
- B) Upper substage (Ashgillian-Memuniat Formation) which represents the uppermost Ordovician (Fig. 5).

According to Massa and Colomb (1960), this Formation occurs only on the western margin of the Murzuq Basin. The absence of most of Ordovician and all of Silurian formations at the northern edge of the Murzuq Basin is attributed to the Caledonian movements which caused an extensive uplift and trough structures that extended in a NNW-SSE direction (Fig. 6).

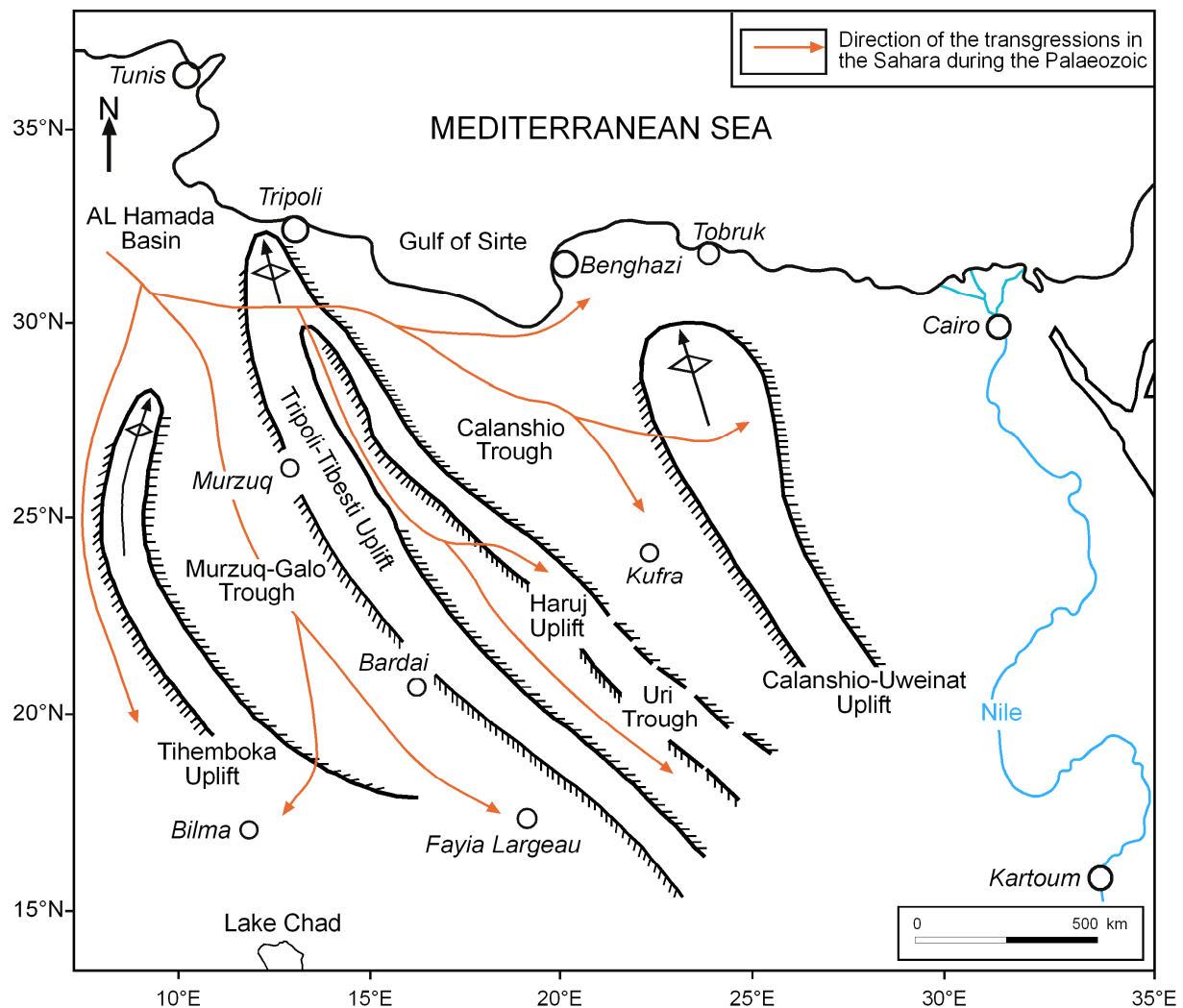


Figure 6. Generalized pattern of major structural elements of the central Sahara during the Caledonian Orogeny. From Klitzsch (1970).

2.4.3 Hercynian structural stage

The Hercynian collision of Gondwana with the Laurasian northern plates resulted in the formation of the Pangaea super-continent, which soon after formation, started to disintegrate through east- west trending fault systems, which was later followed by major transgressions to the west (Klitzsch, 2000). The Hercynian structural stage extends into central Sahara from ENE to WSW (Fig. 7). It began with the Middle Devonian and continued up to the Lower Carboniferous. The formation of the Gargaf Uplift in the north and Tibesti-Sirte Uplift in the southeast resulted in the closure of the old Murzuq-Djado Trough in the N and NE directions.

2.4.4 Middle Cretaceous to Early Tertiary tectonics

In the central part of Murzuq Basin one notices a major unconformity between Jurassic and early Cretaceous Mesak Formation and the overlying Quaternary Aeolian sand deposits, calcrete, lacustrine and fluvial deposits (Fig. 5). It is still uncertain whether this stratigraphic break is due to Uplift during the early to middle Cretaceous (Austrian movement), the early to middle Tertiary (Alpine) Orogeny, or a combination of both. Boote et al. (1998) suggested that both of these tectonic movements caused uplift and erosion of the Murzuq Basin margins, with the middle Cretaceous movement been responsible for most of the significant movements. Davidson et al. (2000) found evidence for reactivated compressional or reactivated transpressional fault systems affecting the outcropping Nubian sandstones (Mesak Formation) and dated this movement as post mid-Cretaceous event.

2.4.5 Upper Cretaceous/ Eocene structural stage

This stage is represented by the Bin Affin Member (Maastrichtian in age). These sediments and the thin overlying Paleogene marine deposits are presently positioned some 500 m above present-day sea level, and clearly demonstrate the effects of renewed post Paleogene uplift. It is believed that this uplift is a consequence of Alpine tectonic movement. No tectonic phenomena were established in the younger structural stages, (i. e. Late Tertiary-Quaternary deposits).

2.5 Current Climate of the Murzuq Basin

The Murzuq Basin lies presently in a completely arid climatic area. The current climate of western North Africa is influenced by Atlantic currents; that of southeastern North Africa is affected by the Indian monsoonal circulation. Stable isotope analysis of speleothems from different locations in North Africa, Namibia, and northern Oman in the southern part of the Arabian Peninsula indicate that during the peaks of interglacial periods, the limit of the monsoon rainfall shifted far north of its present location, and each pluvial period coincided with an interglacial stage of the marine oxygen isotope record.

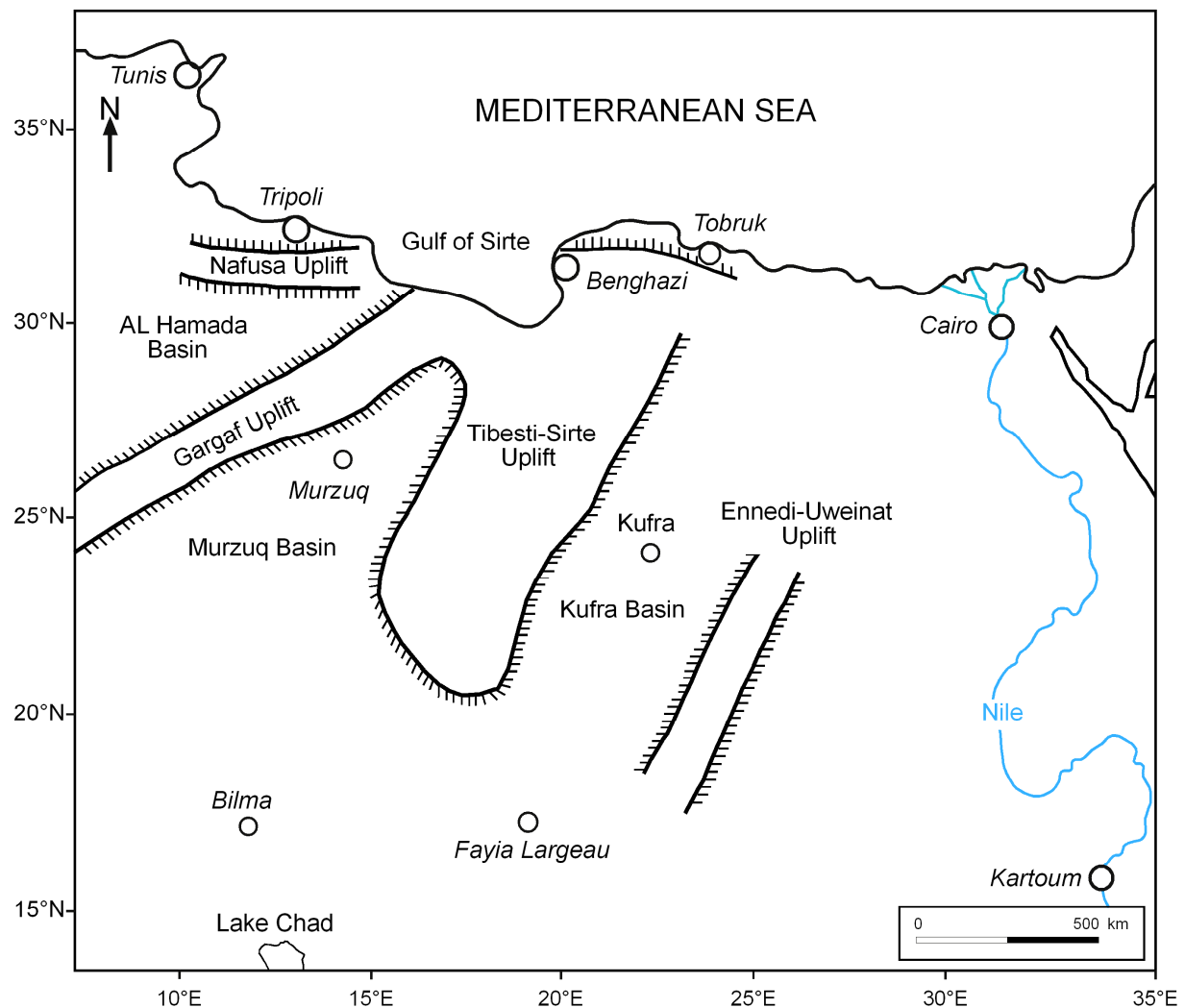


Figure 7. Generalized pattern of major structural elements of Central Sahara during the Hercenian Orogeny. From Klitzsch (1970).

In the early decades of the 20th century a numerous of meteorological stations were established in the Murzuq Basin such as Sabha, Brak, Murzuq, Awbari, Al Qatrur and Ghat etc, which measured daily temperature, rainfall and relative air humidity of Murzuq Basin.

2.5.1 Rainfall in the Murzuq Basin

Rainfall in the Murzuq Basin is very rare. When it occurs, it is only for a short duration, typical of the entire central Sahara. According to Dubief (1963), the highest probability propensity for precipitation in the northern part of the central Sahara

during the winter exists when high tropospheric troughs over southwestern and central Europe extend southward across northern Africa.

In the southern catchment area of the basin, rain falls mostly during the summer (May through October), when the moist air is advected with the Intertropical Convergence Zone (ITCZ) from the Gulf of Guinea northwards

The annual shifts of the ITCZ are responsible for drier climate during the most of the year, when the notheasterly trade winds from the interior of the Sahara prevail (Fig. 8).

Monthly rainfall data for the Murzuq basin is available over 70 years starting from May 1934 to present. The data illustrates that for the past 75 years, rainfall has been rare and irregular. The analyzed metrological data of the basin exhibits that the average annual precipitation under present desert climate is less than 15 mm since the data was record 1934. There is no specific season in the year, which is characterized by precipitation, whereby the summer months July and August are always dry (El Chair, 1984). Nevertheless, in summer seasons rare heavy rainfall has been registered in Murzuq Basin (Klitzsch, 1966). Extremely heavy rainfall sometimes occurs locally (Löhnert and Thiedig, 1998). For example, in November 1937, an exceptionally heavy thunderstorm raged during the night in the area from Idri to Brak, including the southern sand desert, resulting in the collapse of most houses in Aqar village about 20 km west of Brak. In autumn (September–November) 1963, rainstorms filled depressions west of Jabal al Haruj and resulted in large pools of flood water about 2 meters deep. The rain water remained in the depressions and Wadis for up to four months (Kanter, 1967).

2.5.2 Relative humidity

The monthly mean relative humidity ranges between 14 and 69%. The winter months of December, January and February the maximal values lies between 41.6 % and 46.7 %, whereas the summer months June, July and August vary in minimal values from 21.7 to 25% (El Chair, 1984; El Tantawi , 2005).

2.5.3 Temperature

The mean daily temperatures at Sabha town, which is located in the center of the Murzuq Basin, records 12° in the winter and 32° in the summer (Geyh and Thiedig, 2008). The temperatures fluctuate between a minimum of - 4°C measured in January 1953, and a maximum of + 46.5°C in July 1966. The temperature differences between day and night are nearly constant throughout the year (El Chair, 1984).

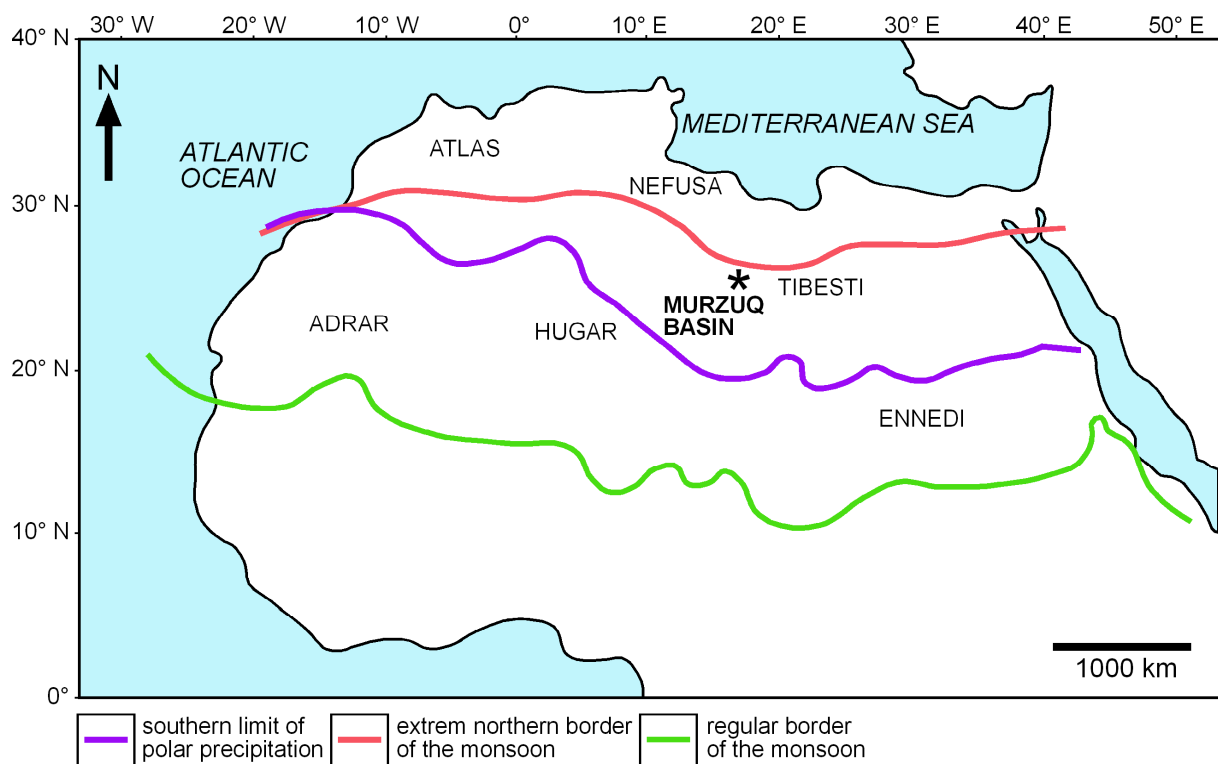


Figure 8. The annual shifts of the ITCZ in northern Africa. Modified Grunert (1983).

2.5.4 Evaporation

The high temperatures and low humidity values of the very dry climate in the Sahara allow for a high potential evaporation throughout the year, especially in the summer season, when temperatures exceed 42-46° C in July/August. As a result, evapotranspiration is extremely high. The Atlas of World Water Balance shows annual potential evaporation as between 2 .25 to 2 .5 m, whereas the potential annual evaporation of the basin is 4 to 5 m (Fig. 9). This high potential evaporation is of importance in assessing whether or not there may be infiltration of precipitation

(including dew) into the groundwater. According to El Chair (1984), most of the short-term and sporadic rainfalls evaporate before any drop of water filters down to the deep groundwater reservoirs.

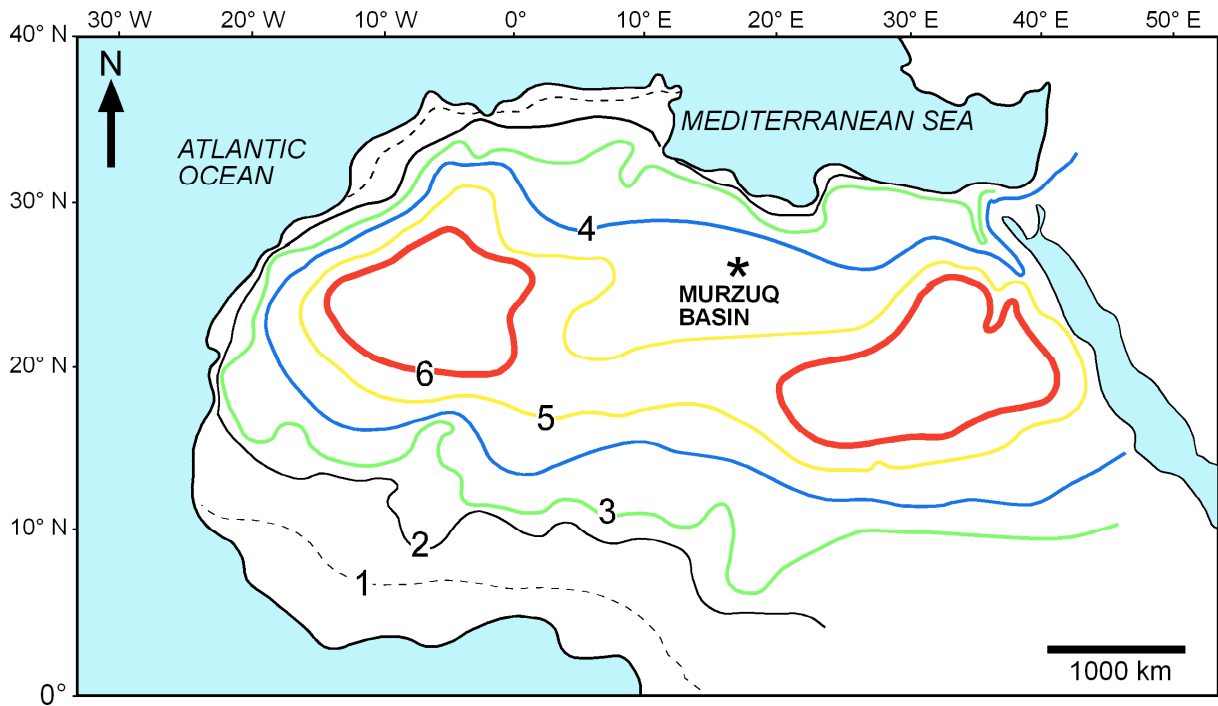


Figure 9. Potential annual evaporation (in meters) in the Sahara. Modified after Grunert (1983).

2.5.5 Dominant wind directions in Murzuq Basin.

Murzuq Basin is located in the middle of the Central Sahara. The Central Sahara is located in the transitional zone between two mainly dominate wind directions. In general, the Central Sahara can be subdivided into two main areas according to predominant wind directions.

The northern part of the Central Sahara is dominated by northwestern Passat winds, whereas the southern part is dominated by northeastern Passat winds.

It is known that the border between the two main wind systems changes and shifts seasonally over the Sahara. During winter, this border lies in the middle of the Central Sahara, crossing the northern Murzuq Basin in Fezzan province extends around 28° N (Dubief, 1971; Grunert, 1983). In the summer, it runs far to the north of the northern African coast. The southern boundary of the Passat wind system is subject to similar seasonal oscillations. In the winter it pushes forward to the Republic

of Sudan, while in summer, due to the advancing Inter Tropic Conversion (ITC) and the subsequent southwest monsoon wind system, the border shifts far to the north to approximately Hoggar-Tibesti (Grunert, 1983), meaning that the core zone of the central Sahara (Murzuq Basin) theoretically remains under the influence of the eastern winds throughout the year.

3

BRAK MEMBER

ABSTRACT

A facies analysis and $^{230}\text{Th}/\text{U}$ dating was performed to clarify if Neogene limestones in the Murzuq Basin are reliable tracers for the occurrence and extension of large northern Sahara lakes in the Pleistocene, previously described as Lake Megafezzan. The Brak Member of the Al Mahruqah Formation is an up to 12 m thick limestone which crops out at the northern flank of the Wadi ash Shati valley in the northern Murzuq Basin and unconformably overlies carboniferous sandstones and claystones. Based on textural and compositional changes, the Brak Mb. can be subdivided into four intervals. A lower interval is transitional between the Palaeozoic siliciclastics and the carbonates, and consists of *in-situ* brecciated deposits with a limestone matrix. A second interval consists of a calcareous matrix-supported conglomerate which contains pisoids. It is overlain by an evaporite-carbonate interval with gypsum, halite, and dolomite. The upper interval of the Brak Mb. is a partly chertified massive limestone with *in-situ* brecciation, circumgranular cracks, fenestral structures, and gravitational cements. Based on these characteristics, the limestones are interpreted as calcrete deposits, i.e. groundwater calcrites. This is contrary to previous interpretation of the Brak Mb. as a lacustrine limestone. The results of the $^{230}\text{Th}/\text{U}$ dating of the Brak Mb. indicate a Middle Pleistocene age and apparently support the concept of middle Pleistocene Megalake Fezzan. However, the $^{230}\text{Th}/\text{U}$ data scatter from indefinite ages to about 240 ka, which could indicate periods of diagenesis in densely cemented carbonates and so does not exclude a Pre-Pleistocene formation age of the limestones. This should be taken into account for further reconstructions of the palaeohydrological regime in the northern Sahara, and especially has a repercussion for the assumption that a pronounced phase of humidity occurred north of the central saharan watershed during the Pleistocene.

3.1 Introduction

The Wadi ash Shati is a depression stretching in an E-W direction, 10 to 20 km wide and about 180 km long at the northern border of the Murzuq Basin. Cambrian, Ordovician, Devonian and Carboniferous sedimentary rocks outcrop, and dip gently to the South. Pale creamy-colored continental carbonates unconformably overlie the Palaeozoic formations, and occur as a series of laterally discontinuous exposures in W-E trending, about 150 km long strip along the northern margin of the Wadi ash Shati (Fig. 10). These carbonates were defined as Al Mahruqah Formation by Seidl and Röhlich (1984, p.89). The name is derived from the village of Al Mahruqah, 25 km W of Brak in Wadi ash Shati, where the formation is typically developed and reaches its maximum thickness of about 12 m.

The Al Mahruqah Formation forms a flat topographic surface “caprock” with an average dip of less than 1 degree to the South. The base of this formation stands approximately 120 m above the bottom of the Wadi ash Shati depression, which is occupied by lacustrine and sabkah deposits (Seidl and Röhlich, 1984).

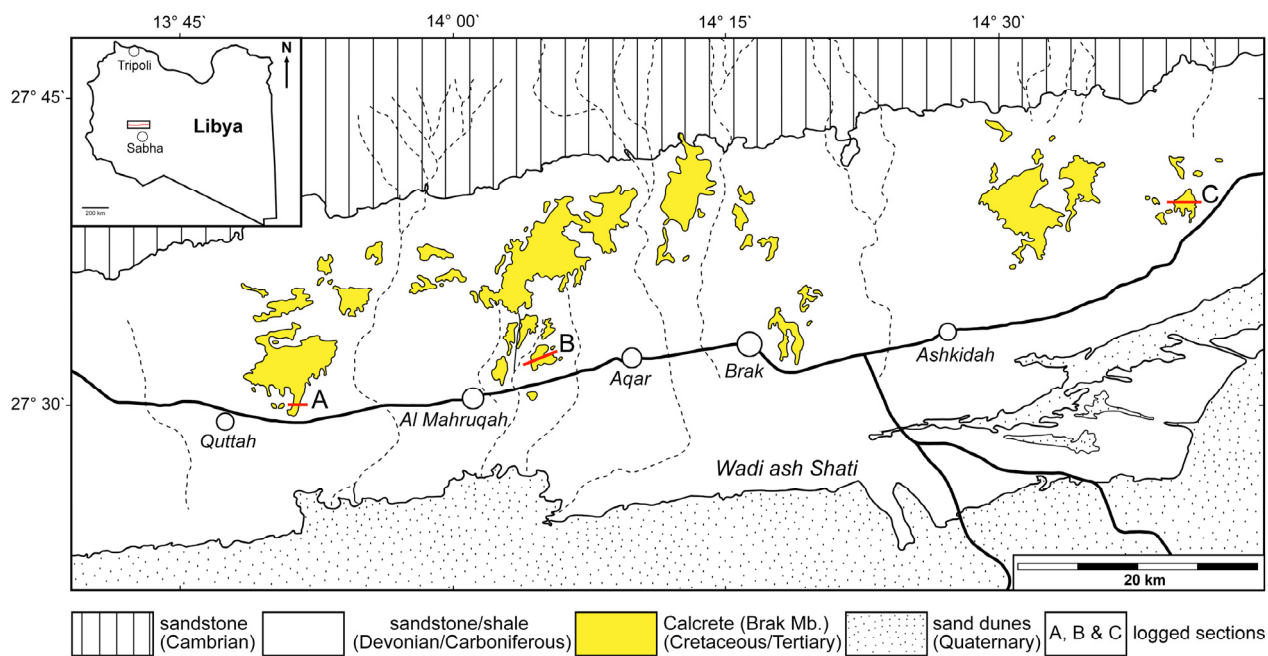


Figure 10. Geological map of the study area showing the main chronostratigraphic units and locations of measured sections (A, B and C) and locations discussed in the text. Section A: 27° 29' N, 013° 51' E, section B: 27° 32' N, 014° 02' E and section C: 27° 38' 49" N, 014° 38' 48" E. Simplified after Seidl and Röhlich (1984).

The limestone was classified as Tertiary lacustrine deposits by Freulon et al. (1955); Collomb (1962); Conant and Goudarzi (1964). Klitzsch (1974) interpreted it as marine deposits and postulated a Late Cretaceous age. Thiedig et al. (2000); Thiedig and Geyh (2004); Geyh and Thiedig (2008) expanded the Al Mahruqah Fm. to include all isolated superficial carbonate deposits in the Murzuq basin. They interpreted these limestones as Quaternary lacustrine deposits and subdivided them into four units: the Antalkhata, the Brak, the Bi'r az Zallaf, and the Aqar members. This interpretation and subdivision gave rise to the notion of "Megalake Fezzan" (Thiedig et al., 2000; Thiedig and Geyh, 2004; Pachur and Altmann, 2006; Geyh and Thiedig, 2008). Lake Megafezzan is proposed to have covered up to about 150.000 km² and to have periodically existed in the Murzuq Basin. It was proposed that it developed during the humid periods of the middle Pleistocene (Geyh and Thiedig, 2008; Armitage et al., 2007; Drake et al., 2008). Age assignments of > 420, 290 - 380, 205 - 260, and 125 - 140 Ka for the distinct limestone members rely on radiometric ²³⁰Th/U dating of random samples from limestones in the Wadi ash Shati, the Wadi za Zallaf, and the Hamada Zegher area (Geyh and Thiedig, 2008). The supposed older to younger sequence of carbonate members are thought to reflect cycles of lacustrine sedimentation followed by erosion, and re-establishment of smaller lakes (Domáci et al., 1991).

The concept of a middle Pleistocene large lake in the northern Sahara to some point is in contradiction with climate proxies retrieved from the marine record. These show that the aridity of the Sahara dates back to major steps of aridification at 3.5 - 3.2, 2.8 - 2.6, 1.7, and 1.0 Ma (Leroy and Dupont, 1994; Dupont and Leroy, 1999; deMenocal, 2004). The probability of a water supply feeding huge lakes was further diminished after 0.95 Ma, when the monsoon front remained south of the central saharan watershed (Larrasoña et al., 2003). Although the distribution of the limestones in the Murzuk Basin was taken to trace the supposed extension of this Megalake Fezzan, no in-depth facies analysis was performed for the different members of the limestones of the Al Mahruqah Fm. Occurrence of coquinas with the aquatic bivalve *Cerastoderma* assigns the youngest Aqar Mb. a lacustrine origin (Petit-Maire et al., 1980; Geyh and Thiedig, 2008). For the Antalkhata Mb., which has a patchy occurrence in the western part of the Murzuq Basin, Rončević (1984) describes a succession of alluvial sands overlain by a calcrete. The sands contain

spores, pollen, lamellibranchs, and gastropods of Pliocene to Quaternary age. For the Brak Mb., characean oogonia, rare lamellibranch debris, ostracods, gastropods, lamellibranchs, and fine organic detritus were mentioned (Seidl and Röhlich, 1984), without, however, a documentation of sample provenance.

For a correct interpretation of the paleohydrological regime of the northern Sahara, a solid knowledge of the facies taken as indicative for widespread aquatic sedimentation, i.e. of the Antalkhata Mb. and the Brak Mb., is essential. This has an impact going further than the understanding of the regional stratigraphy, because the existence of the Megalake Fezzan implies the return to a rather humid phase during the Pleistocene, after a trend of Messinian and Pliocene aridization in northern Africa (Drake et al., 2008). Because the deposits of the Antalkhata Mb. have a very restricted occurrence, the limestone of the Brak Mb. with several outcrops allowing to trace lateral lithological changes appear as a good case to study the genesis of the deposits. Here, a lacustrine origin and the age assignement of the Brak Mb., one of the key deposits for the interpretation of the occurrence of Megalake Fezzan, are challenged. This is based on the occurrence of textures and components which indicate that these limestones are calcrete, i.e. groundwater calcrete deposit. New $^{230}\text{Th}/\text{U}$ measurements in addition question former age assignments of these limestones, and do not exclude a pre-Pleistocene formation age. This has considerable consequences for the reconstruction of the different stages of the Megalake Fezzan, which was much smaller than proposed in different publications.

3.2 Methods

At three locations in the Wadi ash Shati area, sections were logged and sampled in the Brak Mb. of the Al Mahruqah Fm. (Fig. 14). From 150 selected samples, thin sections and slabs were prepared for microscopic analysis. In order to determine the carbonate mineral composition of the limestones, 5 samples from each of the measured sections in the study area were analysed by X – ray diffraction (XRD) with a Philips Diffractometer PW 1830/00. Measurements were performed on smear mounts with 0.02° 2Θ steps and 2 s of scanning time. $^{230}\text{Th}/\text{U}$ dating was performed on a sample from Section B (11.8 m from the base of the section) at the thermal ionisation mass spectrometry laboratory of the Leibniz Institute for Applied

Geophysics in Hannover. Samples for $^{230}\text{Th}/\text{U}$ analysis were sawn from slices of hand specimen with a microdrill and powdered for chemical treatment. Blocks of 1.0 – 1.5 g were taken from homogeneous micritic matrix and from components floating in the matrix.

Uranium-series dating is a commonly used method for dating speleothems (Spötl and Mangini, 2006), travertines (Sierralta et al., in press), corals (Scholz and Hoffmann 2008), and peat (Frechen et al., 2007). Furthermore, calcretes or calcrete-like carbonates formed under semi-arid or arid climate can be dated by $^{230}\text{Th}/\text{U}$ (Candy et al., 2005), which determine the time elapsed since carbonate precipitation or carbonate formation. The different solubility of uranium and thorium in natural waters is the methodological basis of $^{230}\text{Th}/^{234}\text{U}$ -dating of Quaternary deposits (Langmuir 1978; Ivanovich and Harmon, 1992). Since uranium (VI+) has a high solubility and thorium is largely insoluble in groundwater under oxidizing conditions, isotopic disequilibrium evolves during groundwater transport of uranium as uranyl carbonate complex and its co-precipitation with carbonates. Ideally, no thorium precipitates with the carbonate and any ^{230}Th found later developed from radioactive decay of ^{234}U . The activity ratio [$^{230}\text{Th}/^{234}\text{U}$] is a measure of the time elapsed since the evolution of disequilibrium and so this activity ratio is a function of age (Equation 1):

$$\left[\frac{^{230}\text{Th}}{^{234}\text{U}} \right] = \left[\frac{^{238}\text{U}}{^{234}\text{U}} \right] \left(1 - e^{-\lambda_{230}t} \right) + \left(1 - \left[\frac{^{238}\text{U}}{^{234}\text{U}} \right] \right) \frac{\lambda_{230}}{\lambda_{230} - \lambda_{234}} \left(1 - e^{-(\lambda_{230} - \lambda_{234})t} \right) \quad (1)$$

The ratios in brackets are the measured activity ratios, λ_{230} and λ_{234} represent decay constants, and t denotes the time elapsed since formation (Bateman 1910; Kaufman and Broecker, 1965; Ivanovich and Harmon, 1992). Equation 1 can not be solved directly, but for t an iterative procedure has to be used.

Accurate ages can only be produced by the $^{230}\text{Th}/\text{U}$ method if the carbonates have experienced no migration of uranium and thorium since its formation. However, most of such carbonate formations, especially calcretes, are impure and gained various amounts of detrital material mostly clay containing unknown quantities of thorium. Previous studies were concentrated on developing methods to correct for the additionally gained ^{230}Th , most of them based on the detrital amount of ^{232}Th (Ku et

al., 1979; Ku and Liang, 1984; Schwarcz and Latham, 1989; Kaufman, 1993). Ku and Liang (1984) used analyses of the leachate and the insoluble residue to obtain the age of a deposit (L/R-method). Schwarcz and Latham (1989) showed that measured ^{230}Th activities for age calculation can be corrected for the admixed detrital ^{230}Th by analysing leachates of several coeval sub-samples with differing detrital contents (L/L-method) and constructing an isochron (Fig. 11). Kaufman (1993) compared all proposed leaching methods on a well dated sample of impure carbonate. The results indicated that the L/L method yielded valid ages in contrast to analytical schemes combining leachate and residue analyses

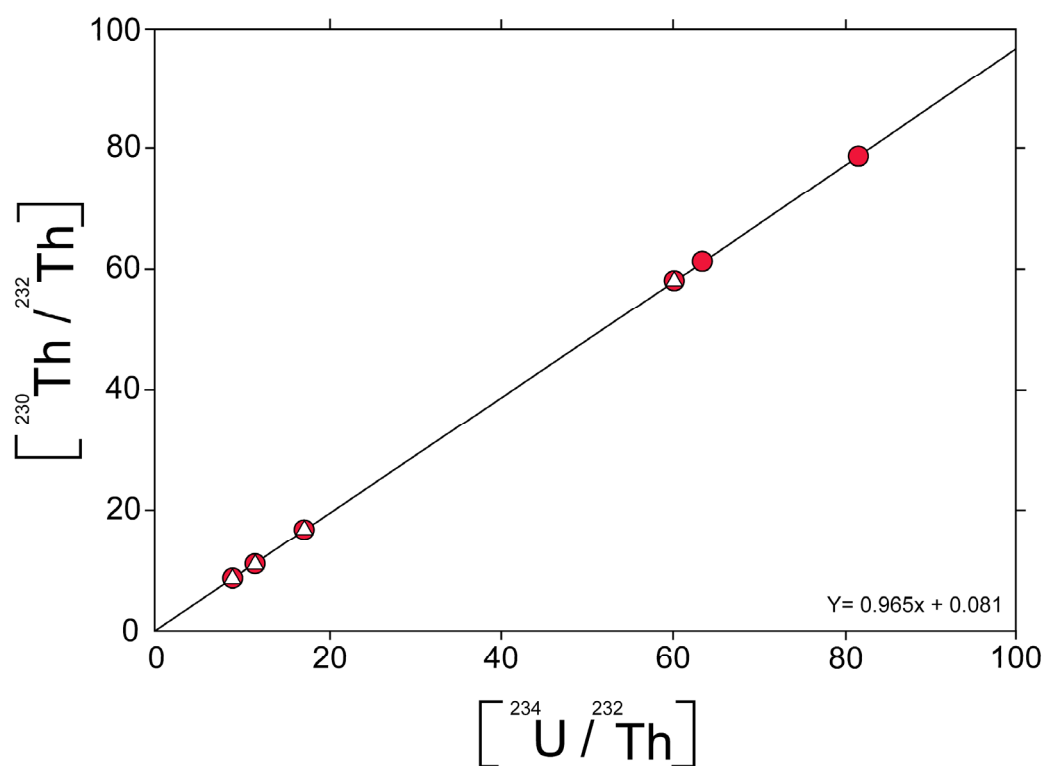


Figure 11. Rosholt -type I diagram of measured isotope activity ratios $^{234}\text{U}/^{232}\text{Th}$ vs. $^{230}\text{Th}/^{232}\text{Th}$ with linear fit to data, so-called isochron diagram. Triangles and circles represent micritic matrix and conglomerate components, respectively

In this study, we applied a similar leaching approach for chemical preparation, as previously described for travertines by Sierralta et al. (in press). The chemistry for the extraction of uranium and thorium for TIMS $^{230}\text{Th}/\text{U}$ dating from the samples was adapted from the leachate/leachate technique (Schwarcz and Latham, 1989; Kaufman, 1993). To meet the isochron requirements at least three coeval dry limestone samples about 0.9 -1.4 g each were crushed gently and heated up to a

temperature of about 900°C for 15 h. The remaining powders were dissolved slowly in a concentrated HNO₃/HCl mixture and processed as described by Sierralta et al. (in press). The isotopic ratios were measured by thermal ionisation mass spectrometry (TIMS; Finnigan MAT262 RPQ) applying the double filament technique. The external reproducibility was determined by measurements of standard solution of NBL-112A (New Brunswick Laboratories Certified Reference Material) and yields a value of 0.3% (1s SD). Three or preferably more coeval samples with different uranium and thorium concentration and so different detrital components, must be analysed to construct isochrons (Fig. 12). To avoid methodologically enlarged errors we used a modified procedure for the calculation of the isochron age, as described by Geyh (2001) and Sierralta et al. (in press). Weakly lithified limestones and nodular limestones, which show evidence of extensive recrystallization or weathering (intervals 2 and 3), were excluded. Well-lithified limestones with non homogeneous textures were considered acceptable for age dating analysis.

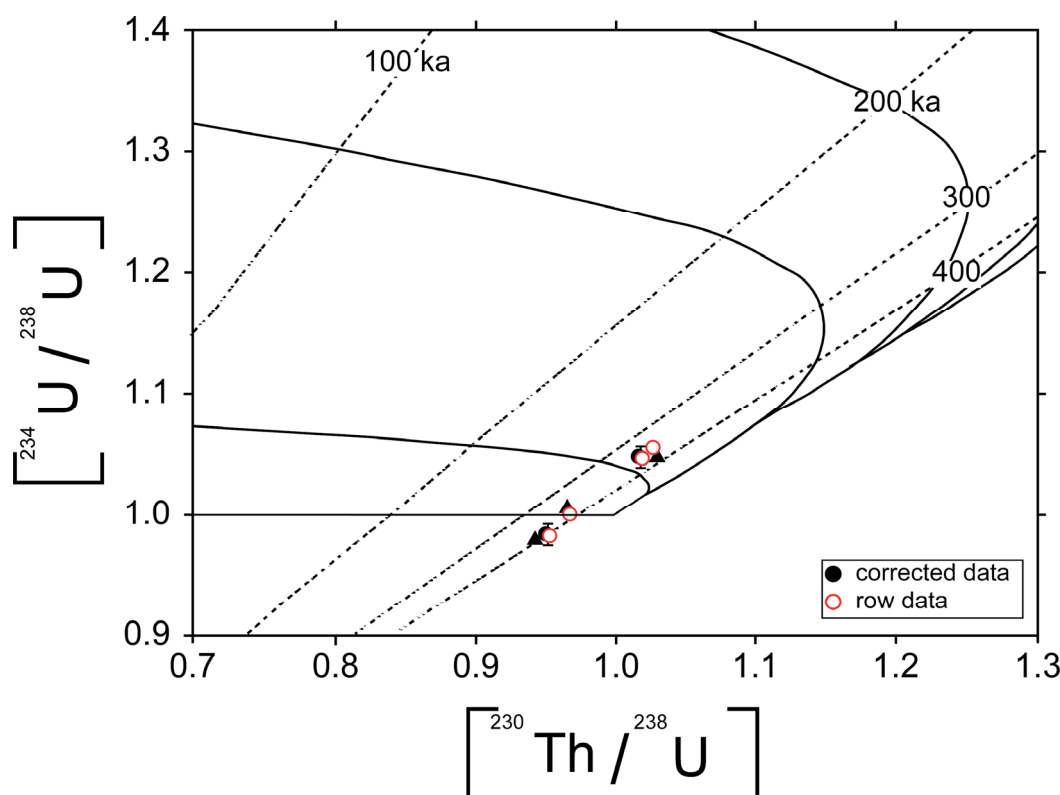


Figure 12. Osmond-Ivanovich diagram of measured isotope activity ratios $^{230}\text{Th}/^{238}\text{U}$ vs $^{234}\text{U}/^{238}\text{U}$ for check of open-system conditions. Curved lines indicate evolution lines of isotope ratios with time, straight dashed lines indicate isochrons (lines of same age). Data plots are given for conglomerate components (circles) and micrite matrix (triangles).

3.3 Results

A representative outcrop of the Al Mahruqah Fm. is shown in Fig. 11. The carbonate-bearing succession overlying the Palaeozoic sandstones and claystones of the Marar Fm. (Seidl and Röhlich, 1984) consists of four distinct intervals which can be differentiated based on macroscopic and microscopic characteristics. These intervals are traceable along all the outcrops of the Wadi ash Shati. From bottom to top the intervals are the following.

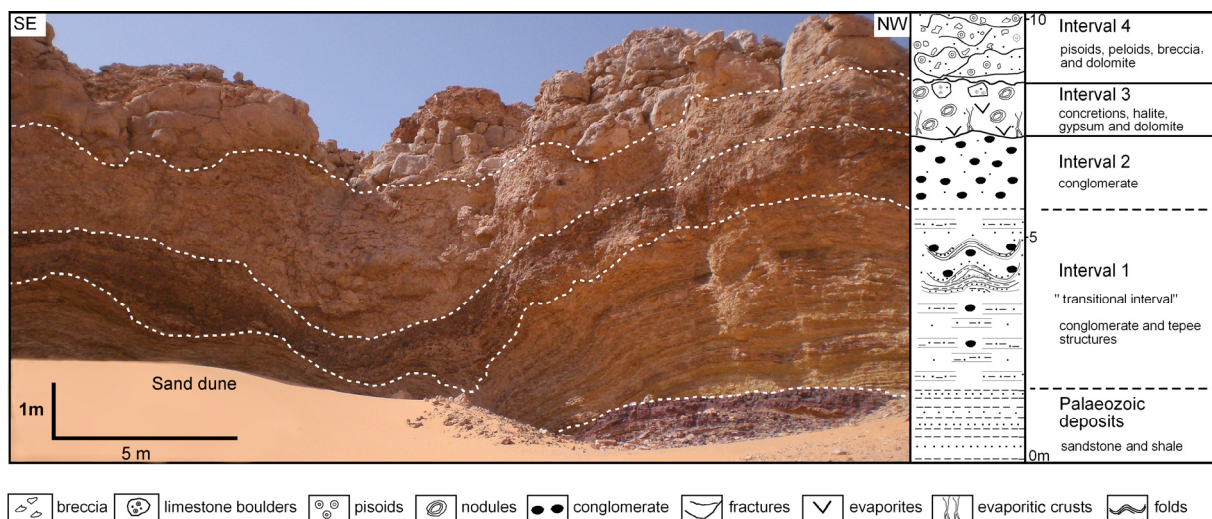


Figure 13. Outcrop photograph showing the Brak Mb. and the proposed subdivision into distinct intervals. Outcrop is located at 450 meter above sea level 40 km E of Brak, in Wadi ash Shati, 27° 38' 40" N, 14° 41' 10" E. See text for details

3.3.1 Transition between Palaeozoic siliciclastics / carbonates (Interval 1)

This transitional interval is up to 3 m thick, and locally wedges out. It consists of bedded or brecciated sandstone beds (Fig. 15 a and b). Interstices between sandstone beds and fractures in the beds are infilled by a light sandy limestone. The brecciated intervals are matrix-supported, and the matrix consists of sandy limestone. Locally, this transitional interval is folded. Folds are up to 1 m high and 2 m wide.

3.3.2 Conglomerate (Interval 2)

The conglomeratic interval is generally around 1-2 m thick (Fig. 15 c). It is matrix-supported and contains irregular subangular to rounded red and brown, 0.5 to 35 cm large clasts of Palaeozoic sandstones and mudstones floating in a sandy calcareous

matrix. The matrix of the conglomerate is a white to brown sandy limestone containing abundant peloids, pisoids, and micritic concretions. Pisoids range in size from 2 mm to 10 cm and accumulated around quartz grains, sandstone pebbles, or in some cases around micritic lithoclast grains (Fig. 15 d). Some of the sandstone clasts are fractured, and fractures are infilled by the sandy limestone matrix.

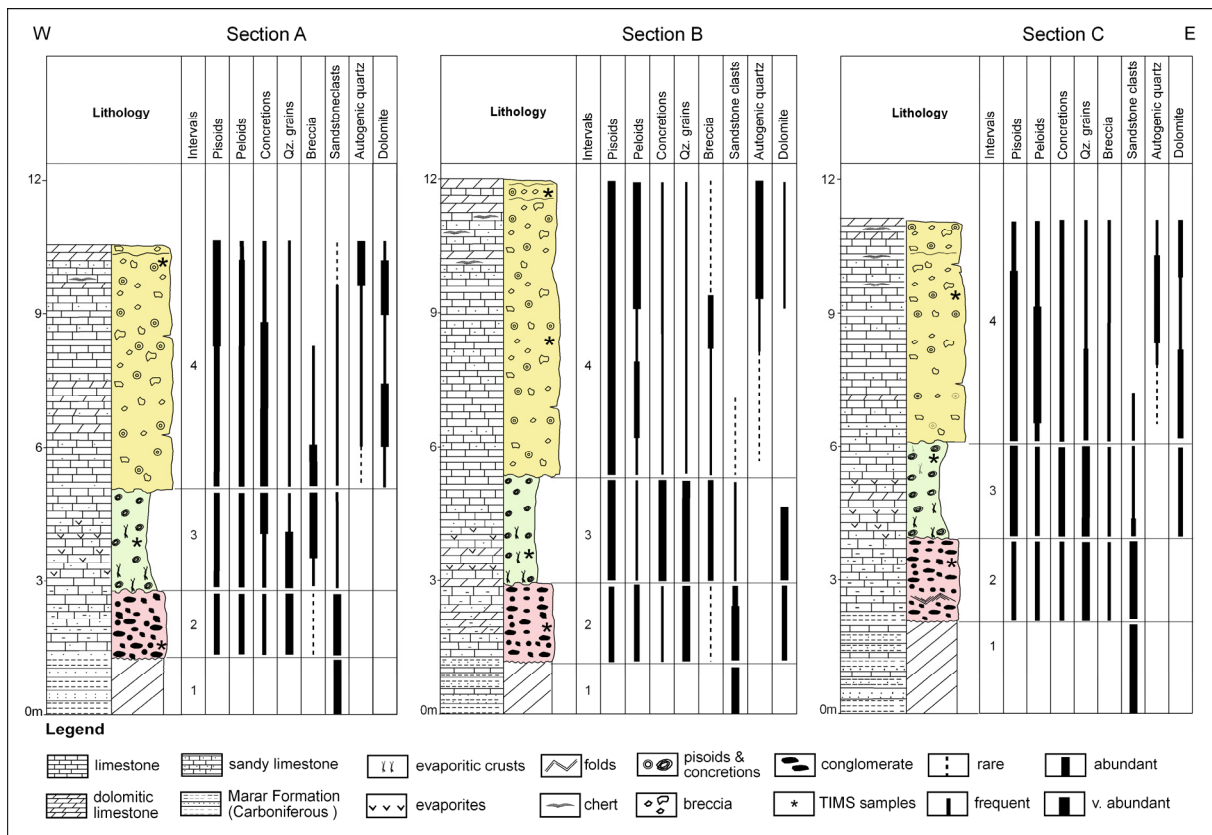


Figure 14. Sections A-C of the Brak Mb. (for localisation see Fig. 10). The lithostratigraphic subdivision into intervals 1 - 4 is shown, as well as the occurrence of major components in the Brak Mb. in Wadi ash Shati

3.3.3 Evaporite-carbonate interval (Interval 3)

The second interval of the Al Mahruqah Fm. passes upward through a wavy boundary into 2-5 m thick interval of evaporites together with a white to creamy nodular limestone with very minor Palaeozoic clasts (Fig. 16 a and b). The limestone of this third interval contains abundant to frequent peloid, pisoids, and quartz grains. The evaporites are halite, gypsum and dolomite. They occur as either isolated 15 cm large nodules or coalesced masses, with a white to cream colour. Nodules are

irregular to spherical in form. At section C, evaporites are cross-cut calcite strings, giving the rock a brecciated appearance (Fig. 16 b). Strings have a lateral extension of up to 1 m in the lower part of the interval, and decrease in size upsection. In some places, up to 50 cm large boulders of limestone and small clasts of sandstone occur as isolated components floating in the evaporites and carbonates (Fig. 16 c).

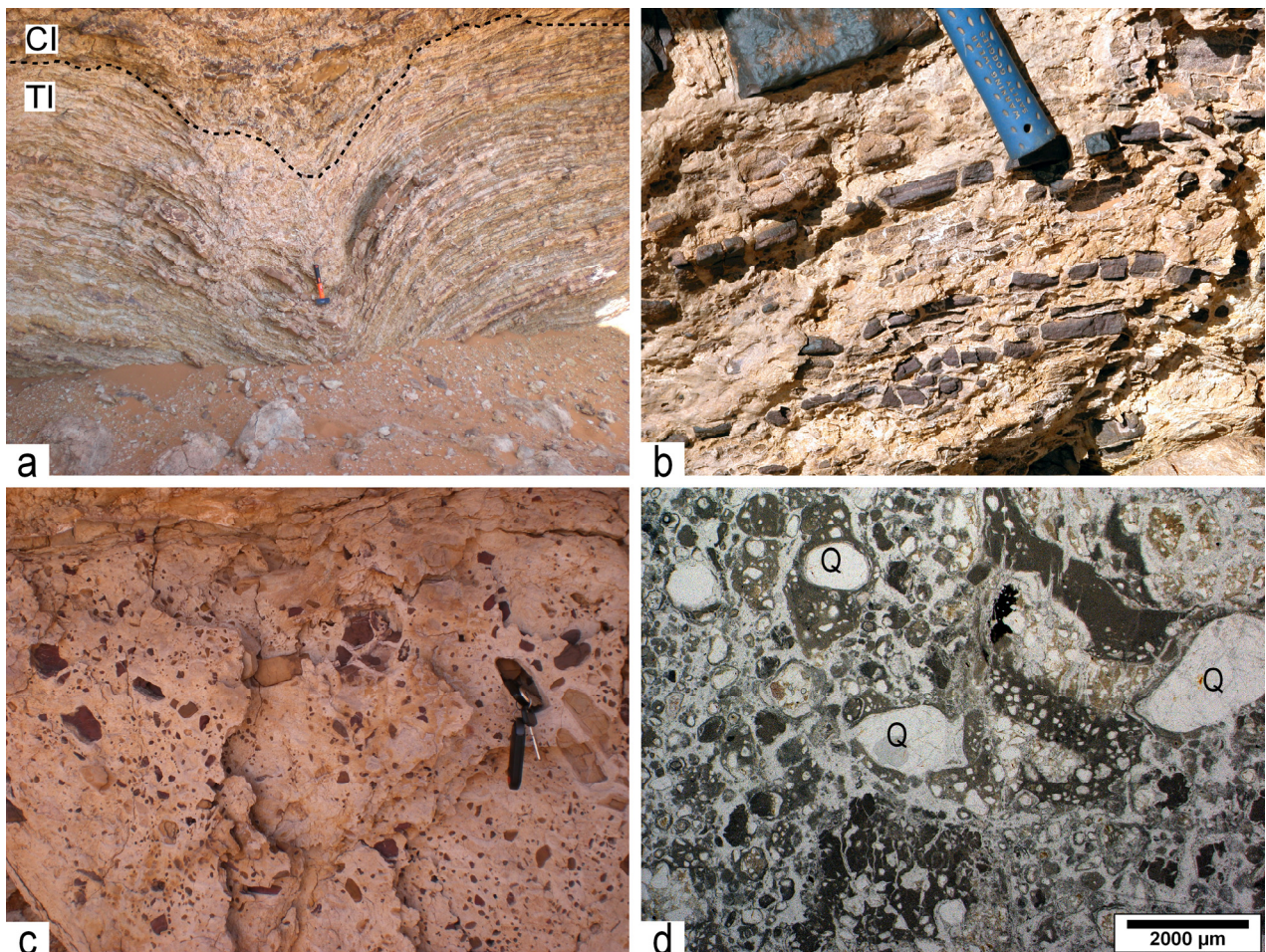


Figure 15. Characteristic features of the transitional and the second interval of the Brak Mb. **a:** Outcrop photograph showing the folded transitional interval (TI) and the conglomeratic interval (CI). Outcrop is located approximately 200 m W of section A. Hammer for scale; **b:** Close-up view of Fig. 15a showing the sandstone clasts in the carbonate matrix; **c:** Close-up view of 15a showing matrix-supported conglomerate of conglomeratic interval, **d:** photomicrograph of the conglomeratic interval showing abundant pisoid grains with quartz grains nuclei (Q). Section C, 3 m from base of section.

3.3.4 Massive limestone (Interval 4)

The upper interval of the Al Mahruqah Fm. is about 6 m thick at section B (Fig. 14), but decreases westward to about 5 m and less at section A. The contact of this interval with the underlying evaporite-carbonate unit is irregular, and at places forms 1-2 m wide and up to 1 m deep pockets.

In its lower part, Interval 4 consists of a massive, well-lithified whitish-grey microcrystalline limestone, changing upsection to a grey to white dolomitic brecciated and fractured limestone. Limestones are commonly fractured throughout Interval 4 (Fig. 16 a). Fractures have different shapes and size with elongated veinlets and joints running in all directions around large disintegrated limestone blocks (Fig. 17 a). In general, these fractures are empty. In some instances, they are filled by sparry calcite. The massive limestones part are characterised by patchy, discontinuous, up to 50 cm thick *in situ* brecciated horizons with abundant horizontal to subvertical fenestral structures. Allochems in the brecciated horizons show dark brown to reddish staining (Fig. 17 b). Brecciation appears to have occurred *in situ*, as indicated by the form fit of the breccia components (Fig. 17 b). Some of the carbonate breccia components have circumgranular cracks. Fenestrae show open porosity or are partially infilled by drusy blocky cements (Fig. 17 c).

In sections B and C (Fig. 14), abundant lenticular chert of diverse colours occurs in the upper part, but they are frequent to scarce in section A (Fig. 14).

The main components of this interval are pisoids, and peloid grains, as well as calcareous concretions. Individual pisoids have clastic grains as nucleus and vary from 0.5 to 10 mm and rarely attain 20 mm in size. Limestones of Interval 4 contain frequent fine to medium clastic quartz grains, which are poorly sorted and subangular to subrounded. The matrix around components is prevalently micritic, with streaks of microsparite to fine pseudosparite. In pores between the components, gravitational cements form the first cement generations. Gravitational cements are fibrous to bladed, and consist of distinct zones separated by thin veneers consisting of silt-sized carbonate grains (Fig. 17 d).

The remaining pore spaces are infilled with bladed and blocky cements (Fig. 17 d).

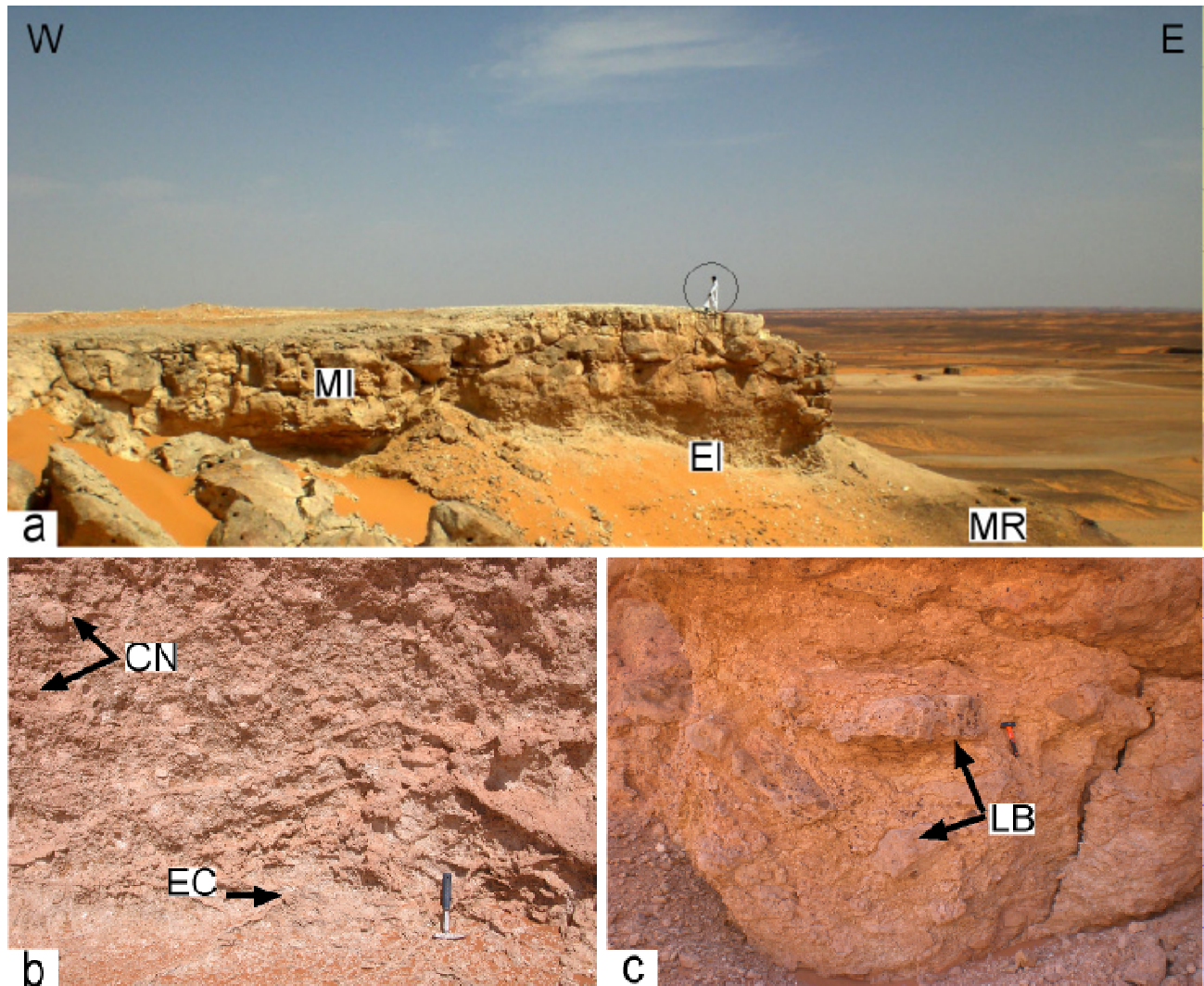


Figure 16. Outcrop views of the evaporite-carbonate interval and the massive limestone interval. **a:** Overview of the evaporite carbonate interval (EI) and the massive limestone interval (MI) resting on Carboniferous Marar Formation (MR). Outcrop is located approximately 20 m E from section A; **b:** Close-up view of lower part of Figure 16 a showing the abundant carbonate nodules (CN) and evaporite crusts (EC) of the evaporitic interval; **c:** Outcrop photograph of the evaporite carbonate interval showing isolated limestone boulders (LB) floating in the evaporites and carbonates. Outcrop is located approximately 70 m N of the section A.

3.3.5 Carbonate mineralogy

XRD analysis shows that the limestone of Al Mahruqah Fm. consists of low-Mg calcite, and that dolomite can make up to 20 % of the rock. Dolomitization is not linked to individual intervals.

3.3.6 $^{230}\text{Th}/\text{U}$ dating

The results of the sampled calcretes from the MH1 ranged from $364 \pm 12\text{ ka}$ to $398 \pm 60\text{ ka}$ (conglomerate components) and $334 \pm 10\text{ ka}$ to $349 \pm 14\text{ ka}$ (micritic matrix) indicating a Middle Pleistocene formation age of this carbonate. However, the comparison of the activity ratios from both analyses (Figs. 11 and 12) clearly demonstrates that a process occurred that shifted the uranium isotope activities. The ages of the primary carbonate phases (conglomerate components) plot nearby the line of radioactive equilibrium and are possibly underestimated. The determined age for the micritic matrix could probably be addressed to a process of re-crystallisation that influenced the isotopic composition of uranium and caused the fractionation of the isotopes.

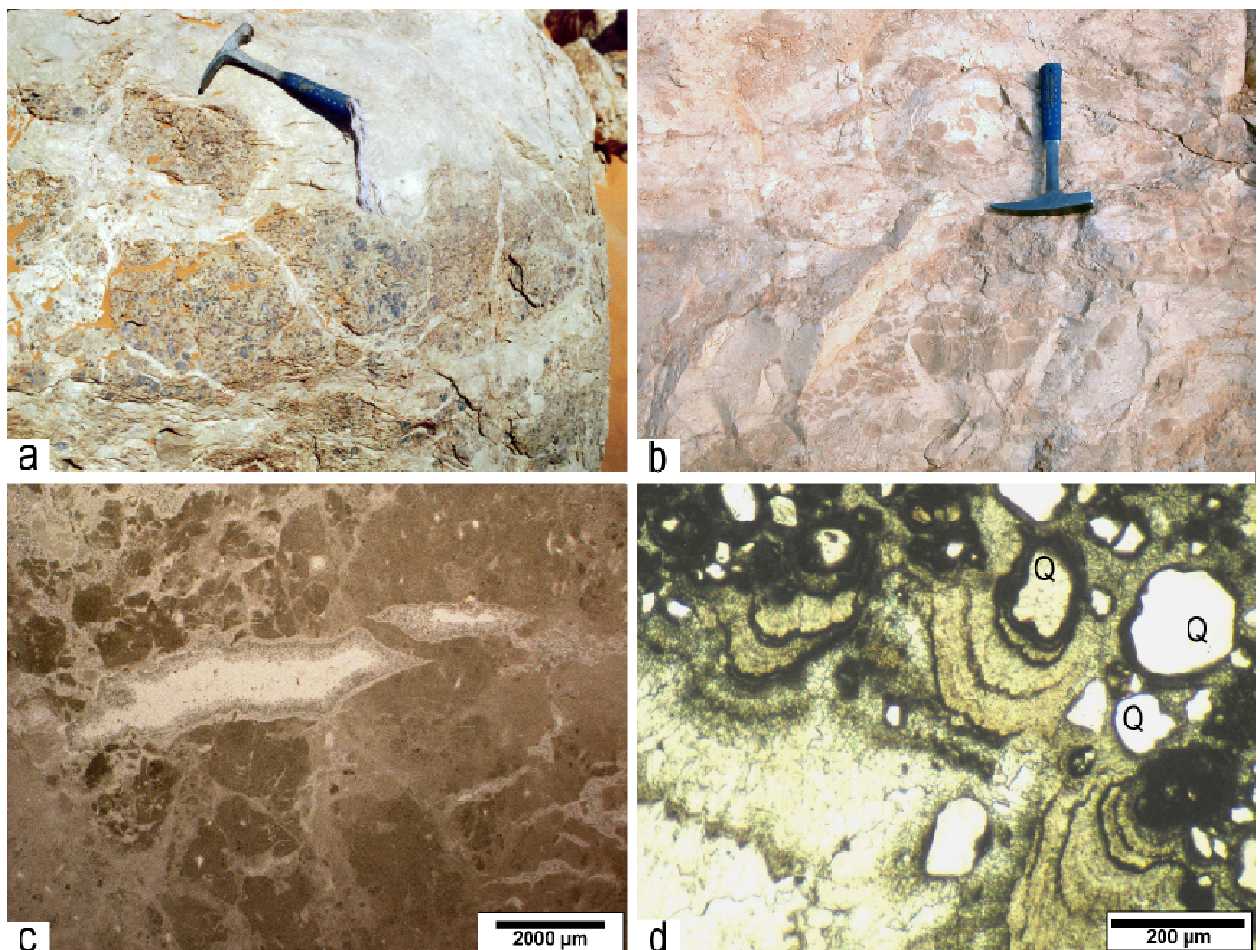


Figure 17. Upper interval of the Brak Mb. **a:** Outcrop photograph of the massive limestone interval showing curved fractures, black spots within the blocks are pisoid grains. Outcrop located approximately 100 m N of Section A; **b:** Outcrop photograph of the massive limestone interval showing well-developed brecciated textures 6 m above the base of Section B; **c:** Photomicrograph of the massive limestone interval showing fenestral structures (Section B, 8 m from base of section); **d:** Photomicrograph of the massive limestone interval showing pisoids grains with quartz grains nuclei (Q). Pisoids are lined by extensive gravitational cement (Section B, 10 m from base of section).

3.4 Interpretation

The analyzed carbonates from the Brak Mb. in the Al Mahruqah Fm. are interpreted as calcrete deposits. The irregular shape of the sandstone clasts in the transitional interval suggests that these clasts are the product of an *in-situ* weathering from the Carboniferous sandstones. Brecciation also appears to have occurred through displacive dislocation of sandstone beds (Figs. 15 b and 17 b), as a result of precipitation of carbonate between the sandstone beds and in fractures cross-cutting the sandstones. Such a displacive carbonate precipitation was reported by Arakel, (1986) and Wright and Tucker, (1991) from the capillary fringe of groundwater

calcretes in central Australia. The paleozoic siliciclastics of the Marar Fm. are dominated by claystones and contain salt and gypsum in the upper formations part (Pařízek et al., 1984; Seidl and Röhlich, 1984). The folds which occur in the lower and second interval (Fig. 15 a) are therefore interpreted to have resulted from the swelling of the clay minerals as well as evaporite dissolution and precipitation under a regime of alternating phases of wetting and drying.

The abundant calcareous and evaporite nodules which occur as a major component in the third interval are interpreted as calcareous soil glaebules (Fig. 16 b) (Braithwaite, 1983; Esteban and Klappa, 1983; Goudie, 1983; Knox, 1977; Wright and Tucker, 1991). Evaporites in the lower part of this interval are interpreted as a primary precipitate from super-saturated groundwater.

Macroscopic and microscopic characteristics from the upper massive limestone interval indicate that it was formed through complex pedogenetic processes, because pisoids, peloids and desiccation features are characteristic for pedogenic calcrete and are less common in groundwater calcrete deposits (Wright and Tucker, 1991). Brecciation and occurrence of circumgranular cracks are further representative for caliche hardpans, which form the topmost horizon of a calcrete profile (Esteban and Klappa, 1983). The occurrence of gravitational cements in vugs of the massive limestone interval is a further indicator for the subaerial formation of the Al Mahruqah limestones. It is proposed that there was a gradual shift from wet to dry conditions during the deposition of the Brak Mb. controlling the vertical facies variations of the calcrete sequence, because the lower part of the formation is dominated by groundwater calcrete whereas in the upper part pedogenic calcrete is prevailed.

Occurrence of cherts in the upper interval of the Brak Mb. is interpreted as silcrete formation. In general the development of silcretes involves the precipitation and/or crystallisation of silica, probably over long periods of comparative landscape stability during which only slow geomorphological and chemical changes took place (Twidale and Hutton, 1985). The origin and presence of the silica in calcretes is attributed to number of sources such as fluctuating ground-water tables, kaolinitization of feldspars and serpentization and proximity to basalt. In addition to upward-moving

silica-rich solutions, possible mixing with downward-percolating alkaline water is a trigger for silcrete growth (Watts, 1980).

3.5 Discussion and conclusion

This study provides new data and interpretations concerning the origin, depositional environment and age of the Al Mahruqah Fm. and the geological history of Murzuq basin. In earlier studies, the Al Mahruqah Formation was interpreted as marine limestone (Desio, 1936; Hecht et al., 1963; Goudarzi, 1970; Klitzsch, 1974; Panerjee, 1980), or as a chemical and biochemical lacustrine sediment (Pangi, 1938; Bellair, 1944, 1947, 1953; Lelubre, 1946 a; Petit-Maire et al., 1980; Gaven, 1982; Seidl and Röhlich, 1984; Thiedig et al., 2000; Thiedig and Geyh, 2004; Geyh and Thiedig, 2008).

Based on the herein presented data and the resulting interpretation, a lacustrine or marine origin of the Brak Mb. of the Al Mahruqah Fm. limestone, however, is excluded because of the lack of independent geological or palaeontological evidence to support such an interpretation. Although Seidl and Röhlich (1984) described the occurrence of limnic gastropods in Al Mahruqah limestones from the Wadi al Shati, this observation cannot be corroborated, despite the analysis of 150 samples in thin section.

It is proposed that the all the features recognized in the Brak Mb. display unequivocal evidence that the limestones are calcrete deposits. Arakel (1986) described groundwater calcrete and dolocrete deposits in Australian very similar to Al Mahruqah Formation. In analogy to such groundwater carbonates (Wright and Tucker, 1991), the Brak Mb. of the Al Mahruqah Fm. does not exhibit a mature pedogenic calcrete profile, but is nodular, brecciated or massive throughout. Groundwater calcrete deposits are commonly kilometres wide (maximum of 10 km), tens of kilometres long (maximum of about 100 km) and have an average thickness of about 10 m (Mann and Horwitz, 1979; Arakel and Mc Conchie, 1982; Carlisle, 1983).

The new findings presented here have consequence for former interpretations of the Neogene paleohydrological evolution of the Murzuq Basin. After the first description of lacustrine limestones in the Murzuq Basin by Seidl and Röhlich (1984), the concept of a Megalake Fezzan was later introduced based on the interpretation of the Brak Mb. limestones of the Wadi al Shati as lacustrine limestones. The Brak limestones were taken as 380 - 420 ka old evidence of significant lake sedimentation in the Murzuq Basin during the Pleistocene, covering about up to 52.000 km² during its maximum extension, and forming during a middle Pleistocene humid period (Thiedig et al., 2000; Thiedig and Geyh, 2004; Geyh and Thiedig, 2008; Armitage et al., 2007; Drake et al., 2008).

The interpretation of the Brak Mb. limestone as a calcrete not only challenges the postulated occurrence of a megalake, but the new age datings also question the age assignment of the Brak limestones as middle Pleistocene. Accurate ²³⁰Th/U ages can only be obtained, if the carbonates did not experience migration of Uranium and Thorium and so formed a closed system since formation, as described in detail by Sierralta et al. (in press). Geyh and Thiedig (2008) summarised the available data concerning the Brak Member. Twelve of fourteen samples yielded ²³⁰Th/U dates between 380 ka and 290 ka, two samples yielded ²³⁰Th/U ages of 257 ka and 243 ka. In the latter study, clasts of older limestone were reported indicating that some of the ²³⁰Th/U ages could be erroneously high. In this study, we determined similar formation ages for the Brak Member limestones, which is in disagreement of the geological estimates of this study.

In principle it is unexpected that uranium-series ages result in discrepancies of such an order of magnitude. There are two explanations likely for the disagreement. One is that the ²³⁰Th/U ages are correct and thus the geological estimates significantly overestimate the true formation age of the Brak Member limestone. The samples passed all quality criteria, such as the correction for the admixed detrital ²³⁰Th and the Osmond Ivanovich diagram indicating a closed system. The other is that the ²³⁰Th/U dating significantly underestimates for the formation age of the calcretes and thus is unsuitable for providing reliable ages for the calcretes under study owing to diagenetic alteration of the calcretes, as shown in thin slices of this study. One criteria for an open system could be the large scatter of the isotope data. In contrast,

lake carbonates should have a homogenous isotope distribution and undergo no or minor carbonate recrystallisation.

Following this, it is not possible to draw a final conclusion on the chronological framework and stratigraphy of the Brak Member calcrites based on $^{230}\text{Th}/\text{U}$ age dating. It is proposed that the Brak Mb. is much older than forwarded by Thiedig et al. (2000). If one accepts the calcrete model as valid, then the limestones formed as a laterally extensive rock body, before incision of the Wadi ash Shati valley. This valley formed through erosion of the Nashu palaeoriver, which flew out from the Murzuq Basin into the Mediterranean Sea (Drake et al., 2008). The river course was interrupted between 24.9 - 8.0 Ma, when it was blocked through formation of volcanic edifices. The herein presented data do not allow for a further age assignment, but the limestones may be as old as upper Cretaceous, as already proposed by Klitzsch (1974).

4

BI'R AZ ZALLAF MEMBER

ABSTRACT

A mixed carbonate/siliciclastic sequence occurs in the center of the Wadi Zallaf depression, which comprises a complex alternation of green, weakly consolidated sands together with thin laminated carbonate beds. Sands are weakly cemented and some intervals are rich in halite and sylvine, with minor quantities of gypsum. Locally, the deposits are bioturbated by vertical and sub horizontal burrows, which are mostly lined by carbonate. Sediments are interpreted as alluvial and aeolian in origin. Carbonates are thin-bedded dolomitic limestones and dolomites, with intercalations of thin green salty sandstones laminae. Rare to frequent fossils such as ostracodes, pelecypods, gastropods, and charophyte debris occur in these carbonate sediments. Carbonates are interpreted as lacustrine in origin, having formed in shallow saline playa lakes. Four intervals of lacustrine limestones stages, separated by siliciclastics and evaporites were defined, two different facies are distinguished, which can be assigned to shallow lakes environments. Alternation of siliciclastics and carbonates is thought to reflect climatic variations. Arid to semi-arid times are characterized by the siliciclastics and evaporites, more humid stages allowed the development of shallow carbonate-rich playa lakes. It is proposed that the sands and carbonates, which were previously attributed to the Pleistocene, are older.

4.1 Introduction

The Bi'r az Zallaf Member consists of green, weakly consolidated sands together with thin laminated carbonate beds, which form distinctive pale grey marker beds in the weakly cemented green sand layers. The deposits of the Bi'r az Zallaf Mb. occur stuck between the recent sand dunes, and crop out in a series of laterally discontinuous exposures in W-E direction extending over 50 km along the southern margin of the Wadi az zallaf depression (Fig. 18).

The Bi'r az Zallaf Mb. unconformably overlies the carboniferous Marar Formation (Seidl and Röhlich, 1984). The name of the member is derived from the Wadi azZallaf area, where the Bi'r az Zallaf Mb. is typically developed and reaches its maximum thickness of about 25 m (Thiedig et al., 2000). Bi'r az Zallaf Mb. has been recorded at heights varying from 350 m in the east up to 410 m above sea level in the west (Thiedig. et al., 2000). Bi'r az Zallaf deposits were mapped and classified as Miocene lacustrine deposits by Collomb (1962). Conant and Goudarzi (1964) and Seidl and Röhlich (1984) defined them as Tertiary- to Quaternary continental rocks.

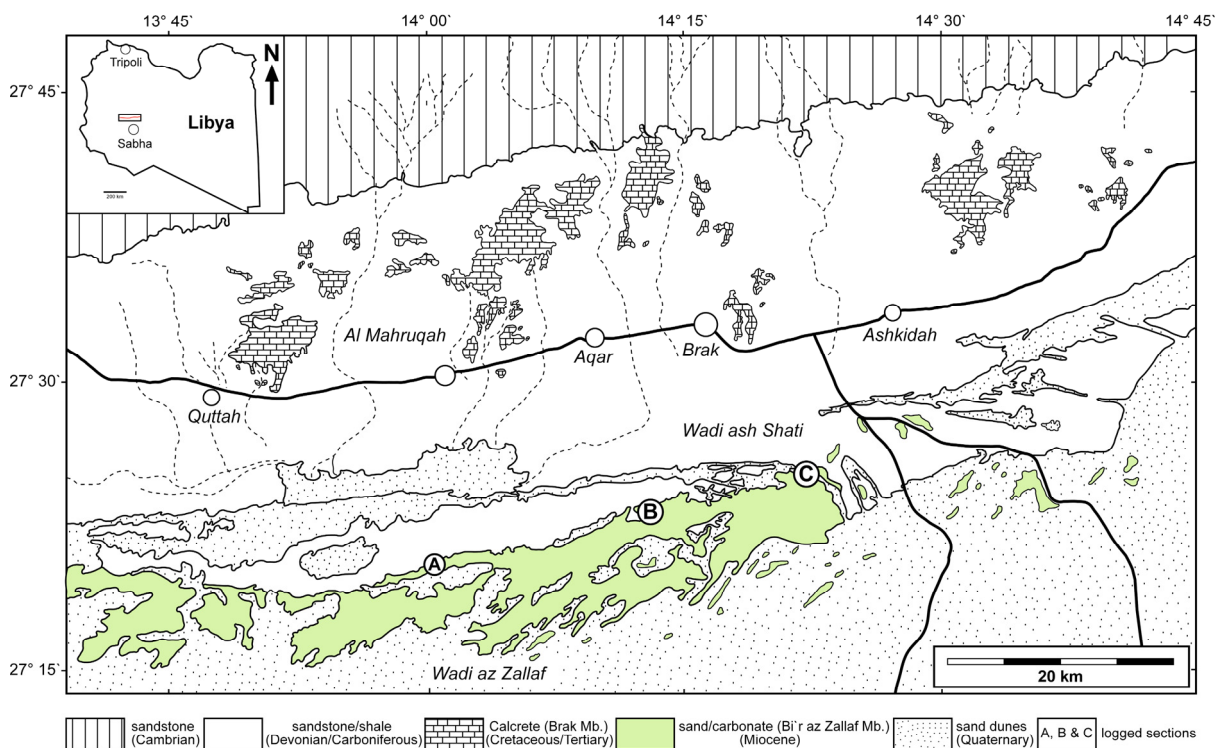


Figure 18. Geological map of study area showing the distribution of Bi'r az Zallaf Member, indicating the location of measured Sections (A, B and C) and the position of the localities discussed in the text. Section A: 27° 21' 14" N, 014° 01' 28" E, Section B: 27° 23' 07" N, 014° 13' 23" E and Section C: 27° 25' 27" N, 014° 23' 13" E. Simplified after Seidl and Röhlich, (1984).

Recently, these deposits were interpreted as fresh water sediments Thiedig et al. (2000) and taken as evidence for a large fresh water lake which was termed "Megalake Fezzan" (Thiedig et al., 2000; Drake et al., 2008; Armitage et al., 2007). The maximum size of the lake attained before outflow over the catchments rim is postulated to cover $130,000 \pm 7000 \text{ km}^2$ (Thiedig el al., 2000; Thiedig and Geyh, 2004; Geyh and Thiedig 2008; Drake et al., 2008; Armitage et al., 2007).

Using $^{230}\text{Th}/\text{U}$ dating, Thiedig et al. (2000), Thiedig and Geyh, (2004), and Geyh and Thiedig, (2008), assigned the Bi'r az Zallaf Mb. an age of 240 and 350 ka. Armitage et al. (2007) applied OSL methods on the three sand intervals at Section C (Fig. 18). The upper sand bed in the section yielded $420 \pm 2.4 \text{ ka}$, while the lowers sand layers were beyond the range of the method (Armitage et al., 2007).

The principal objective of this part of study is the characterisation of the sedimentary facies developed in these mixed deposits, with particular emphasis on the thinly bedded carbonate beds in order to clarify their components, structure, sedimentary facies and origin. In order to achieve these, several outcrops in the Wadi az Zallaf area were analysed. It will be demonstrated that weakly consolidated sands together with thin laminated carbonate beds of Bi'r az Zallaf Mb., previously interpreted as lacustrine deposits of the "Megalake Fezzan" (Thiedig el al. 2000; Thiedig and Geyh, 2004, Geyh and Thiedig 2008; Drake et al., 2008; Armitage et al., 2007), were in fact deposited in smaller shallower ephemeral playa lakes. This is indicated by the occurrence of textures, facies and components which are characteristic for playa lake deposits.

4.2 Geological setting

The Wadi az Zallaf is an about 80 km long and 10 to 12 km wide endorheic depression. The depression extends in E-W direction parallel to Wadi ash Shati on the northern margin of Murzuq Basin, between lat. 27° 15' N and long. 13° 00' E and lat. 27° 25' N, long. 14° 30' E (Fig. 18).

Field studies and photogeological mapping show that the northern margin of Wadi az Zallaf forms a stepped and curvy high escarpment. To the south the depression is bordered by high Quaternary sand dunes (Fig. 18). The basement of Wadi az Zallaf consists of the Palaeozoic rocks with a rugged and irregular relief (Seidl and Röhlich, 1984). Devonian and Carboniferous rocks occur at the western margin of the Wadi depression and they formed small isolated hills. High Quaternary sand dunes are intermittently distributed in the middle part of the Wadi depression, whereas they occupied southern margin of the depression. Throughout the Wadi azZallaf area there are numerous exposures of several thin bedded carbonate beds underlain by yellowish-green sands and poorly lithified sandstone. The carbonate deposits are subdivided into several intervals. These are packages of well-lithified beds, separated from each other by weakly cemented sands (Fig. 19). These deposits extent from east to west along Wadi az Zallaf and cover an area of about 5400 km² (Thiedig et al., 2000). The top of the Bi'r az Zallaf Mb. is located at an elevation of around 350-410 m above sea level (Geyh and Thiedig, 2008).

The first formal stratigraphic scheme and classification of Bi'r az Zallaf mixed carbonate-siliciclastic sequence was presented by Collomb (1962), who interpreted the sequence as lacustrine deposits of Miocene age, whereas Conant and Goudarzi (1964); Seidl and Rhölich (1984) classified it as lacustrine sediments of Tertiary-Quaternary age. Thiedig et al. (2000); Thiedig and Geyh (2004); Geyh and Thiedig (2008) interpreted the Bi'r az Zallaf Mb. deposits as Middle Pleistocene fresh water lacustrine sediments, which were formed in the large regional Megalake Fezzan (Thiedig et al., 2000; Thiedig and Geyh, 2004; Geyh and Thiedig, 2008; Drake et al., 2008; Armitage et al., 2007; White et al., 2006). The maximum thickness of the Bi'r az Zallaf Mb. is about 25 m in the eastern part of Wadi az Zallaf depression, decreasing westwards to about 18 m and less.



Figure 19. Field photo showing general view of Bi'r az Zallaf Mb. Outcrop location, 15 km south of Al Mahrouqah village in Wadi ash Shati, 27° 21' 14" N, 14° 01' 28" E.

4.3 Methods

Three detailed sections were logged sampled (Fig. 18). Thin sections and polished slabs were made from 100 oriented samples. Carbonate lithofacies were defined petrographically using texture, fabric and mineralogy. X-ray diffraction (XRD) analyses were used in order to determine the carbonate mineralogy. For the X-ray analysis, a Philips Diffractometer PW 1830/00 X-ray generator was used by the powder and orientated aggregate method. 25 samples from four carbonate intervals at section C (Fig. 20) were powdered and analyzed by XRD to discriminate the main carbonate mineralogy of these carbonate deposits. Three sand samples were taken by using metal pipes (25 cm long and 3.5 cm in diameter) from three sand intervals from section C Fig. 20 (2, 3 and 4) and were analyzed by optically stimulated luminescence (OSL) to determine the age of the sand beds.

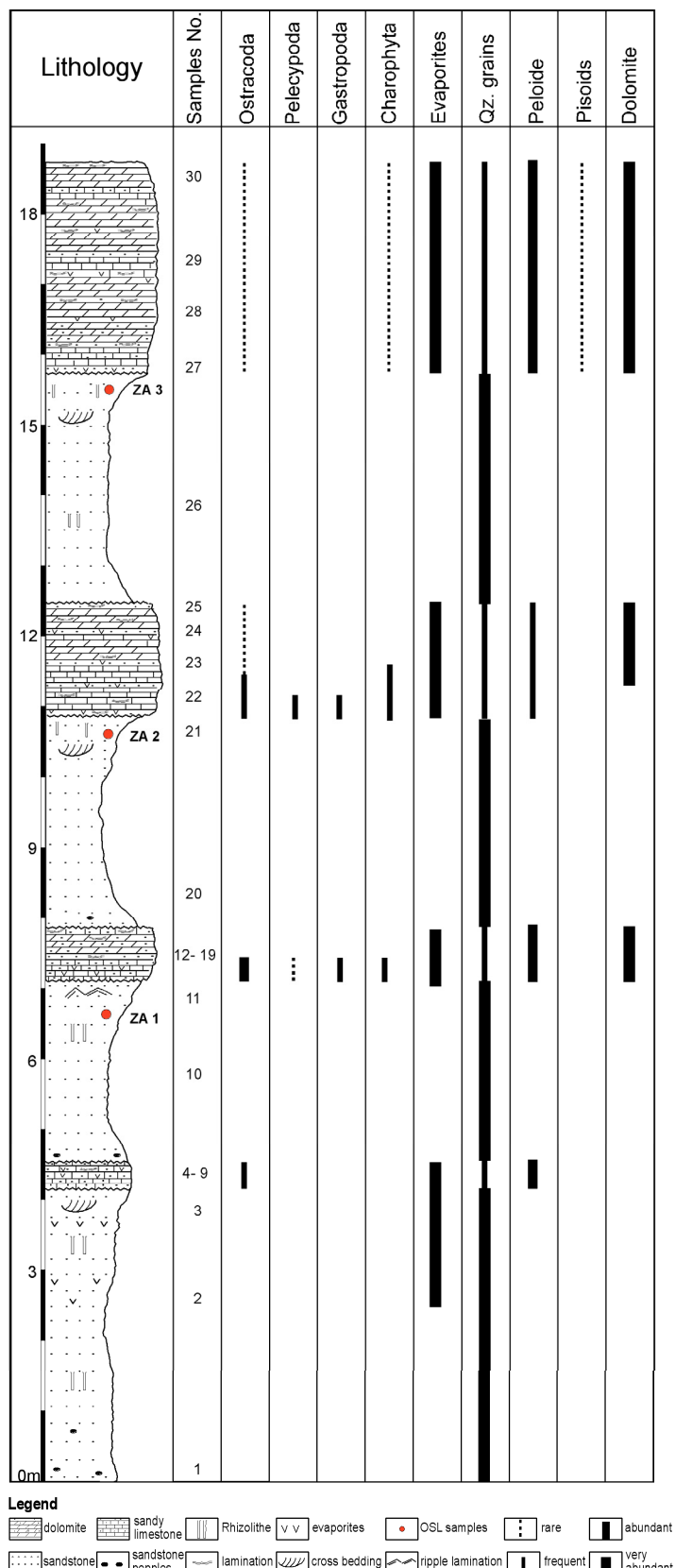


Figure 20. Measured sedimentary log of the mixed sequence of Bi'r az Zallaf Member (Section C, Fig. 18) in the eastern side of Wadi az Zallaf depression. Outcrop location, 27° 25' 27" N, 014° 23' 13" E.

4.4 Results

4.4.1 Lithology and Sedimentary facies

Detailed graphic logs of the measured sections A, B and C in Wadi az Zallaf area are provided in Fig. 20, and 30. Section C (Fig. 20) shows the lithology and vertical distribution of different key components in the succession presented bed by bed.

4.4.1.1 Sand facies

Occurrence

In the analyzed section C sand facies forms four intervals (Fig. 20). The lower interval lies between the base of the section and 4.15 m. The second interval extends from 4.50 to 7.10 m. The base of the third interval appears at 7.80 m and terminates at 11 m. The fourth interval is between 12.30 to 15.70 m.

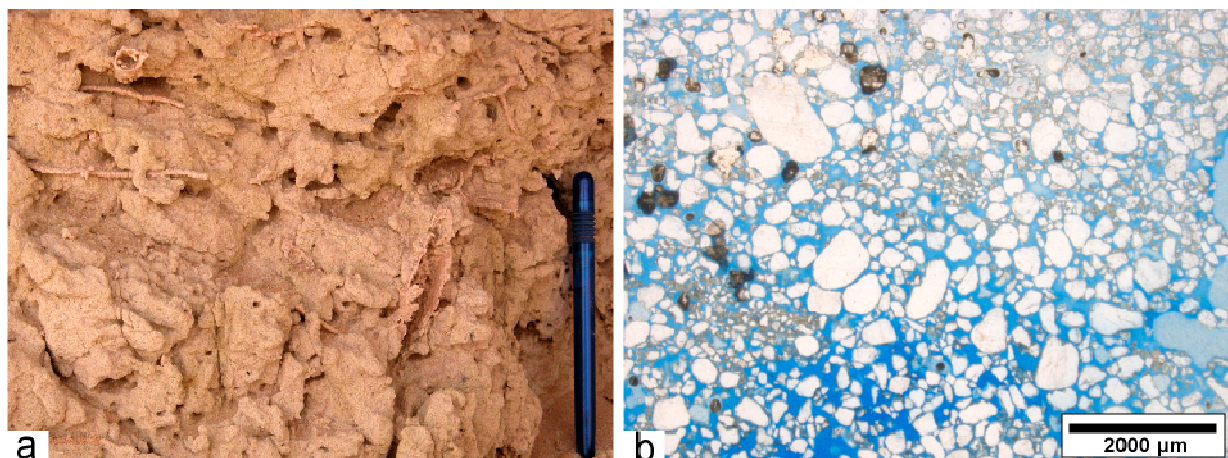


Figure. 21. a: Field photo showing abundant bioturbation of different form and size of rootlets in sand facies in lower sand interval at Section C; **b:** Thin section photo of the lower sand facies (2 m from the base of the Section C). Note the poorly sorted sand grains and high porosity in this facies.

Description

At section C, sands make up about 12 m of the Bi'r az Zallaf Mb., a value which increases westward to about 18 m at Section A (Fig. 30). The contact of the sands with the overlying thin bedded carbonates is an undulating surface. Sands are varicoloured reddish-yellow and grey to light green argillaceous and weakly

cemented (Fig. 19 a). The sand grains are poorly sorted, subangular to rounded, and are medium to fine-grained in size (Fig. 21 b).

At all investigated Sections A, B and C (Fig. 20 and Fig. 30), the lower intervals of this facies contain frequent red to black sandstone pebbles (size 0,5-3 cm □) as well as fragments of whitish sandy limestones. Sedimentation continued upwards with yellowish-green to white argillaceous sands and salty sands. At section C (Fig. 20), the size of sand grains becomes finer with a significant increase in the proportion of silt and clay upsection. Frequent calcareous concretions and abundant thin intercalations of evaporites (halite, gypsum and dolomite) commonly occur in the sands. In thin sections, sand grains are mostly none supported by any matrix, but in some cases calcareous, argillaceous and ferruginous matrix has been observed. In general, sand grains are non to weakly cemented by halite cement and rarely by calcareous cement (Fig. 21 b).



Figure 22. Field photo showing the lower sand interval, at Section A. Note the mega ripple structures below the contact between sand bed and the carbonate.

Sedimentary structures of this facies are represented by poorly developed planar cross bedding. Cross beds are mostly planar and up to 10 cm large, locally trough cross-bedding structures were observed. Megaripple lamination occurs sporadically in the lower sand interval at Section A (Fig. 22).

The sands are devoid of fossils, with exception of extensive bioturbation characterized by vertical and subhorizontal burrows, which have different shape and size (Fig. 21 a). The diameter of the burrows ranges from 0.5 to 3 cm. Mostly they are lined by carbonate.

4.4.1.2 Carbonate facies

Four intervals of thin-bedded carbonates have a cumulative thickness of about 6 m at section C (Fig. 20) and consist mainly of white to creamy thinly bedded dolomites and sandy limestones. Carbonate packages are separated by weakly cemented light green sand beds.

The lower interval occurs between 4.15 and 4.45 m of the section, the second occurs between 7.2 and 7.8 m. Both intervals are restricted to section C (Fig. 20). The third interval is between 11 and 12.5 m, and the uppermost interval (4) is between 15.8 m and the top of the logged section. The upper two carbonate intervals (3 and 4) are well exposed in sections B and C (Fig. 30) and traceable over long distances along the eastern margin of the Wadi az Zallaf.

4.4.1.2.1 Lower carbonate Interval

The lower (first) carbonate interval consists of thin bedded white sandy-dolomitic limestone beds intercalated with green salty sands (Fig. 23 and Fig. 24). The contact between the carbonates and weakly cemented sands is transitional and occurs as wavy surface (Fig 24). At Section C (Fig. 20) the lower carbonate interval occurs as centimeter-scale alternations of dense white carbonate layers and green salty sandstones. The total thickness of this interval is about 30 cm.



Figure 23. Field photo showing the thin bedded lower carbonate interval of Bi'r az Zallaf Member. Section C, sample 5, metre 4.2. Outcrop location 18 km to the south of Brak village in Wadi ash Shati, $27^{\circ} 25' 27''$ N, $014^{\circ} 23' 13''$ E.

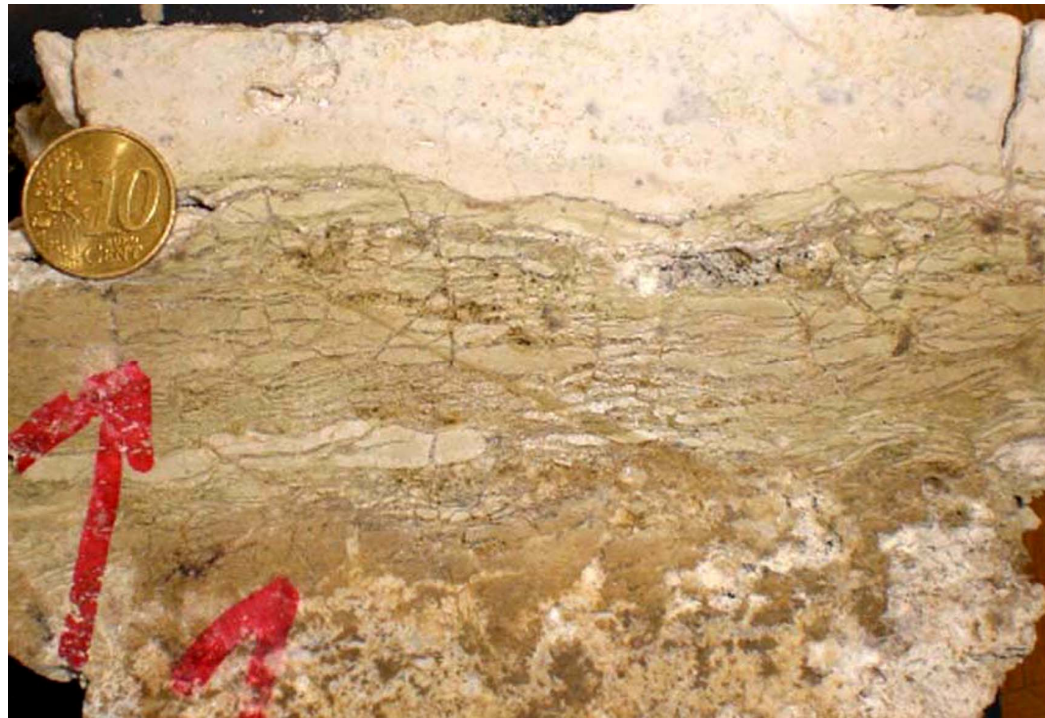


Figure 24. Polished slab showing a close view of the thin bedded lower carbonate interval, which is provided in Fig. 23. Note the wavy and fractured contact between carbonate and sand layers and the high concentration of evaporites in the lowermost part of the photograph. Diameter of the coin is 15 mm.

Individual carbonate layers are well-lithified, white to creamy in colour. Their thickness decrease laterally and ranges between 2-3 cm (Fig. 24). Carbonates are fractured to brecciated and have irregular surfaces (Fig. 24). Sands are light green weakly cemented, between 3 and 5 cm thick, and contain high amounts of evaporites.

Carbonates contain abundant peloids and fine quartz grains. Other components are rare bioclasts, which are represented mainly by poorly preserved fragments of ostracods debris. The components in carbonate beds are embedded in a matrix consisting of clotted micrite and dolomite. The matrix is recrystallized to various degrees. Poorly developed cement occurs in this facies locally with stripes and streaks of pseudosparite. In general, the lower carbonate interval exhibits poorly developed lamination, comparing with the other carbonate intervals

4.4.1.2.2 Middle (second) carbonate Interval

The second carbonate interval consists of white-creamy sandy dolomitic limestone with a maximum thickness of 60 cm (Section C, Fig. 20). It is characterised by a well-cemented massive lower part, which contains high concentration of salt and displays wavy to irregular structures. The upper part of this interval changes abruptly upward from massive to thin bedded to fine laminated intercalations of sandy dolomitic limestones, which are interbedded with thin light green coloured salty sandstones. In the upper part of this interval the individual wavy to irregular carbonate laminae, which are brecciated, range from 1 mm to 2 cm in thickness, whereas weakly cemented sand laminae are 1-5 mm thick.

This second carbonate interval is characterised by high dolomite and sand content. The main components are abundant fine to medium quartz grains and frequent to abundant peloids. Frequent quartz grains are well sorted and subangular to subrounded in shape. Other components are represented by rare to frequent poorly preserved bioclast fragments of ostracodes, and pelecypod debris. Bioclast debris occurs sporadically distributed in the matrix between sand and peloids. The matrix around the components is micrite and occurs in various degrees of recrystallization. The interstitial pores are mostly open or rarely filled with partly recrystallized micrite or with minor rims of blocky calcite cements around the bioclasts. Poorly developed

ripple lamination, brecciation, vertical fractures, lenticular structures and pseudo-convolute bedding were observed in this carbonate interval.

4.4.1.2.3 Upper (third) carbonate Interval

The third carbonate interval is about 1.7 m thick at section C (Fig. 20) and 1.5 m thick at section B (Fig. 30). It is missing in section A (Fig. 30). The base of this interval rests directly on the top of the bioturbated green sands of the third sand interval with an erosive irregular lower surface (Fig. 20). The lower part of this carbonate interval begins with 20 cm thick massive white carbonate bed. In section B and C it passes upward gradually to form thin bedded to fine laminated white-creamy carbonate laminae, which are intercalating with thin green salty and sandy laminae. In the upper part, the carbonate content increases while the sand intercalations decrease in thickness. Laminated evaporites occur at the top of the interval.

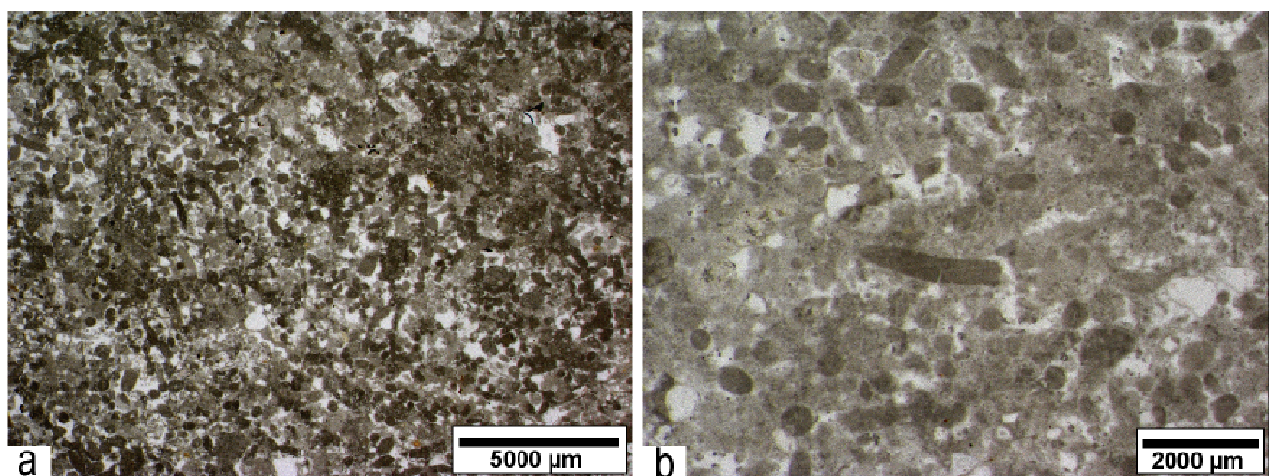


Figure 25. a: Thin section showing the abundant peloid grains in thin bedded carbonate facies (Section C, sample 24, meter 12; **b:** Thin section of the same facies shows the splitting of peloid grains in the middle part of the photograph (Section C, sample 24, meter 12).

The main components of this interval are frequent to abundant fine to medium quartz grains and peloids of by smooth-surface, ovoid, spherical and ellipsoidal form (Fig. 25 a and b). Their size ranges from 0.5 to 2 mm. Individual peloids are black, structureless and occur as either isolated or have point contact with each other. In some thin sections, the ellipsoidal peloids commonly split into two or three small pieces by micro vertical cracks (Fig. 25 b). Peloids of this interval are partly to entirely

recrystallized to very fine dolomite, which fill the spaces between the components as a fine matrix (Fig. 25 b). Quartz grains are abundant in the lower part of this interval, and they occur commonly distributed between the peloid grains. Some of quartz grains are partially surrounded by poorly developed micrite rims (Fig. 25 b). In addition to the peloids and quartz grains, this interval contains frequent biogenic components, which mostly occur in the lower part of the interval. Biogenic components represented by frequent fragmented ostracodes, gastropods, charophytes debris (Fig. 29 b), with low to moderate degree of fragmentation (Fig. 29 b). The matrix around the components is prevalently micritic to fine dolomite with a clotty recrystallized texture. In places, stripes and streaks of sparite and pseudosparite cements occur filling some voids or fractures between the components. The remaining spaces between the components are filled with blocky cements. This interval is characterised by presence of abundant fine wavy to laminated structures (Fig. 28 a), interpreted as cyanobacterial lamination. Abundant vertical microfractures and elongated fenstral structures were observed parallel to the bedding surface in this interval. In some instances, they are filled by sparry calcite cements.

4.4.1.2.4 Uppermost (fourth) carbonate Interval

This interval is about 3 m thick at section C (Fig. 20). It decreases in thickness to 2.5 m at section B (Fig. 30) and is also entirely missing at section A (Fig. 30). In the measured, this interval represents the top of Bi'r az Zallaf Mb. in both sections (B and C). The base of this interval is erosive and occurs as wavy surface above the underneath sand bed (Fig. 26). The uppermost carbonate interval is characterized by a uniform appearance from the base to the top in comparison with former mentioned intervals (Fig. 26). The carbonates are creamy to white in colour and thin bedded to finely laminated. The laminae are regular and slightly undulated. They are centimetres to millimetres-thick and are interpreted as cyanobacterial mat deposits (Fig. 26). Laminae consist of intercalation of couplets of carbonate and thin evaporite layers (Fig. 26). Carbonate laminae have a white-creamy colour and consist of fine crystallised dolomite. Their thickness is about 0.5 to 1cm. They have a fractured to brecciated texture and display wavy to irregular structures. Carbonate laminae are separated from one another by fine light green to colourless evaporite laminae.



Figure 26. Field photo showing the thin bedded uppermost carbonate interval of the Bi'r az Zallaf Mb. deposits. Section C, outcrop location, 18 km south of Brak village in Wadi ash Shati, $27^{\circ} 25' 27''$ N, $014^{\circ} 23' 13''$ E.

Evaporite laminae are 1-5 mm thick and consist of abundant clay, silt and fine sand grains with abundant halite and gypsum crystals. Evaporite laminae display curved to wavy irregular bedding and small diapir-like structures (Fig. 26). Abundant elongated fenestrae occur parallel to the bedding surfaces. In thin sections, the dominant components in this interval are microcrystalline anhedral dolomite crystals and recrystallised peloid grains. The small dolomite crystals display a mosaic texture and have an unimodal size distribution (Fig. 29 a). Other components are represented by frequent to abundant small quartz grains and rare to frequent micritic nodules. Biogenic components are very scarce and partly to entirely recrystallized. Among the recrystallised bioclast fragments, ostracodes are the only skeletal components which can be identified in this carbonate interval. The matrix is cryptocrystalline dolomicrite to dolomite. Ripple mark lamination and lenticular bedding are common structures within this interval (Figs. 26 and 27). Abundant vertical cracks and fenestral voids were observed parallel to stratification (Figs. 27 and 28 b). Pseudo-microcarst cavities, rootlet and algal mat wavy structures occur commonly in this interval.



Figure 27. Polished slab showing the irregular bedding in the uppermost carbonate interval of Bi'r az Zallaf Mb. Section C. Sample 30, meter 18. 5. Outcrop location, 18 km to the south of Brak village in Wadi ash Shati, $27^{\circ} 25' 27''$ N, $014^{\circ} 23' 13''$ E. The scale bar divisions are in centimeters.

4.4.3 Fossil content

Fossils in the of Bi'r az Zallaf Mb. deposits are poorly preserved and represented by fragments of ostracodes, pelecypods, gastropods and charophytes (Fig. 29 b). Ostracods are represented by *Cyprideis trosta* (Seidl and Röhlich, 1984). Flora

remains are represented by rare to frequent and indeterminable oogonia of Charophytes. Seidl and Röhlich (1984) reported sporadic remains of the angiosperm *Phragmites* sp. which indicates a late Tertiary to Quaternary age. According to same workers relicts and moulds of small fish of family *Centropomidae* (*Ambassidae*) were found in the uppermost interval of Bi'r az Zallaf carbonate deposits.

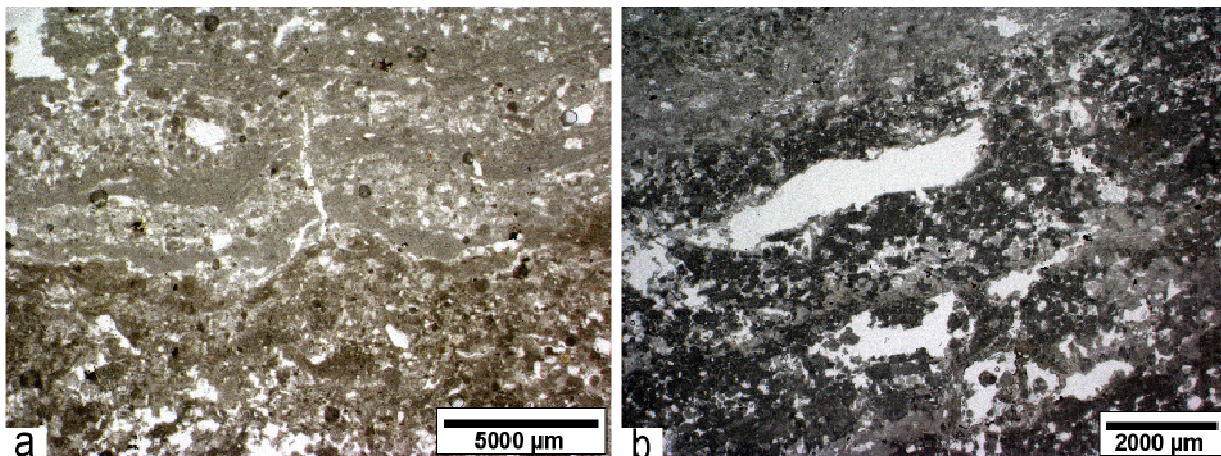


Figure 28. **a:** Thin section of the thin bedded carbonate showing the wavy structure and vertical desiccation cracks in the thin bedded carbonate facies. (Section C, sample 25, meter 12.5); **b:** Fenestral voids in the thin bedded carbonate facies. Same locality as a.

4.4.4 Carbonate Mineralogy

The carbonate minerals are dominated by dolomite (80%) and contain 10- 20 % of calcite or less a few examined samples. This calcite appears to be mostly high Mg-calcite. Because of the very small quantity of the mineral and low intensity of the X-ray peaks, estimation of the Mg content is difficult. We suspect that this small amount of calcite is biogenic in nature, derived mainly from ostracod, pelecypod and gastropod shells. Other minor minerals detected by X-ray diffraction are principally halite, gypsum, ankerite and sylvite.

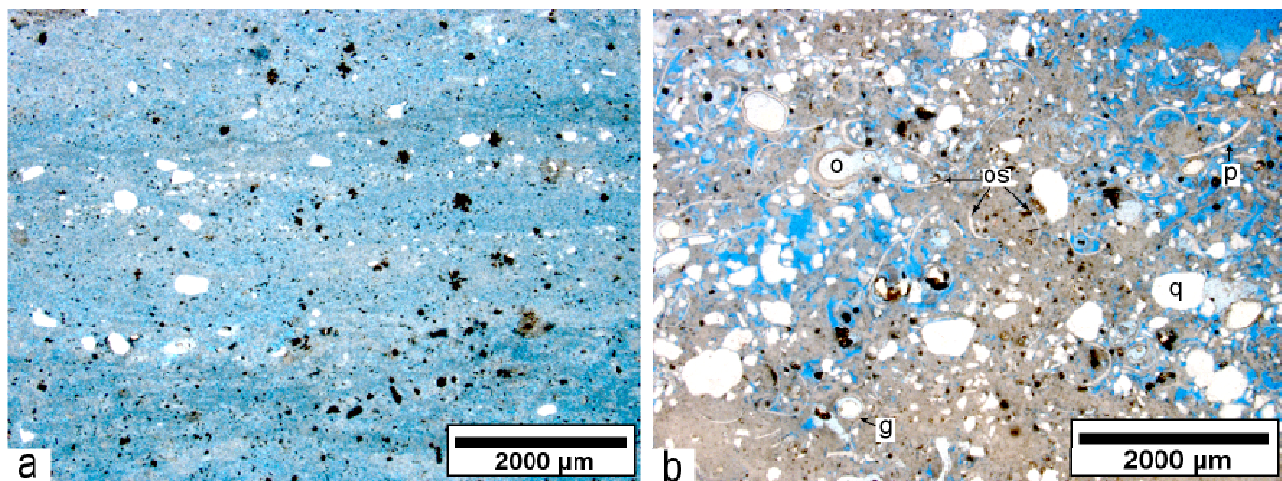


Figure 29. **a:** Thin section photo of thin bedded carbonate facies showing the microcrystallized dolomite (Section C, sample 29, meter 17.5). Note the fine wavy structures within this facies; **b:** Thin section photo showing the frequent bioclasts debris in this thin laminated carbonate facies. P: pelecypods, os: ostracods, o: oogonia of charophytes, g: gastropods and q: quartz grains. (Section C, sample 22, meter 11)

4.4.5 OSL age determinations

OSL dating of the three samples collected from Bi'r az Zallaf Mb. sand intervals (Zas 2, Zas 3, and Zas 4 Section C Fig. 20) confirms the findings of Armitage et al. (2007) that these sand intervals are extremely old. The upper sand interval (sample ZaS4), yielded an absolute age (410 ± 50 ka), indicating that the lower sand intervals (Zas1 and Zas2) are of a very great antiquity. OSL results suggest that the Bi'r az Zallaf deposits are clearly older than the uranium-series estimated Quaternary ages of 240-260 ka, which were carried out and published by Thiedig et al. (2000); Thiedig and Geyh (2004) and by Geyh and Thiedig (2008).

Result of X-ray analysis determination of carbonate mineralogy in this study challenge the previous interpretations as limestone beds and questioned the reliability of the published $^{230}\text{Th}/\text{U}$ dating due to high dolomite content in the laminated carbonate intervals.

The mixed carbonate/siliciclastic sequence presented herein is comparable to the Neogene lacustrine deposits (Qarat Weddah Formation) between Al Jaghub and Jalū in Sirte Basin, which were described by Di Cesare et al. (1963) and by Domàćí et al. (1991). Thus a Middle Miocene age for these lacustrine deposit is suggested,

which was proposed by Collomb, (1962) and corresponds very well with our observations in study area.

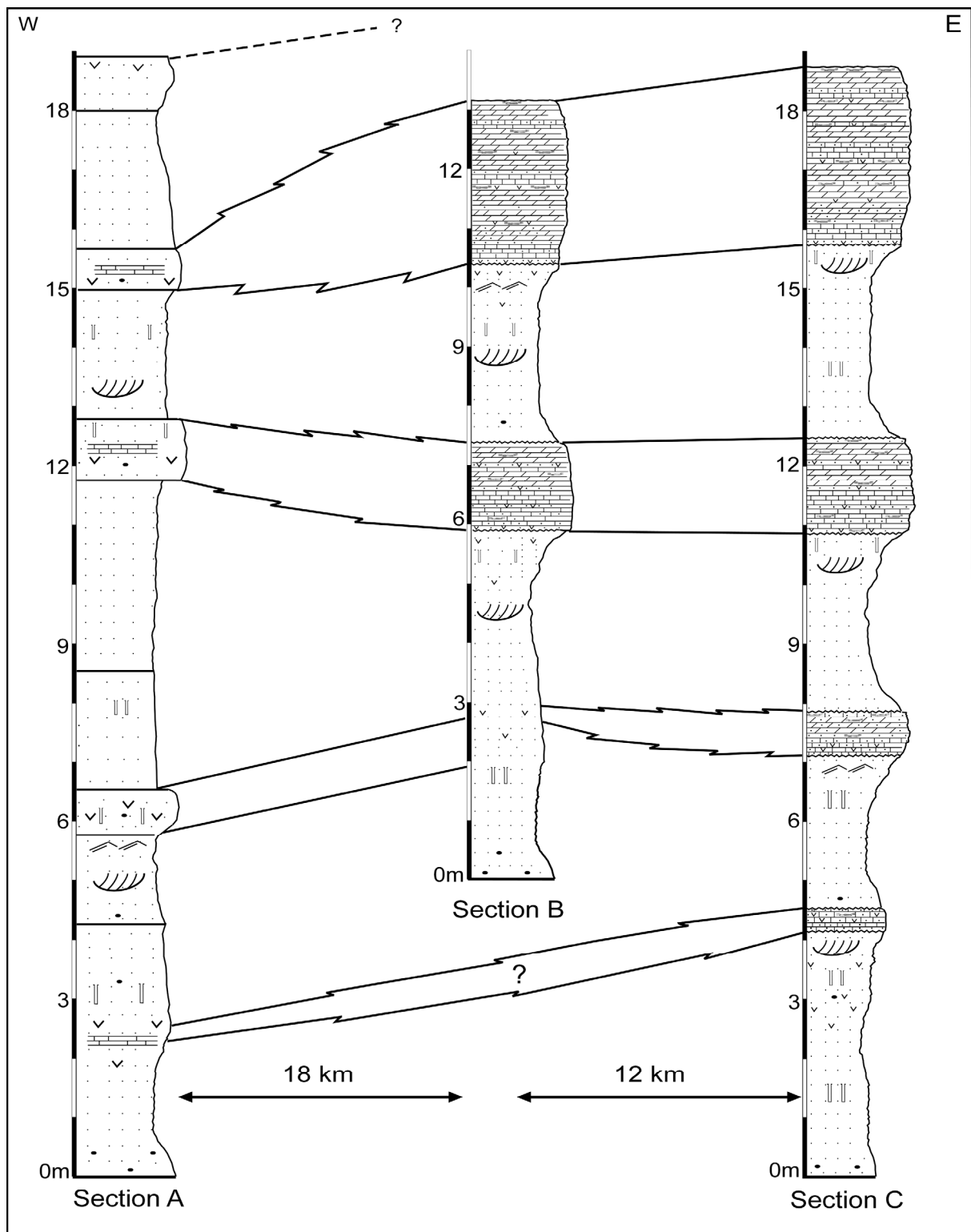


Figure 30. Sections logged on the Wadi az Zallaf depression illustrating correlation of sand facies and the thin bedded carbonate facies a long Wadi az Zallaf area.

4.5 Interpretation

4.5.1 Facies interpretation

4.5.1.1 Sand facies

The investigated mixed carbonate/siliciclastic sequence of Bi'r az Zallaf Mb. are interpreted as inland playa lake deposits. Conglomerate clasts or pebbles of sandstones in the sand facies are interpreted as fragments of Palaeozoic sandstone formations in the study area. The presence of these sandstone fragments suggests that the sands were deposited by occasional heavy wadis floods, which is supported by the cross bedding and ripple mark structures. A high proportion of fine grains such as silt and clay components within the sand facies can be interpreted as a result of pedogenetic processes, which are indicated by dense rootlets vertical borrows in the sand facies (Völker, 1990; Freytet and Plaziat, 1982). The abundant rootlets structures within this facies indicate humid conditions, as demonstrated by abundant roots, vertical borrows, iron staining and silicate weathering (varicoloured impregnations of sand grains). Large root cavities may indicate intensive desiccation periods since the root system must have had to penetrate deeply to reach the water.

4.5.1.2 Carbonate facies

Carbonates are interpreted to have formed in ephemeral lakes. The irregular wavy bedding, fine lamination and small wavy structures are attributed to adhesion ripples, which are characteristic for shallow playa lake and sabkhas deposits (Reineck and Singh, 1980). The rare to frequent biogenic components associated of this facies suggest very shallow aquatic brackish- to slightly saline waters, inferring a lake or pond sedimentation. The presence of fossils in this facies indicates aquatic phases, when climate was sufficiently humid in order to allow lake formation.

Peloid grains in this facies are interpreted as *in situ* formed algal and cyanobacterial peloids, which occur in microbial mats of shallow saline lakes and sabkhas (Flügel, 2004; Tucker and Wright, 1990). Some of peloid grains probably were produced by deposit-feeding animals; such grains are mostly oval or ellipsoidal in shape, which are similar to these peloid grains, whereby the original grains have lost their inner

structures and have been completely micritized by endolithic micro-organisms. In general, peloids is a polygenetic group of grains. Identifying their exact origin is often impossible, since they can be produced by different processes (Tucker and Wright, 1990). Quartz grains in the carbonates are thought to reflect aeolian influx or flooding phases of adjacent fluvial channels.

Primary deposition of dolomite in ancient and modern saline lakes is reported by many authors such as Von der Borch (1976); Talbot and Allen (1996); Mahran (1999) and Schulz et al. (2002). Valero (1993) mentioned that during the lowstand of a lacustrine system, the chemical composition of water may very substantially, and as a result, primary dolomite may precipitate. Eugster and Hardte (1978) found that the dolomite formed in saline lakes was due to an increasing Mg concentration.

The presences of abundant vertical cracks and fractures, fenestral voids and Pseudo-microcarst in this facies are interpreted in this study as desiccation features. They may indicate frequent periods of sub aerial exposure. Thus, low water level in the playa-lake with periodic and/or complete desiccation of the shallow lake, contributed to the development a large sabkha setting.

4.5.2 Depositional model

Based on the investigated and correlated sections (Fig. 30) a depositional model is proposed for the mixed carbonate/siliciclastic sequence studied in the Wadi az Zallaf depression (Fig. 31). The evolution of the lacustrine area can be subdivided into several sedimentary cycles (Section C, Fig. 20). According to this model the sand facies is mainly documented in the western part of the depression, while the thin carbonate facies is dominated in the eastern part. Between the both facies there is a transitional zone which is characterized by deposition of high concentration of evaporates

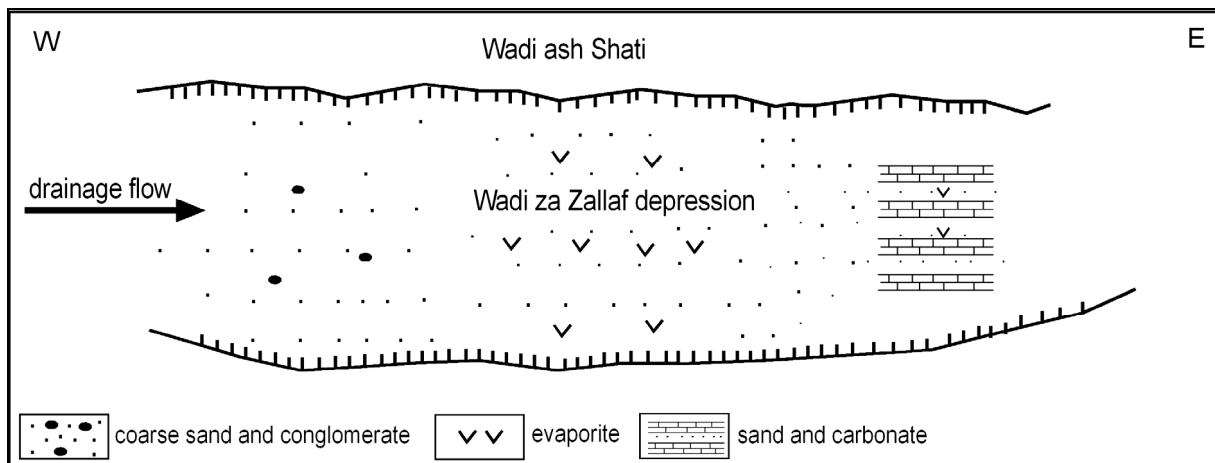


Figure 31. Depositional model showing facies distribution of the main sediment types of Bi'r az Zallaf Mb.

4.5.2.1 Alluvial stages

Sands are interpreted to have been supplied by tractive flows carrying silt, sand and gravel. Correlation between the measured logs (Fig. 30) demonstrates a reduced terrigenous supply from the proximal area in the west to more distal zones in the East (Fig. 31). It is suggested that sands were frequently subjected to subaerial conditions leading to the cementation of the sands by salts. All analyzed sections show that sand intervals are organized in fining-upward sequences. This implies changes in the energetic conditions of the wadi flow during its development.

4.5.2.1 Lacustrine stages

Carbonates are interpreted as deposits of carbonate-rich shallow playa-lakes, under humid conditions. At the onset of every stage of the playa lake the water level was high, and the salinity was low to moderate. During this time the playa lake was essentially a shallow carbonate-rich lake, with ostracodes, gastropods and charophytes. During these stages, the water depth could have reached 0.5-3 m. At the periphery of the lake, notably in western sector, an essentially detrital sedimentation took place. Both characteristics of carbonate facies and the vertical sequence indicate that during these periods water level fluctuations occurred and terrigenous supplies flowed into the lake predominantly during its initial development.

This model contradicts the former interpretation of a large perennial lake (Thiedig et al., 2000; Armitage et al., 2007; Drake et al., 2008). The lakes were initially fed by surface runoff and occasionally wadi flows. Late stages of the playa lakes were relative bigger and should have been lasted longer comparing with earlier stages. This can be indicated by thickness and laterally extension of the third and fourth carbonate intervals. However, all playa lake stages received most of their water from surface runoff, wadis, and spring discharge. The sequence of deposits indicates not only significant long-term changes in climatic conditions but also frequent short-term oscillations.

4.6 Discussion

The results of this chapter present new interpretations and depositional model for the continental carbonate and siliciclastic deposits of Bi'r az Zallaf Mb., which has enable the reconstruction of the geology of Murzuq Basin and Palaeogeography of the Central Sahara region during Late Tertiary and Quaternary periods.

The results of this chapter contradict all former interpretation, classification, and age determinations of Bi'r az Zallaf Mb. as a fresh water lacustrine deposits by Colomb 1964; Seidl and Röhlich 1984; Thiedig et al. 2000; Thiedig and Geyh 2004; Armitage 2007; Geyh and Thiedig, 2008 within the context of "Megalake Fezzan"

Based on $^{230}\text{Th}/\text{U}$ method the age of Bi'r az Zallaf Mb. ranges between 240 and 260 ka (Thiedig et al., 2000; Thiedig and Geyh, 2004; Geyh and Thiedig, 2008). This Member was taken as evidence of existence of the third phase of "Megalake Fezzan", which followed the orbitally-forced (Milankovitch) eccentricity cycle of 100 ka during the middle Pleistocene (Thiedig et al., 2000; Thiedig and Geyh, 2004; Armitage et al., 2007; White et al., 2001; Geyh and Thiedig, 2008).

According to Thiedig et al. (2000) the middle Pleistocene Megalake stage of Bi'r az Zallaf Mb. covered most of the Murzuq Basin with maximum extension of about 53.000 km². The proposed Megalake was separated into two large lakes by the Mesak Plateau between the Awbari and Murzuq Sand Seas.

The results of this study show that, the Bi'r az Zallaf Mb. in the study area consist of an intercalation of thin bedded to fine laminated carbonate, weakly consolidated sands and evaporites (dolomite, halite and gypsum).

Four carbonate and sand intervals were recognized and described in Wadi az Zallaf area. Carbonate beds are made mainly of dolomite, sandy limestones and evaporite minerals. Abundant peloids and fine quartz grains are the main components of the carbonate beds. Rare bioclasts of poorly preserved fragments of ostracods, gastropods, and charophyte debris were found in the thinly laminated carbonate intervals. The Carbonate intervals are characterized by intercalations of laterally continuous laminations consisting of couplets of carbonate and thin evaporite layers, which are suggestive of deposition by vertical accretion in an ephemeral saline lake.

XRD analysis proved that carbonate minerals of Bi'r az Zallaf Mb are dominated by dolomite (80%) and contain less than 10-20 % of calcite. High dolomite content of Bi'r az Zallaf Mb. questioned the former $^{230}\text{Th}/\text{U}$ age determinations, which were performed by several geologist (Thiedig et al., 2000; Thiedig and Geyh, 2004; Geyh and Thiedig, 2008).

Result of OSL dating on three sand samples of Bi'r az Zallaf Mb. confirms the findings of Armitage et al. (2007) that these sand intervals are older than middle Pleistocene.

The high evaporite and dolomite content of the thinly bedded to laminated carbonate beds of Bi'r az Zallaf Mb. suggests that they are temporary shallow playa lake deposits.

According to Reineck and Singh (1980), inland playa lakes are characterized by salt crusts formed from rapid evaporation of water. Moreover the sediments of these shallow lakes are parallel-bedded and show intercalations of with thin sandy layers with gypsum layers and dolomite (Eugster and Kelts, 1983).

The results presented here also agree with the findings of Glennie (1970) and William (1971) on desert Lake and inland sabkha deposits. They also described thin bedded to laminated carbonate and evaporite and interpreted it as adhesion ripples in shallow playa lake environment.

The deposits of Bi'r az Zallaf Member are modern analogue of the laminated carbonate deposits described from the Sinai Peninsula by Krumbein et al. (1979).

Bell (1989) described similar fine-laminated carbonate beds from the Codocedo Limestone Member in the Atacama region of northern Chile, which consists mainly dolomite, quartz grains and cyanobacterial peloids with frequent bioclast fragments including ostracods, gastropods and charophytes debris.

According to Soulie'-Màrsche (2008) and Zalat, 1996 abundant charophyte gyrogonites, and ostracods were found within several inland sabkhas deposits in North Africa. She stated that the presence of charophyte gyrogonites in sabkha sediments indicate obligatory low saline phases.

Finally our results also suggest that the carbonate intervals of Bi'r az Zallaf Mb. represent a relatively short period of shallow playa lake deposition within an essentially terrigenous succession. The playa lakes were possibly formed quite suddenly and fed mainly by groundwater and occasionally by wadi inflows. Sedimentation in the ephemeral lakes was predominantly cyclical. Seasonal biogenic and algal blooms produced millimetre-scale laminations. Interbedded with these laminites are centimetre-scale beds of evaporitic gypsum, anhydrite and halite.

The former misinterpretation of the Bi'r az Zallaf Mb. as middle Pleistocene fresh water lacustrine deposits led to development of the concept of "Megalake Fezzan" by several geologists (Thiedig et al., 2000; Thiedig and Geyh, 2004; Armitage et al., 2007; White et al., 2006; Pachur, 2006 ; Drake et al., 2008; Geyh and Thiedig, 2008).

Based on this interpretation, they reconstructed the Palaeoclimate of Murzuq Basin and the Central North Africa as a humid climate area during the Middle Pleistocene period. They thought that they had found a coincidence between pluvial phases in the arid North Africa and the interglacial events in the moderate climate zones (Thiedig et al., 2000).

The present research does not support the existence of Megalake stage of Bi'r az Zallaf Mb. and consequently the lacustrine fresh water origin of Bi'r az zallaf Mb. is dismissed because of lack of any evidence to support that interpretation.

It is obvious from the results of this study that without comprehensive sedimentological studies including facies analysis, and relying solely on geographical, chronological and chemical examination such deposits may be mistaken as fresh water lake sediments, and the presence of bioclast debris and thin bedded to fine laminated carbonate may be misinterpreted as lake stratification.

4.7 Conclusions

The Bi'r az Zallaf Mb. consists of an intercalation of lacustrine carbonate and weakly consolidated sands and evaporites. These deposits are interpreted as playa-lake deposits. Alternation from sands and carbonates indicate four aridity periods, which were followed respectively by a more humid climate.

Carbonate beds of Bi'r az Zallaf Mb. are mainly composed of dolomite (80%) and 10-20 % of calcite.

OSL age determination show that Bi'r az Zallaf Mb. deposits are older than middle Pleistocene and they may date back to Middle Miocene, which was proposed by Collomb, (1962) and corresponds very well with our observations in study area.

5

AQAR MEMBER

ABSTRACT

Discontinuous outcrops of coquinas occur in the Wadi ash Shati, south of the Palaeozoic Gargaf Uplift in the northern margin of the Murzuq Basin. The coquinas were termed the Aqar Member. The Aqar Mb. was interpreted as lacustrine deposits which were deposited in the last stage of the Megalake Fezzan development and therefore it was considered it as the younger member of Al Mahruqah Formation.

The main objective of this chapter is to document the composition, fossil contents, and the sedimentary facies of these sediments with respect to the depositional environment and to present a depositional model.

In order to achieve these goals the Aqar Mb. coquinas were analyzed along Wadi ash Shati area. Two representative sites in the north-western margin of Wadi ash Shati were selected and sampled. Abundant *Cerastoderma glaucum* shells, ostracodes, gastropods, rare to frequent charophytes were found and described. These biogenic components were found interbedded with abundant admixture of mud to boulder sized siliciclastics.

The coquinas are characterised by medium to large-scale steeply inclined cross bedding and trough cross bedding. Based on these new finding, it is proposed that the deposits are recent wadi sediments, and that the shells are reworked from older lakes sediments.

5.1 Introduction

Cerastoderma glaucum coquina deposits were discovered in the middle of Sahara more than 130 years ago (Tournouér, 1878). Marés (1857) reported the existence of these fossils in the south of Oran province, Algeria and scattered outcrops in the vicinity of Timbuctu in Mali and interpreted them as marine deposits. Their widespread distribution in the Sahara with presence of ostracodes and foraminiferas gave rise to the notion of “Saharian Seas”, opening respectively to the Mediterranean Sea and the Atlantic Ocean (Palaziat, 1991).

New studies, carried out in recent years provide more precise information concerning the distribution, ecological significant, and age of the *Cerastoderma* shell deposits in the North African Sahara (Gaven, 1981; Petit-Maire, 1982; Plaziat, 1991; Conrad, 1969; Conrad and Lappartient, 1991). More than 25 outcrops containing these fossils were found in North Africa and Middle East, and interpreted as lacustrine deposits (Fig. 43). The majority of the sites mark the middle Pleistocene lacustrine phase dating back from approximately 80 to 150 ka ago (Petit-Maire, 1980; Gaven et al., 1981). According to several authors, the *Cerastoderma glaucum* were transported to the Sahara by migrating birds (Petit-Maire, 1980, 1991; Gaven et al., 1981; Conrad and Lappartient, 1991).

In study area coquinas extend along the northwestern edge of the endorheic depression of Wadi ash Shati (Fig. 32). They crop out in a series of laterally discontinuous W-E trending exposures, about 100 km descending from approximatlly 350 to 290 m elevations along the Wadi ash Shati (Petit-Maire et al., 1980; Petit-Maire, 1982). Along the southern and eastern edges, the coquinas are entirely absent and fine sand, silt and marl deposits are prevalent (Gaven et al., 1982; Seidl and Röhlich, 1984). Coquina beds consist mainly of abundant *Cerastoderma glaucum* shells with frequent to rare gastropods, ostracodess and charophytes (Lelubre, 1946 a, b; Müller-Feuga, 1954; Desio, 1971; Petit-Maireet al., 1980; Gaillard and Testud, 1980; Gaven et al., 1981; Seidl and Röhlich, 1984; Pařízek et al., 1984). Petit-Maire et al. (1980); Gaven et al. (1982) carried out the first $^{230}\text{Th}/\text{U}$ age determinations on these deposits. The published radiometric $^{230}\text{Th}/\text{U}$ ages of coquina shells range from 90 to 136 ka (Petit-Maire et al., 1980; Gaven, 1981, 1982).

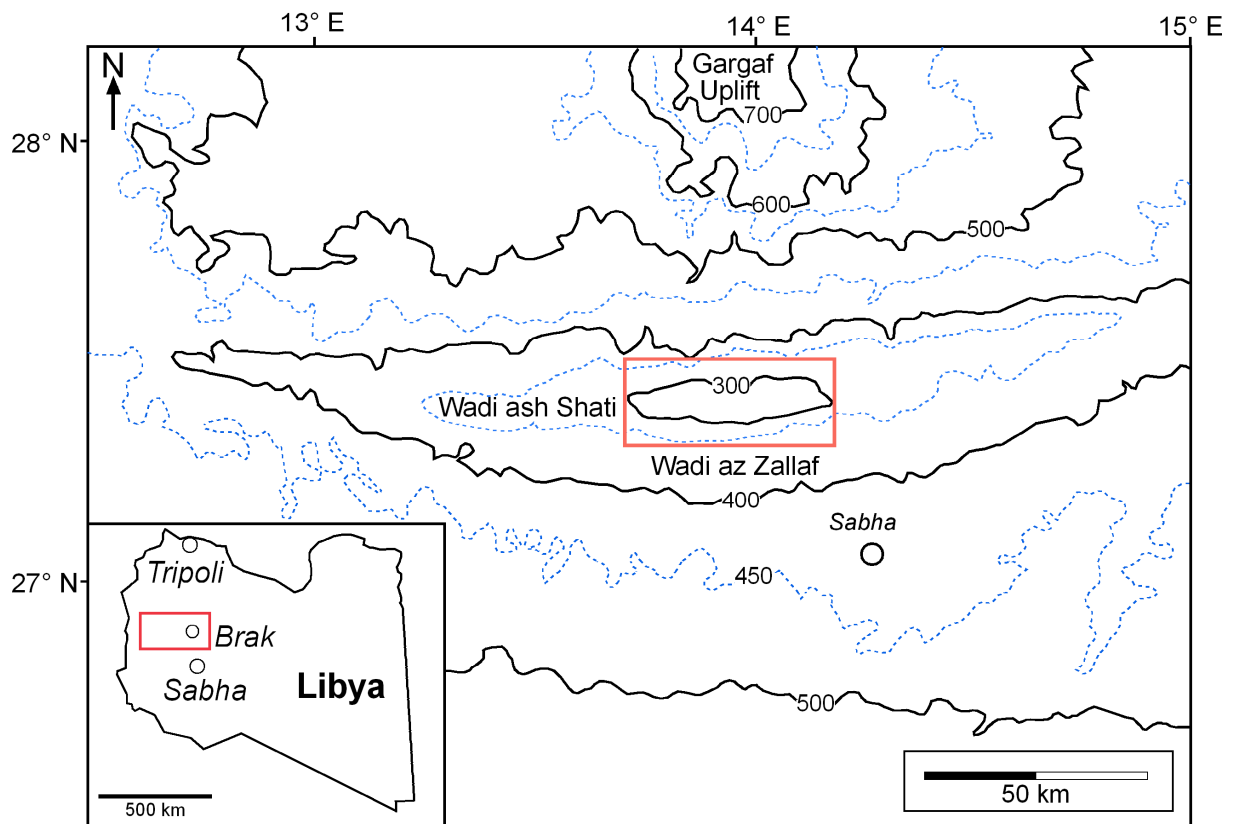


Figure 32. Topographical map showing topography and location of the endorheic depression of Wadi ash Shati and study area.

The most recent observations and age determinations of these sediments were performed by Thiedig et al. (2000), Thiedig and Geyh (2004); Geyh and Thiedig (2008). They classified them as middle Pleistocene lacustrine deposits and termed these coquina deposits as Aqar Member of Al Mahruqah Formation. Their age determinations confirm the former suggested Pleistocene age of these lumachelles. In spite of many geological studies were carried out on the coquina deposits in Wadi ash Shati, However, a sedimentological assessment was not attempted and the characteristic facies and sedimentary structures were not incorporated in the paleo-environmental interpretation.

The main objective of this chapter is to document the composition, fossil contents, and the sedimentary facies of these sediments with respect to the depositional environment and to present a depositional model.

The lumachelle is characterised by medium to large-scale steeply inclined cross bedding and trough cross bedding in the lower part of the sedimentary bodies and by tabular cross bedding is in the upper part.

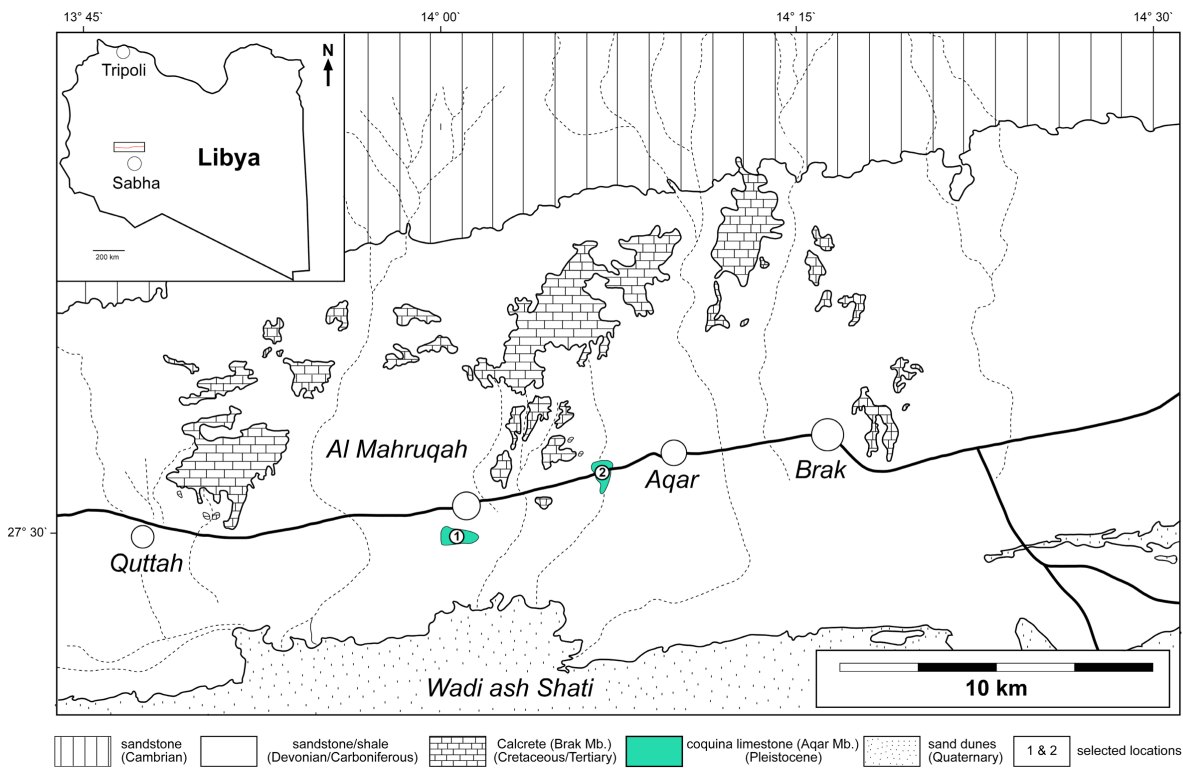


Figure 33. Geological map of study area showing the distribution of Aqar Mb. deposits in the study area and indicating the location of investigated sites (1 and 2) and the position of the localities discussed in the text. Simplified after Seidl and Röhlich (1984).

Based on these characteristics the limestones are interpreted as recent Wadi deposits which contain reworked shells which were originally accumulated in a shallow fresh to brackish restricted small isolated palaeolake in the Wadi ash Shati depression. Reworking is thought to have been controlled by local wadis.

5.2 Geological setting

The study area, the Wadi ash Shati depression, is located in northern margin of the Murzuq Basin in the province of Fezzan in SW Libya. Wadi ash Shati, which is approximately 180 km long and represents a deep stretching endorheic depression, running from the West to the East from $12^{\circ}30'$ to $15^{\circ}00'$ E, along the southern slope of the Garqaf Uplift (Fig. 32). According to Desio (1971) and Drake et al. (2008) the Wadi ash Shati was incised by one of the several rivers flowing north-eastwards towards the Mediterranean Sea, which was gradually cut off by the thermal uplift of the region and the Haruj al Aswad lava flows towards Jabal Sawda.

K/Ar dating of the volcanic rocks at Haruj al Aswad indicates that volcanism started near the beginning of the Messinian (Desio, 1971; Drake et al., 2008).

The blocking of the rivers by volcanic activity formed a closed basin at the northern margin of the Murzuq Basin (Drake et al., 2008). Hence, the endorheic situation in the Wadi ash Shati begins at the latest during late Miocene Age (Drake et al., 2008). Cambrian, Ordovician, Devonian and Carboniferous sedimentary rocks respectively outcrop in the study area and dip gently from north to south (Fig. 33). Lacustrine deposits were observed in Wadi ash Shati depression and were attributed to the Pleistocene (Lelubre, 1946 a, b; Müller-Feuga, 1954; Desio, 1971; Petit-Maire, 1980; Gaven et al., 1981; Thiedig et al., 2000). They occur as small denudations and relicts along the floor of the wadi depression lying between 40 and 50 m elevated above the present sabkhas, which occupy the deepest areas at elevations ranges from 280 to 300 m a.s.l (Figs. 33 and 34). The fossiliferous coquina beds extend along the western and northern edges of the endorheic depression of Wadi ash Shati, where they were prevalently developed (Petit-Maire et al., 1980; Seidl and Röhlich, 1984)).



Figure 34. Field photo showing a coquina bed of *Cerastoderma glaucum* shells resting unconformably on the Carboniferous Marar Formation, site 1, 1 km south of Al Mahrurah village in Wadi ash Shati, 27° 29' 32" N, 14° 00' 39" E

5.3 Methods

Our Field work started with revisiting the lacustrine outcrops along Wadi ash Shati, which were mapped firstly by Petit-Maire, 1980; Seidl and Röhlich (1984). The

second step was investigating the lithology, the fossil content and the stratigraphy of the coquina beds through sampling at two selected sites in the western part of Wadi ash Shati (sites, 1 and 2 Fig. 33). Ten samples were taken from each site. The selected locations are representative of the Aqar Mb. deposits in Wadi ash Shati endorheic depression. Small Molluscs, ostracods, and charophyte gyrogonites fossils were obtained from eight samples by washing and wet sieving for eight samples from both investigated sites.

5.4 Results

5.4.1 Palaeontology

The Aqar Mb. coquina beds in Wadi ash Shati contain bivalves, gastropods, ostracodes and charophytes. The species composition of the samples collected from the study area (sites 1 and 2 in Fig. 33) is described by order of abundance as follows:

5.4.1.1 Bivalves

Pelecypods are represented by *Cerastoderma glaucum*. The shells are very abundant in two studied sites 1 and 2 (Fig. 33). *Cerastoderma glaucum* shells are solid, thick, globular and broadly oval in outline, up to 4 cm long but usually less. The outer surface is white, yellowish or light brown, while the inner surface is dull white (Fig. 35 a). In both locations *Cerastoderma glaucum* shells were often found scattered, weathered and mostly with disconnected valves or broken shells. At site 2, they are associated with abundant sandstone pebbles and sand grains.

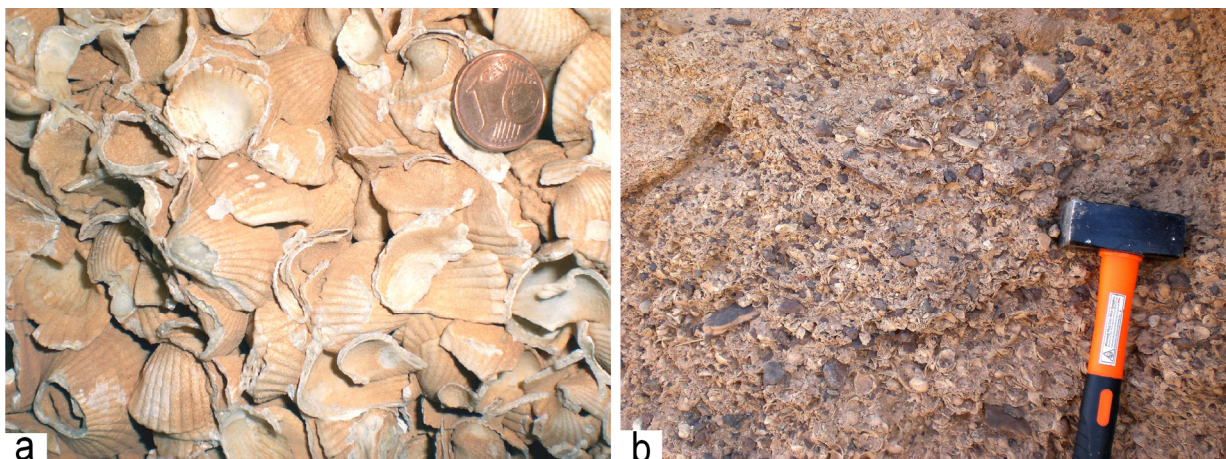


Figure 35 a: Close view of Figure 34 showing densely packed and disarticulated *Cerastoderma glaucum* shells (Site 1, Fig. 31) diameter of coin 1.5 cm; **b:** *Cerastoderma* shells interbedded with abundant admixture of mud to boulder sized siliciclastics at site 2, Fig. 31. Hammer for scale

The fossil shells show little differences in size and shape. Shell valves are completely symmetrical and equal sized. The radiating ribs and the ligament area are easily observed. Other shell features include prominent umbones and 22-28 radial ribs with equal size muscle scars.

5.4.1.2 Gastropods

Gastropods are more diversified in the study area and represented by three species. Abundant and poorly preserved *Hydrobia* shells were found in two samples along with *Cerastoderma glaucum* shells (Fig. 36 a). All shells are small spiralling, mostly up to 3-4 mm in height, and are brown to yellow in colour.

Melanoides tuberculata shells were found rarely in two samples derived from the investigated locations in Fig. 33. *Melanoides tuberculata* is easily recognised by its conical shape with usually five whorls. The shells are light brown in colour and are frequently mottled (Fig. 36 b). The average shell length is around 2-3 cm.

Rare *Gyraulus* sp. shells were obtained in the 125 µm fraction from five samples from site 2 (Fig. 38 a). The shells are silky to glossy and transparent with fine growth lines. The flattened shell consists of four whorls, which are regularly and rapidly increasing with a clear visible to deep suture (Fig. 38 a). The shells range between 0.5 – 3.0 mm in diameter and 1.0-1.2 mm in height.

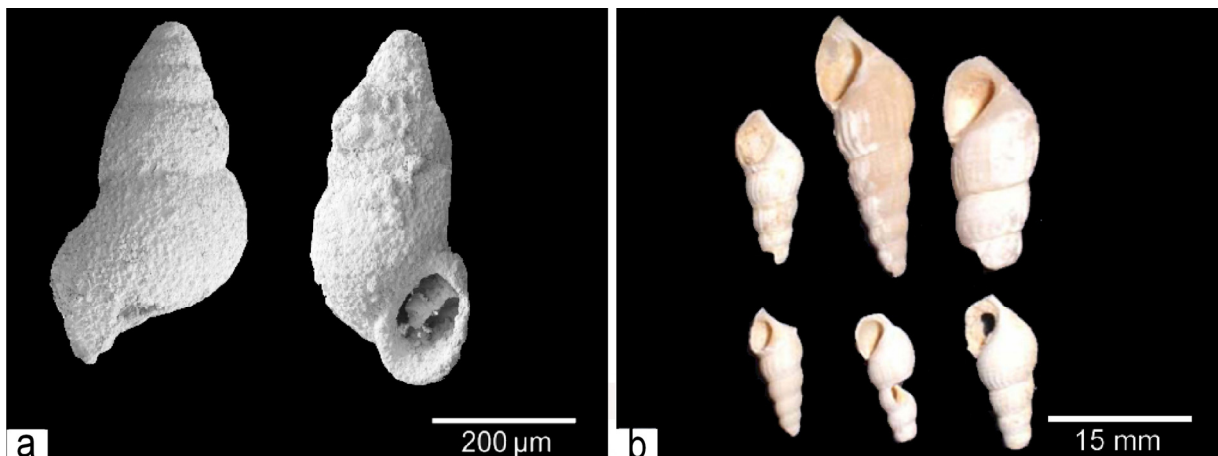


Figure 36. Gastropod fossils collected from Cerastoderma coquina bed of Aqar Mb. in both investigated sites **a:** *Hydrobia* sp. Shells; **b:** *Melanoides tuberculata* shells collected from Cerastoderma facies. Note the mottling and bad preservation of the *Melanoides tuberculata* and *Hydrobia* shells.

5.4.1.3 Ostracodes

Frequent, well-preserved ostracodes occur in the 125 μm fraction from locations 1 and 2 (Fig. 33). The most common species is represented by *Cypridies trosta* (Fig. 37).

5.4.1.4 Charophytes

Charophytes were found in all investigated samples from locations 1 and 2. Fifty gyrogonites of the two locations were measured and identified. The gyrogonites are similar and belong to one species (Fig. 38 b). The average size is about 510 μm in length and 390 μm in width and the average L / W ratio of 1.31. The morphology and the measurements of the gyrogonites compared most closely to *Lamprothamnium* sp., a modern species, well-known from North African localities (Zalat, 1996). This species is also known to exist in several localities in Mediterranean regions, central Iran and India (Soulié-Märsche, 1993 a,b; Djamali. et al., 2006).

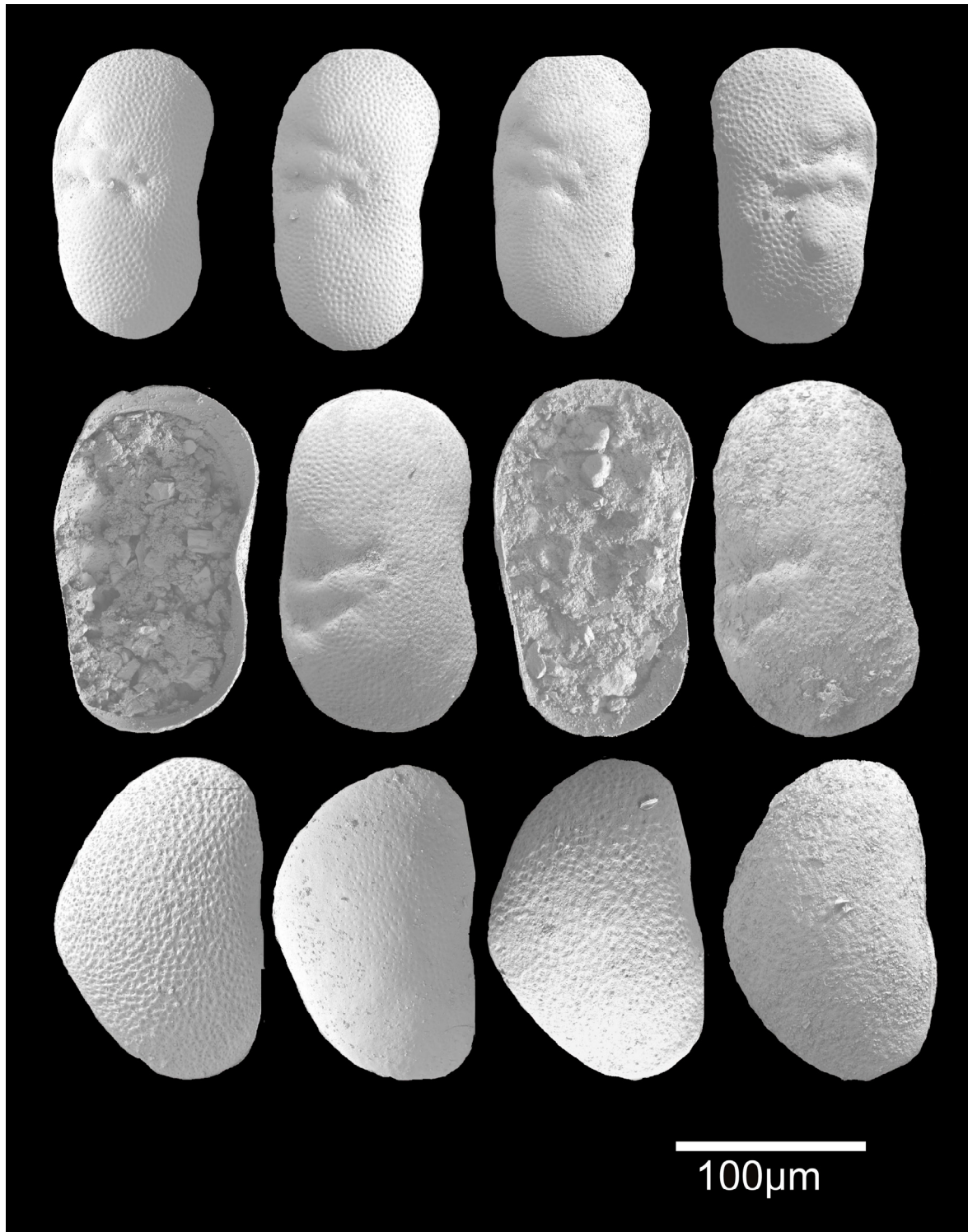


Figure 37. Abundant ostracod shells recovered from Aqar Mb. from both investigated sites (1 and 2) in Wadi ash Shati area.

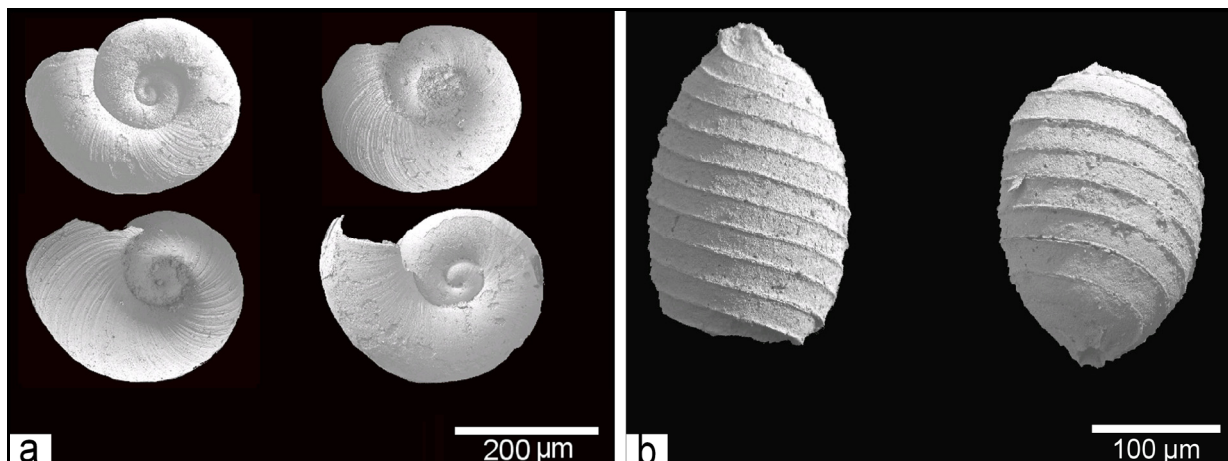


Figure 38. Microfossils fossils recovered from coquina beds of Aqar Mb. from both sites (1 and 2) in study area **a:** *Gyraulus* sp. shells (gastropod); **b:** Charophytes gyrogonites .

5.4.2 Depositional model

The lumachelles are arranged in up to 3 m thick beds. A typical outcrop view of *Cerastoderma* facies is shown in Figs. 39 a/b and Fig. 40 with calcirudites beds, having diffuse, undulating internal layers. The limestones unconformably overlie the carboniferous siliciclastic substrate (Figs. 34, 39 and 40). The lateral extension of the lumachelle patches is less than 20 meters.

At site 2, *Cerastoderma* shells are interbedded with abundant black to dark grey admixture of clastic materials. This admixture is composed of abundant conglomerate clasts and pebbles and boulders of sandstones, in addition to mud, silt and sand grains. The conglomerate gravels are poorly sorted, mostly subangular to subround with small ferruginous concretions. The size of the individual clast of the sandstone pebbles varies from 2 to 10 cm. These sandstone pebbles locally are imbricated.

The *Cerastoderma* facies is weakly consolidated through cements at the shell contacts. Interstices are empty or partly filled by small abundant gastropods *Hydrobia* fossils (Fig. 36 a), silt, fine sand grains and gypsum crystals. Gypsum crystals are present in both sites 1 and 2, mostly as microcrystals and agglomerated transparent gypsum plates. The shell fragments of *Cerastoderma* are occasionally cemented by gypsum.

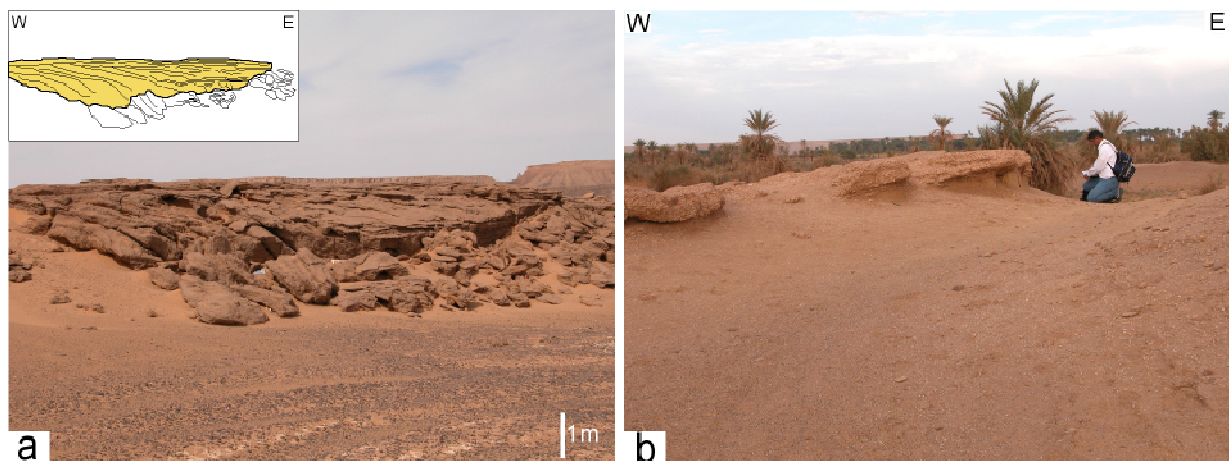


Figure 39. Field photographs showing geometry Cerastoderma coquina beds of Aqar Mb. in study area. **a:** Typical of small fan delta geometry with different cross bedding structures of coquina beds at investigated site 2 at road cut 5 km W of Aqar village, $27^{\circ} 31' N$, $014^{\circ} 06' E$; **b:** Large-scale steeply inclined cross bedding structures at site 1, 1 km S of Al Mahruqah village, $27^{\circ} 29' N$, $014^{\circ} 00' E$

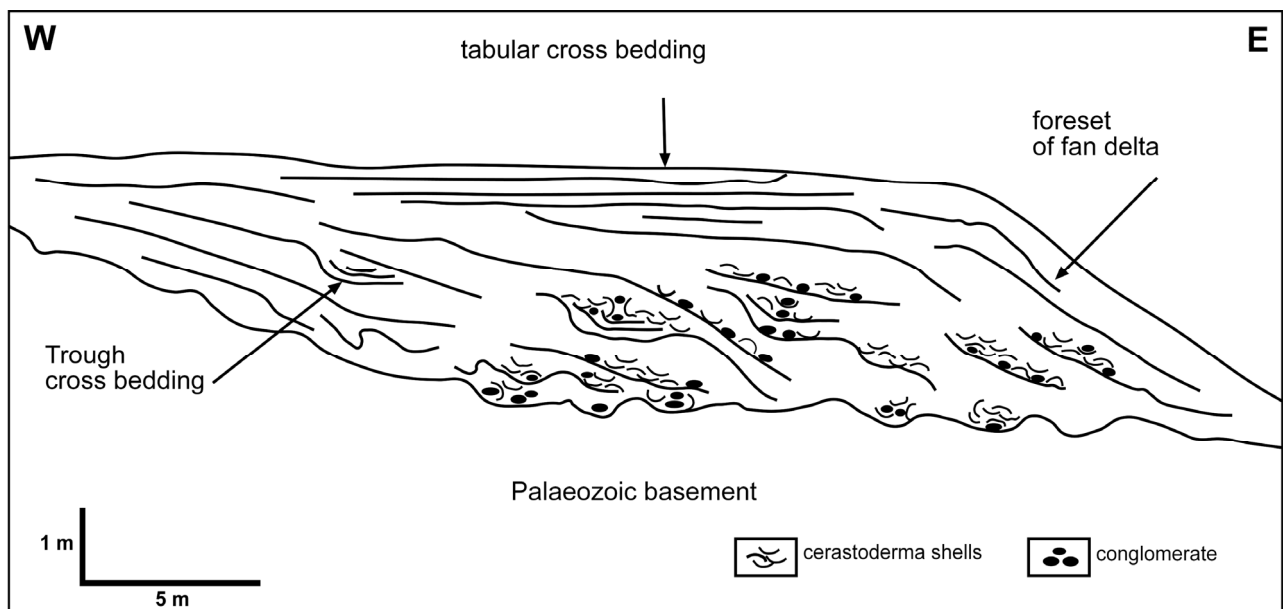


Figure 40. Simplified sketch drawing and interpretation of the field photographs and outcrops data provided in Figure 39 **a** & **b**, showing Typical small fan delta geometry, progradation features and different types of cross bedding structures can be distinguished.

At site 2, medium to large-scale steeply inclined cross bedding and trough cross bedding occurs in the lower part of the sedimentary bodies and tabular cross bedding in the upper part (Fig. 41 a, b, c, and d). Large inclined cross-bedding bodies dip as much as 30° and display graded bedding structures between them (Fig. 41 c). The steeply inclined cross bedding measurements show a very conspicuous and ubiquitous WNW ESE trend of cross bedding structures throughout the study area. Field works show that the lumachelle accumulations are similar everywhere in the western margin of Wadi ash Shati.

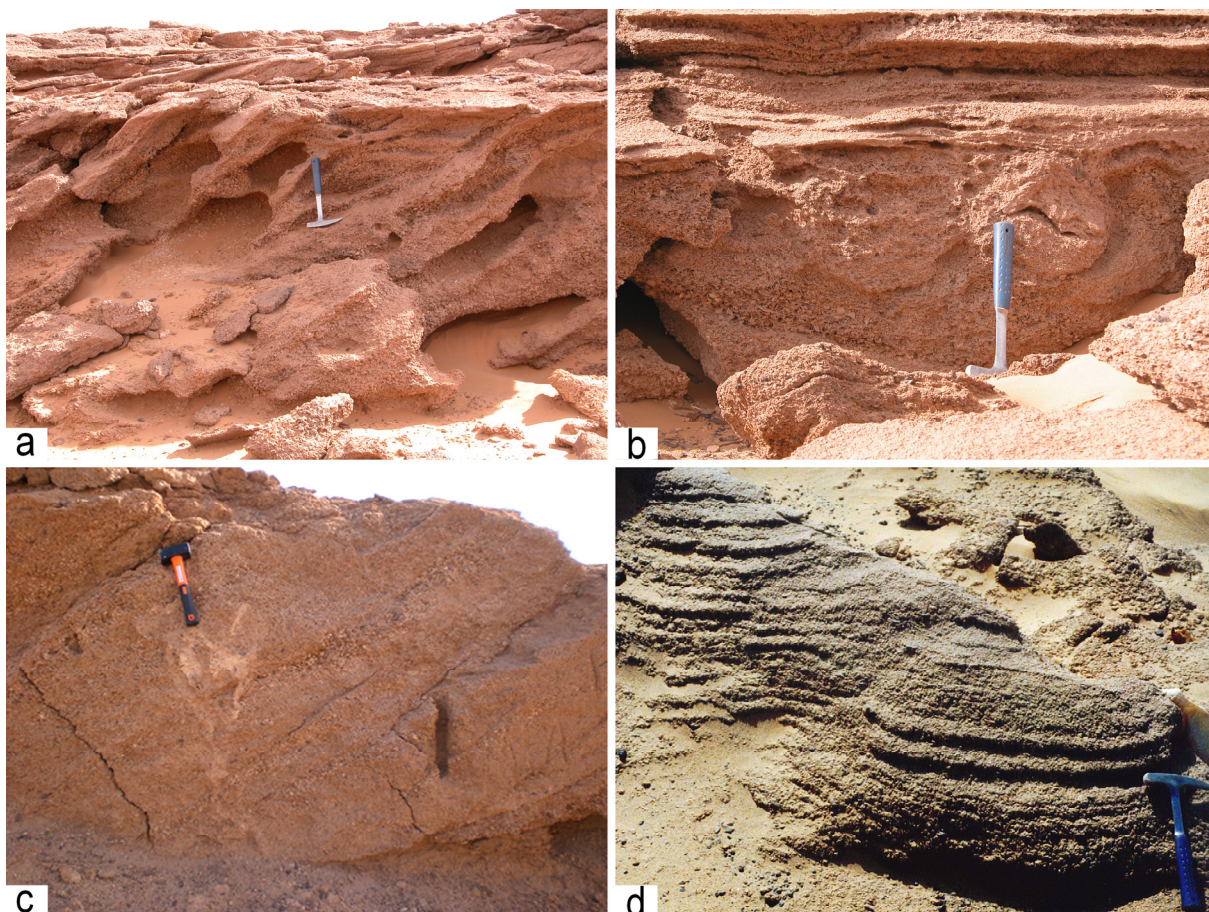


Figure 41. Field photograph showing poorly preserved different types of cross bedding structures in Cerastoderma facies; **a:** Middle to large cross bedding in the lower part of the photo capped by horizontal (planner) in the top of the photo; **b:** Trough cross bedding covered by tabular one. Note the graded bedding in the lower part of the photo; **c:** Field photograph showing a large-scale cross bedding structures which interpreted as small progradation structures, which were made by Wadi fan delta. Note the graded bedding within the sediment wedges structures, also the coarsing upward structures within the sediment bodies; **d:** Trough cross bedding in the Cerastoderma facies. Road cut about 5 km W of Aqar village, 27° 31' N, 014° 06' E;

5.4.3 Interpretation

Interpretation of the deposits relies on the palaeoecology of the fossils, the components, and the sedimentary structures. The correlation of sections and the analysis of depositional geometries are based on the physical tracing of deposits in outcrops and outcrop photographs.

Cerastoderma glaucum inhabits diverse environments, ranging from temperate to tropical shallow water areas, including marine, lagoons, estuaries and saline lakes (Petit-Maire, 1980; Gaven et al., 1981). They can tolerate wide ranges of salinity with values of 5 to 38 ‰ and water temperature between 0° and 25 °C (Boyden and Russell, 1972; Petit-Maire, 1980; Gaven et al., 1981). Their resistance to low salinity is generally emphasized, but they also tolerate eusaline to hypersaline waters (Petit-Maire, 1980; Gaven et al., 1981; Plaziat, 1991). Presently, *Cerastoderma* faunas are found in Egypt, in Birket Qarun of the Fayum depression, which is located 200 km from the sea. The salinity in Birket Qarun is 35 / 50 ppm (Plaziat, 1991). *Cerastoderma* preferentially settle and burrow shallowly in soft sediments with a usual borrowing-depth of less than 5 cm. *Cerastoderma* prefers clean sand, muddy sand or muddy gravel substrate.

Melanoides tuberculatus is a fresh water snail in the family Thiaridae, even though it can also live in brackish to highly salt water. It tolerates salinities of up to 29 ‰ (Petit-Maire, 1980; Gaven et al., 1981). *Hydrobia sp.* is a characteristic gastropods of fresh and brackish water in the northern continents. They are well represented in NW Africa, but rare in tropical region. They presently live in brackish water in Tunisia and Egypt at Birket Qarun and Sinai (Van Damme, 1984). In general, *Melanoides tuberculata* and *Hydrobia sp.* fossil assemblage indicate a shallow water community (depth <10 m) living on sandy substrate. It also suggests a temperature of about 20° C and a minimum salinity of 3 ‰ (Gaven et al., 1981).

Ostracodes are planktic, swimming, or benthic, crawling on or in the mud on the bottom. They live predominately in marine and terrestrial environments and their fossil record extends back to the Cambrian (Lehmann and Hillmer, 1980).

The presence and distribution of charophytes in Wadi ash Shati clearly indicate a paleolake with predominantly fluvio-lacustrine zones, where large seasonal inflows of fresh water occurred. The association of brackish water mollusks, such as *Melanoides tuberculata*, *Hydrobas*, *Cyprideis trosta*, and *Cerastoderma glaucum*, which tolerate a wide range of salinity, with freshwater or very low salinity-tolerant species such as *Gyraulus* and *Charohpytes*, may seem astonishing. However, the same association exists today in Lakes Chad, Albert and Tanganyika (Petit-Maire, 1980; Gaven et al., 1981).

The high proportion of dismembered bivalve shells suggests a strong reworking and transport for short distances due to powerful currents of local Wadis. This transport led to mixing the shells with clastic material, which were winnowed. The gypsum with this facies may originate either from lake evaporation processes or capillary rise of groundwater during recent periods.

Large-scale steeply inclined cross bedding and trough cross bedding structures are interpreted as small fan delta progradation features, caused by sporadic and abrupt fluvial wadi activity. Progradational geometry may indicate a lack of accommodation space in the shallow lake. Poor sorting of the components and the presence of abundant detritus components such as sandstone clasts, silt and mud grains in the *Cerastoderma* facies denotes that they were deposited in the highest part of the depositional system as proximal deposits. The gradual gentle slope of the facies toward the current sabkha depressions may be attributed to the light decline of the lake shore line during the deposition of the sediments.

A simple conceptual depositional model is presented in Fig. 42. This model shows the evolution and described the depositional pattern of the Aqar Mb. deposits, is presented in Fig 42. This model consists of two stages, which are displaying the development of these sediments in three separated cycles including the deposition, erosion and redeposition of the coquina deposits.

Stage “A” shows that the *Cerastoderma* shells were initially accumulated on the shallow lake beaches mixed with smaller organisms such as ostracods, charophytes and gastropods.

Stage B is characterised by low lake level or by entirely drying out of the shallow lake and may be development of new lake, the *Cerastoderma* shells were subjected to erosion and reworking by occasionally power full wadi inflows. These wadi inflows are responsible for mixing the shells with sandstone pebbles and conglomerate and finally redeposited them as shall fan delta, which can be indicated by progradation and cross bedding features.

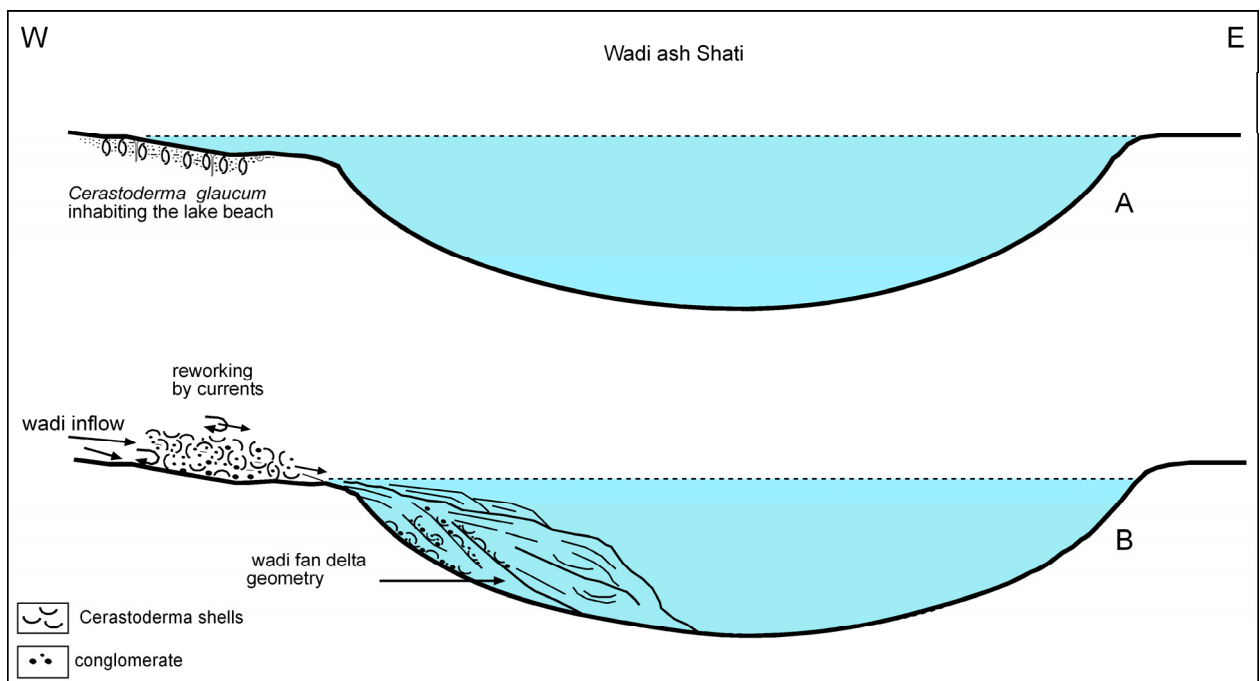


Figure. 42. Depositional model showing the geometry and depositional environment of the Aqar Member in Wadi ash Shati area.

In the analyzed deposits there are no features pointing to the lacustrine nature or origin of this facies. All depositional and sedimentological features display evidence for strong control by currents.

Based on the herein presented data and the resulting interpretation the depositional environment of the Aqar Mb. deposits are regarded as fluvial deposits. *Cerastoderma* shells were deposited around the shallow lake level and mostly within the shallow beach sector during high lake level stages. After the death of the bivalves their shells remained buried under a thin sediment cover of a former lake stage. During more humid episodes, the shells were reworked and transported by wadi flows over short

distances and finally accumulated near the downstream limit of the flow in form of a wadi fan.

5.5 Discussion

Cerastoderma coquina deposits are widely distributed in the Sahara (Fig. 43). Today, they are found approximately 250 to 900 km from the nearest shore (Tournouér, 1878; Marés 1857; Lelubre, 1946 a, b; Müller-Feuga, 1954; Desio, 1971; Petit-Maire, 1980; Gaillard and Testud, 1980; Gaven et al., 1981; Seidl and Röhlich, 1984; Pařízek et al., 1984; Fontes et al. 1985; Gasse et al., 1987, Plaziat, 1991, 1993; Gibert et al., 1990; Thiedig et al., 2000, 2004; Armitage et al. 2007; Geyh and Thiedig, 2008).



Figure 43. Distribution of *Cerastoderma coquina* deposits in the North African Sahara and in the Middle East.

More than 20 $^{230}\text{Th}/\text{U}$ dates have been carried out by Petit-Maire et al. (1980) and Gaven (1982) on the *Cerastoderma glaucum* shells collected from Wadi ash Shati area. The determined age ranges from 165 and 89 ka. Geyh and Thiedig (2008) carried out new $^{230}\text{Th}/\text{U}$ dates on more than 50 shells collected from different sites from the same deposits in Wadi ash Shati. They confirmed, more or less, Petit-Maire et al. (1980) and Gaven (1982) yielding an age between 140 and 125 ka.

Armitage et al. (2007) applied OSL (optically stimulated luminescence) on two samples of these coquina deposits. The coquina samples yielded OSL ages from 100 to 110 ka. Petit-Maire et al. (2002) published very similar $^{230}\text{Th}/\text{U}$ determined ages of *Cerastoderma glaucum* shells. They crop out far away from our study area, namely in the Mudawwara and Tabuk depression, which is located along the border between Jordan and Saudi Arabia (Fig. 43). Their age determinations range from 88 to 170 ka. It may be concluded that all ages of these shells in Wadi ash Shati, and the Mudawwara and Tabuk depression match the stratigraphy and indicate isotopic substages 7, 5e and 5a. From the other Sahara sites there are no age determinations available to present.

In the study area, eleven scattered and isolated outcrops of fossiliferous coquina beds of Aqar Mb. were investigated. The thickness of the succession varies between 1 and 5 m. Based on fossil content, topographical elevation, and on $^{230}\text{Th}/\text{U}$ chronological age determinations Aqar Mb. deposits were interpreted as middle Pleistocene lacustrine deposits of a paleo-lake called "Megalake Fezzan" (Thiedig et al., 2000; Thiedig and Geyh, 2004; Geyh and Thiedig, 2008; Armitage et al., 2007). According to former interpretations, the Megalake was 180 km long, 50 km wide with a maximum water depth of 40-50 m (Petit-Maire, 1991). Thiedig et al. (2000) proposed that the lake had covered an area of about 2000 km². This implies that the whole area of the Wadi ash Shati depression and the northern margin of Murzuq Basin was filled by huge "Megalake Fezzan" during the middle Pleistocene (Petit-Maire et al., 1980; Petit-Maire, 1980; Gaven et al., 1980; Seidl and Röhlich, 1984; Thiedig et al., 2000; Thiedig and Geyh, 2004; Geyh and Thiedig, 2008; Armitage, et al., 2007; Drake et al., 2008; Soulé-Märsche, 2008).

In former studies, the outcrop-discontinuity of Aqar Mb. deposits was taken as evidence of a continuous receding of the shore line of the ancient lake (Lelubre 1946 a,b; Muller-Feuga, 1954; Desio, 1971; Petit-Maire et al., 1980; Gaven et al., 1980, 1981; Seidl and Röhlich, 1984; Thiedig et al., 2000; Thiedig and Geyh, 2004, 2007; Armitage et al., 2007; Geyh and Thiedig, 2008).

Contrary to expectations, a sedimentological assessment has not been performed until present. Therefore, the characteristic sedimentary structures of the Aqar Mb. deposits, such as cross bedding, graded bedding, and fan delta geometries, were not incorporated in the paleo-environmental interpretation.

This chapter documents well-exposed Aqar Mb. outcrops in two selected sites in the Wadi ash Shati area. The investigated coquinas form up to 3 m thick beds, which display diffuse and undulating internal layerings. They consist mainly of abundant *Cerastoderma glaucum* shells, which are often scattered, weathered and found mostly with disconnected valves or broken shells in both investigated locations. Additionally, frequent to abundant ostracodes, gastropods shells, and charophyte debris were found in the deposits. Biogenic components are interbedded with an abundant admixture of mud to boulder sized siliciclastics. Aqar Mb. deposits are characterized by medium to large-scale steeply inclined cross bedding, trough cross bedding, tabular cross bedding and graded bedding structures (Figs. 39 a, b and c). Large-scale steeply inclined cross bedding and trough cross bedding structures are interpreted as small fan delta progradation features, deposited under ephemeral fluvial high-energy conditions, which are common for arid regions.

William (1971) described in detail sedimentary structures and sequences of the ephemeral stream deposits from central Australia, which display great similarity with the Aqar Mb. deposits. According to Picard and High (1973), the ephemeral fluvial sequence begins with a basal erosional contact with lag deposits. They are characterised by high-angle cross bedding (large scale), capped by thin laminated or tabular cross bedding structures. Most of the ephemeral stream sediments accumulate near to where stream terminates in the form of fan-shaped bodies. Usually many fan-shaped bodies overlap each other (Solle, 1966; Glennie, 1970).

There is no doubt that the *Cerastoderma* shells in study area were deposited initially in a shallow lake environment. Still today, *Cerastoderma* shells are found in various intracontinental small lakes in North Africa and in Middle East (41). According to Plaziat (1993) such shells are reported from several small lakes close to Siwa Oasis in northwestern Egypt: These lakes are located about 250 km from the Mediterranean Sea. Additionally it can be mentioned that *Cerastodermas* live presently in the Birket Qarun, which located in Fayum, Egypt. Birket Qarun is a brackish to saline small lake located in a landlocked depression below sea level, some 200 km from the Mediterranean Sea (Rose, 1972; Plaziat, 1991).

Based on sedimentological criteria the coquina deposits of Aqar Mb. were subjected to erosion, transport and redeposition by powerful fluvial wadi activity, which is indicated by the presence of abundant sandstone gravel mixed with eroded and disarticulated *Cerastoderma* shells (Fig. 33 b).

Field observations indicate that there were no *Cerastoderma* shells ever found *in-situ* anywhere along the Wadi ash Shati depression. Therefore, in contradiction to former interpretations and based on sedimentary geometry, the abundance of siliciclastic deposits, and the high degree of shell fragmentation, the investigated Aqar Mb. deposits are interpreted as fluvial wadi deposits.

In addition, the existence of a large, 180 km long and 50 m deep large lake filling the whole depression of Wadi ash Shati during the middle Pleistocene period conflict with all marine climate proxies retrieved from the marine records, which point to a dominance of arid to semi-arid climate conditions in the central Sahara during the last 3 million years. This implies that the monsoon rain belt had shifted away from the middle Sahara to the south of the central Sahara watershed before the onset of the Pleistocene time (Larrasoana et al., 2003), although, short humid periods were known to have occurred during the Pleistocene and the Holocene periods.

Based on the new data presented in this chapter, the logical and sensible interpretation of discontinuity of Aqar Mb. coquina beds can be explained satisfactorily by assuming that the *Cerastoderma* shells had initially inhabited several small recent playa lakes in Wadi ash Shati area. This assumption is supported by the fact that the Wadi ash Shati has an irregular topography and furthermore by the differences in the thickness of coquina deposits in distinct outcrops, which range between 1 to 10 m (Seidl and Röhlich, 1984). Fontes et al. (1985) and Gasse et al. (1987) described similar *Cerastoderma* shell deposits from several Holocene small isolated lakes in the region of Oran and at the northern edge of the Great Western Erg in Algeria. These lakes initially were supplied by emergent, dilute groundwater nappe, later were independently salinized as evaporation increased during relatively short (tens of years to centuries) periods (Plaziat, 1993).

Finally, the thesis of Wadi ash Shati was a huge depression with several successive lacustrine phases suggests that the lake was not at all times a single, continuous water body, but rather had finally split into a number of separate brackish to saline

lakes and ponds. These were found in the region from Wadi ash Shati to Wadi Al Hayat on the southern side of the Awbari sand sea (Burdon and Gonfiantini, 1991).

The existence and distribution of these ancient lakes would agree with the current existence and distribution of more than 11 small lakes in the Awbari sand sea area.

Depending on surface and depth, each individual water body thus would have had its specific water regime and particular salinity (Burdon and Gonfiantini, 1991; Soulié-Märsche, 2008).

A simple conceptual depositional model for the Aqar Mb. is presented (Fig. 40), showing at least two depositional stages in the studied area. The *Cerastoderma* shells initially accumulated on shallow lake beaches (Fig. 40 a). Thereupon they were subject to reworking and transportation over short distances due to the high-energetic currents of local wadis (Fig. 40 b). Turbulent conditions during the transport led to mixing of shells and clastic material, which originated from the surrounding area. Finally, sedimentation took place in small wadi fan deltas, which are indicated by characteristic cross bedding and geometry features (Figs. 37, 38 and 39).

This chapter presents a description, interpretation and sequence stratigraphic model for the Aqar Mb. coquina deposits. The investigated coquina beds consist mainly of abundant *Cerastoderma glaucum* shells with ostracodes, gastropods shells, and charophyte debris. They are characterized by medium to large-scale steeply inclined cross bedding, trough cross bedding, tabular cross bedding and graded bedding structures.

Based on these new findings, the coquina beds are interpreted as recent wadi sediments, which were deposited under ephemeral fluvial dynamic conditions. The former interpretation of the Aqar Mb. sediments being lacustrine deposits of large single lake deposits of middle Pleistocene can not be maintained.

5.6 Conclusion

Cerastoderma lumachelles are interpreted as wadi deposits. The sedimentological features can only demonstrate that the shells were deposited in shallow lake environments and were thereafter subjected to reworking and a short distance transport. The shells could only have been reworked and redeposited by temporary wadi flows, indicated by small prograding fan delta foreset geometries.

The presence of *Cerastoderma* shells with other associated fossils testifies to the existence of several palaeolakes in Wadi ash Shati depression during the upper Pleistocene. The water in these lakes must have been brackish - a minimum of 3‰ is required for *Cerastoderma glaucum* to survive. The water supply to the ancient lakes most probably originated from the ground water, the Wadi ash Shati run off and from the precipitation, which had greatly increased during the development of these coquina deposits. The discontinuity of the coquina deposits and the variation of thickness from one outcrop to another indicate the existence of several small lakes and steady decline of the ancient lake shorelines, due to irregular lake floor topography and seasonal climate changes.

6

GENERAL CONCLUSIONS AND OUTLOOK

6.1 CONCLUSIONS

A comprehensive facies analysis has been carried out on three members of Al Mahruqah Formation in the Murzuq Basin SW Libya in order to reconstruct the different stages of “Megalake Fezzan” concept in Central Sahara during Pleistocene interglacial periods. XRD, $^{230}\text{Th}/\text{U}$ and OSL age dating analysis were used in this study to provide another evidence to support the interpretation concerning the age assignments, origin, and depositional environment of the investigated deposits.

The results of sedimentological analysis in this study suggests beyond reasonable doubt that the former notion of a large Megalake Fezzan didn't exist in the study area and the interpretations of Al Mahruqah Formation as lacustrine deposits are entirely wrong.

Brak Member is a groundwater calcrete deposits, which has a long history of development in the Wadi ash Shati area. $^{230}\text{Th}/\text{U}$ age determination shows that the calcrete deposits of this member are older than previously reported and could be as old as Late Cretaceous.

Bi'r az Zallaf Mb. is a shallow brackish to saline playa lake (sabkhas) deposit. Four alternating arid and very humid *intervals* were recognized in Wadi az Zallaf depression. The carbonate beds of Bi'r az Zallaf Mb. consist mainly of dolomite (80%) and 10-20 % of calcite. The fine lamination of the carbonate beds reflects

continuous fluctuation in Water levels in the shallow inland lakes due to high evaporation condition and concentration of evaporates in the lake. The lakes were supplied mainly by groundwater and by local run off. The rare fossiliferous components of this member (e.g. ostracodes, pelecypods, gastropods and charophyte debris) are attributed to the initial stages of playa lake developments. OSL age determination proved that the Bi'r az Zallaf Mb. deposits are older than middle Pleistocene. We agree with the proposal of Collomb (1962) that this member is of Middle Miocene age.

Aqar Mb. *Cerastoderma* lumachelles are interpreted as wadi deposits. Sedimentological evidence only demonstrated that the shells were deposited in shallow lake environments and were thereafter subjected to reworking and a short distance transport. The water in these lakes must have been brackish. The water supply to the ancient lakes most probably originated from the ground water, the Wadi ash Shati run off and from precipitation, which had greatly increased during the development of these coquina deposits.

6.2 OUTLOOK

Although the results presented in this study provided a new interpretations, facies and depositional models of the Brak Mb., Bi'r az Zallaf Mb. and Aqar Mb. of Al Mahruqah Formation in Wadi ash Shati and Wadi az Zallaf, there are still open questions, leaving space for future investigations and more precise tracing of the other occurrences of carbonate deposits in the southern and eastern margins of Murzuq Basin.

The new data, and resulting interpretations presented in this study provided a good basis for further examinations and reconstructions of the geology and palaeogeography of the Murzuq Basin and Central Sahara region from Late Cretaceous to the present time.

REFERENCES

- Abugares, Y.I. and Ramaekers, P. (1993) Short notes and guidebook on the Palaeozoic geology of the Ghat area, SW Libya. Field trip, October 14-17, 1993. Earth Science Society of Libya, Interprint Ltd., Malta, 84 pp
- Arakel, A. V. (1986) Evolution of calcrete in palaeodrainages of the Lake Napperby area, Central Australia. In: *Palaeoenvironment of salt Lakes*. (Eds. A. Chivas, R. Torgersen, and T., Bowler,), *Palaeogeography, Palaeoclimatology, Palaeoecology*, **54**, 283-303.
- Arakel, A.V. and Mc Conchie, D. (1982) Classification and genesis of calcrete and gypsum lithofacies in palaeodrainage systems of inland Australia and their relationship to carnotite mineralisation, *Journal Sedimentary Petrology*, **52**, 1149-170.
- Armitage, S.J., Drake, N.A., Stokes, S., El-Hawat, A., Salem, M.J., White, K., Turner, P. and McLaren, S.J. (2007) Multiple phases of North African humidity recorded in lacustrine sediments from the Fazzan Basin, *Libyan Sahara. Quaternary Geochronology*, **2**, 18-86.
- Bateman, H. (1910) Solution of a system of differential equations occurring in the theory of radioactive transformations. *Proceedings of the Cambridge Philosophical Society* **15**, 423-427.
- Bell, C.M. (1989) Saline lake carbonates within an Upper Jurassic-Lower Cretaceous continental red bed sequence in the Atacama region of northern Chile. *Sedimentology*, **36**, 651-663
- Bellair, P. (1944) Sur l' âge du Calcaire de Mourzouk (Fezzan). *C.R. Somm. Seances Acad. Sci.* **219**, 490-491.
- Bellair, P. (1947) Sur l' âge des affleurements calcaires de Mourzouk, de Zouila et d' El Gatron. *Trav. Inst. Rech. Sahara*, **4**, 155-163.

- Bellair, P. (1953) Le Quaternaire de Tejerhi. Mission au Fezzan (1949). *Sci. Inst.Hauts Etude*, **1**, 9-16.
- Belleni, E. and Massa, D. (1980) A stratigraphic contribution to the Palaeozoic of the southern basins of Libya. In: *The Geology of Libya I* (Eds. M.J. Salem and M.T. Busrewil), Academic Press, London, 3-56.
- Berendeyev, V.S. (1985) Geological Map of Libya 1:250.000, Sheet: Hamadat Tanghirt, (NH 32-16), Explanatory Booklet, Industrial Research Centre, Tripoli, p. 125
- Boote, D.R.D., Clark-Lowes, D.D., and Traut, M.W. (1998) Palaeozoic petroleum systems in North Africa, In: *Petroleum Geology of North Africa* ((Eds. D.S. Macgregor, R.T.J. Moody and D.D. Clark-Lowes), *Geological Society London special Publication*, **132**, 7-68.
- Boyden, R. C. and Russel, P. J. C. (1972) The distribution and habitat range of the brackish water cockle (*Cardium (Cerastoderma) glaucum*), in; the British Isles. *Journal of Animal Ecology*, **43**, 719-734.
- Braithwaite, C.J.R. (1983) Calcrete and other soils in Quaternary limestones structures, processes and applications. *Journal of geological Society London*. **140**, 351-363.
- Burdon, D.J. and Gonfiantini, R. (1991) Lakes in the Awbari Sand Sea of Fezzan Libya. In: *The Geology of Libya V* (Eds. M.j. Salem and M.N. Belaid), Elsevier, Amsterdam, 2026-2041.
- Candy, I., Black, S. and Sellwood, B.W. (2005) U-series isochron dating of immature and mature calcretes as a basis for constructing Quaternary landform chronologies for the Sorbas Basin, southeast Spain. *Quaternary Research*, **64**, 100-111.
- Carlisle, D. (1983) Concentration of uranium and vanadium in calcrete and gypcretes. In: *Residual Deposits*, (Ed. R.C.L Wilson), *Geological Society London Special Publication*, No. **11**, 185-195.

- Collomb, G.R. (1962) Etude géologique du jabel Fezzan et de sa bordure paléozoïque. *Notes Mém. Comp. Fr. Pétrole*, **1**, p 35.
- Conant, L.C. and Goudarzi, G.H. (1964) Geological Map of Kingdom of Libya. U. S. Geol Survey, Misc. Geol. Inv. Map, 1-350 A, scale 1: 2, 000 000, Washington. Second edition (modified), 1977, Geological map of Libya, same scale, Industrial Research Centre, Tripoli-Libya.
- Conrad, G. (1969) L' évolution continentale post hercynienne du Sahara Algérien Centre national de la Recherche scientifique, Paris, France. *Mémoire. du Centre de Recherche. sur les zones arides*, 10.
- Conrad, G. and Lappatent, J.R. (1991) The appearance of Cardium fauna and foraminifers in the great lakes of the Early Quaternary periods in the Algerian Central Sahara Desert. *Journal of African Earth Sciences*, **12**, 375-382.
- Davidson, L., Beswetherick, S., Craig, J. Eales, M., Fisher, A., Himmali, A., Jho, J., Mejrab, B. and Smart, J. (2000) The structure, stratigraphy and petroleum geology of the Murzuq Basin, southwest Libya. In: *Geological Exploration in the Murzuq Basin* (Eds. M.A. Sola and D. Worsley), Elsevier, Amsterdam, 295-320.
- DeMenocal P.B. (2004) African climate change and faunal evolution during the Pliocene-Pleistocene. *Earth and Planetary science letters*, **220**, 3-24.
- Desio, A. (1936) Riassunto sulla costituzione geologica del Fezzan. *Bollettino della Società Geologica Italiana*, **55**, 319-356.
- Desio, A. (1971) Outlines and problems of the geomorphological evolution of Libya from the Tertiary to the present day. In: *Symposium Geology of Libya* (Ed. C. Gray) Faculty of science university of Libya, Tripoli, 11-36.
- Di Cesare, F., Franchino, A. and Sommaruga, C., (1963) The Pliocene-Quaternary of Giarabub erg region. *Revue de L' Institute Français du Pétrole*, **18**, 1344-1362.
- Djamali, M., Soulie-Märsche, I., Esu, D., Glioza, E. and Okhravi, R. (2006) Palaeoenvironment of a Late Quaternary lacustrine-palustrine carbonate

- complex: Zarand Basin, Saveh, Central Iran. *Palaeogeography, Palaeoclimatology, Palaeoecology*, 237, 315-334.
- Domáci, L., Röhlich, P. and Bosa k, P. (1991) Neogene to Pleistocene continental deposits in Northern Fezzan and Central Sirt Basin. In: *The Geology of Libya* V (Eds. M.J. Salem and M.N. Belaid), Elsevier, Amsterdam, 1785-1801.
- Drake, N.A., El-Hawat, A.S., Turner, P., Armitage, S.J., Salem, M.J., White, K.H. and McLaren, S. (2008) Palaeohydrology of the Fezzan Basin and Surrounding Regions: the Last 7 Million Years. *Palaeogeography, Palaeoclimatology, Palaeoecology*, 263, 131-145.
- Dubief, J. (1971) Die Sahara, eine Klima-Wüste. In: *Die Sahara und ihre Randgebiete* (Eds. H. Schiffer), 1: 227-348.
- Dupont, L.M., Leroy, S.A.G. (1999) Climate changes in the Late Pliocene of NW Africa from a pollen record on an astronomically tuned timescale. In: *The Pliocene: Time of Change* (Eds. J.H. Wrenn, J.-P. Suc and S.A.G. Leroy), American Association of Stratigraphic Palynologists Foundation, 145-161.
- El Chair, M.M. (1984) Zur Hydrogeologie, Hydrochemie und Isotopenzusammensetzung der Grundwässer des Murzuq-Beckens, Fezzan/Libyen. Unpublished Dissertation Naturwissenschaften Fakultät Universität Tübingen, Germany, 214 pp.
- El Tantawi, A. (2005) Climate change in Libya and Desertification of Jifara Plain. Using Geographical Information System and Remote Sensing Techniques Unpublished Dissertation Naturwissenschaften Fakultät Universität in Mainz, Germany, 246 pp.
- Esteban, M. and Klappa, C.F. (1983) Subaerial exposure environments. *AAPG Memoir*, 33, 1-54.
- Eugster, H.P., Hardte, L.A. (1978) Saline lakes In: *Physics and Chemistry of Lakes* (Ed. A. Lerman), Springer Verlag. New York, 238-293.

- Eugster, H.P., Kelts, K. (1983) Lacustrine chemical sediments. In: *Chemical Sediments and Geomorphology* (Eds. A. Goudie and K. Pye), Academic Press, London, 321- 368.
- Flügel, E. (2004) Microfacies of Carbonate Rocks Analysis, Interpretation and Application. Springer Verlag, Berlin, 976 pp.
- Fontes, J.Ch., Gasse, F., Callot, Y., Plaziat, J. C., Carbonel, P., Dupeubic, P.A., and Kaczmarska, I. (1985) Freshwater to marine-like environments from Holocene lakes in northern Sahara. *Nature*, **317**, 608-610.
- Frechen, M., Sierralta, M., Oezen, D. and Urban, B. (2006) Uranium-series dating of peat from Central and Northern Europe. In: *The climate of past interglacials* (Eds. F. Sirocko, M. Claussen, T. Litt and M.F. Sàncchez Goni), Elsevier, Amsterdam, 93-118.
- Freulon, J.M., Lefranc, J.P., and Lelubre, M. (1955) *Carte géologique de reconnaissance du Sahara Libyen, Feuille NG 33 N-O "Sebha"* au 1/500.000. Publication du l'Institute Recherche du. Sahara.
- Freytet, P. And Plaziat, J.C. (1982) Continental carbonate sedimentation and pedogenesis. Late Cretaceous and Early Tertiary of Southern France, Contribution to Semimentology, **12**. Springer Verlag, Stuttgart, 213 pp.
- Fürst, M., and Klitzsch, E. (1963) Late Caledonian paleogeography of the Murzuq Basin. *Revue de L' Institute Français du Pétrole*, **18**, 1472-1484.
- Gaillard, J.M. and Testud, A.M. (1980) Comparative study of Quaternary and Present-day lagon populations of *Cardium glaucum* (syn. *Cerastoderma glaucum* (Bruguiere)) Mollusca, Bivalvia. In: *The Geology of Libya III* (Eds. M.J. Salem and M.T. Busrewil), Academic Press, London, 809-814.
- Gasse, F., Fontes, J.Ch., Plaziat, J.C., Carbonel, P., Kaczmarska, I., de Deckker, P., oulie`-Märsche, I., Callot, Y. and Dupeubic, P.A. (1987) Biological remains, geochemistry and stable isotopes for the reconstruction of environmental and Hydrological changes in the Holocene lakes from North Sahara. *Palaeogeography, Paleoclimatology, Palaeoecology*, **60**, 1- 46.

- Gaven, C. (1981) A Pleistocene lacustrine episode in southeastern Libya. *Nature*, **290**, 131-133.
- Gaven, C. (1982) Radiochronologie Isotopique Thorium-Uranium. In: Le Shati. Lac pléistocène du Fezzan (Libye). Editions du Centre National de la Recherche Scientifique (C.N.R.S.), (Ed. N. Petit-Maire), Paris, 44-54.
- Geyh, M.A. (2001) Reflections on the $^{230}\text{Th}/\text{U}$ dating of dirty material. *Geochronometria* **20**, 9-14.
- Geyh, M. and Thiedig, F. (2008) The Middle Pleistocene Al Mahrúqah Formation in the Murzuq Basin, northern Sahara, Libya evidence for orbitally-forced humid episodes during the last 500,000 years. *Palaeogeography, Palaeoclimatology, Palaeoecology*, **257**, 1-21.
- Gibert, E., Arnold, M., Conrad, G., De Deckker, P., Fontes, J.Ch., Gasse, F. and Kassir, A. (1990) Retour des conditions humides au Tardiglaciaire au Sahara septentrional (Sebkha Mellala, Algérié). *Bulletin de la Société Géologique de France*, 497-504.
- Glennie, K.W. (1970) Desert sedimentary environment Developments *Sedimentology*, **14**, 222 pp.
- Goudarzi, G.H. (1970) Geology and mineral resources of Libya- a reconnaissance. Geological Survey Professional Paper 660, 104 pp.
- Goudie, A.S. (1983) Calcrete. In: *Chemical Sediments and Geomorphology* (Eds. A.S. Goudie and K. Pye), Academic Press, London, 93-131.
- Grubić, A., Dimitrijević, M., Galećić, M., Jakovljević, Z., Komarnicki, S., Protić, D., Radulović, P., and Roncevic, G. (1991) Stratigraphy of western Fezzan (SW Libya). In: *The Geology of Libya IV* (Eds. M.J. Salem and M.N. Belaid), Academic Press, London, 1529 -1564.
- Grunert, J.(1983) Relief Boden Paläoklima. Geomorphologie der Schichtstufen am Westrand des Murzuk-Beckens (Zentrale Sahara). Gebrüder Borntraeger. Berlin, 271 pp.

- Hecht, F., Fürst, M. and Klitzsch, E. (1963) Zur Geologie von Libyen. *Geologische Rundschau*, **53**, 413-470.
- Ivanovich, M. and Harmon, R.S. (1992) Uranium-series disequilibrium: Application to earth, marine, and environmental sciences. Clarendon Press, Oxford, 910 pp.
- Jacqué, M. (1962) Reconnaissance géologique du Fezzan oriental. *Notes Mém. Comp. Fr. Pétroles*, **5**, 43 pp.
- Kanter, H. (1967) Libyen: Eine geographisch-medizinische Landeskunde (A Geomedical Monograph). In: *Medizinischr Länderkunde* (Ed. H. Jusatz), Heidelberg.
- Kaufman, A. (1993) An evaluation of several methods for determining $^{230}\text{Th}/\text{U}$ in impure carbonates. *Geochimica Cosmochimica Acta*, **57**, 2303-2317.
- Kaufman, A. and Broecker, W. (1965) Comparison of ^{14}C and ^{230}Th ages for carbonate minerals from lakes Lahontan and Bonneville. *Journal of Geophysical Research*, **70**, 4039-4054.
- Klitzsch, E. (1963) Geology of the north-east flank of the Murzuq basin (Djebel Ben Ghenema-Dor El Gussa area). *Revue de L'Institut Français du Pétrole*, **18**, 1411-1427.
- Klitzsch, E. (1966) Comments on the geology of the central parts of southern Libya and northern Chad. *Petroleum Exploration Society of Libya*, 8th Ann. Field Conf., 1-17.
- Klitzsch, E. (1970) Die Strukturgegeschichte der Zentralsahara. Neue Erkenntnisse zum Bau und zur Paläogeographie eins Taffellands. *Geologische Rundschau*, **59**, 459-527.
- Klitzsch, E. (1974) Bau und Genese der Garets und Alter des Grossreliefs in Nordost Fezzan (Südlibyen). *Zeitschrift für Geomorphology. N. F.*, **18**, 99-116.
- Klitzsch, E. (2000) The structural development of the Murzuq and Kufra basins-significance for oil and mineral exploration. In: *Geological Exploration in the*

- Murzuq Basin (Eds. M.A. Sola and D. Worsley), Elsevier, Amsterdam, 143-150.
- Knox, G.F. (1977) Caliche profile formation, Saldanha Bay (South Africa). *Sedimentology*, **24**, 657- 674.
- Korab, T. (1984) Geological map of Libya, 1:250 000. Sheet Tmassah NG (33-7). Explanatory Booklet, Industrial Research Centre, Tripoli, 87 pp.
- Krumbein, W.E. (1979) Photolithotroipic chemoorganotropic activity of bacteria and algae as related to beachrock formation and degradation (Gulf of Aqaba, Sinai) *Geomicrobiology Journal* **1**, 139-198.
- Ku, T.L., Bull, W.B., Freeman, S.T. and Knauss, K.G. (1979) $^{230}\text{Th}/^{234}\text{U}$ Dating of pedogenic carbonates in gravelly desert soils of Vidal valley, south eastern California. *Bulletin of the Geological Society of America*, **90**, 1063-1073.
- Ku, T.L. and Liang, Z.C. (1984) The dating of impure carbonates with decay-series isotopes. *Nuclear Instruments and Methods in Physics Research*, **223**, 563-571.
- Langmuir, D. (1978) Uranium solution-mineral equilibria at low temperatures. *Geochimica et Cosmochimica Acta*, **42**, (6B), 547-569.
- Larrasoña, J.C., Roberts, A.P., Rohling, E.J., Winklhofer, M. and Wehausen, R. (2003) Three million years of monsoon variability over the northern Sahara. *Climate Dynamics*, **21**, 689-698.
- Lehmann, U., and Hillmer, G. (1980) Wirbellose Tiere der Vorzeit. Ferdinand Enke Verlag, Stuttgart, 320 pp.
- Lelubre, M. (1946a). À propos de calcaires de Mourzouk (Fezzan). *Comptes Rendus de l' Academie des Sciences*, Paris, **222**, 1403-1404.
- Lelubre, M. (1946b) Le Tibesti septentrional. Esquisse morphologique et structurale. *Comptes Rendus de l' Academie des Sciences*, Colon, **6**, 337-357.

- Lelubre, M. (1952) Aperçu sur la géologie du Fezzan. Travaux Récents des Collaborateurs. *Bulletin du service de Carte Géologique Algérie*, **3**, 109-148.
- Leroy, S.A.G. and Dupont, L.M. (1994) Development of vegetation and continental aridity in northwestern Africa during the Late Pliocene: the pollen record of ODP Site 658. *Palaeogeography, Palaeoclimatology, Palaeoecology*, **109**, 295-316.
- Löhnert, E. and Thiedig, F. (1998) Ein starkes Niederschlagsereignis in der Sahara (Südwest-Libyen). *Zentralblatt für Geologie und Paläoontologie*. Teil 1, H. 1/2, 161-174.
- Mahran, T.M. (1999) Late Oligocene lacustrine deposition of the Sodmin Formation, Abu Hammad Basin, Red Sea, Egypt: Sedimentology and factors controlling palustrine carbonates. *Journal of African Earth Sciences*, **29**, 576-592.
- Mamgain, V.D. (1980) The Pre-Mesozoic (Precambrian to Palaeozoic) Stratigraphy of Libya- A Reappraisal. *Department of geological Researches and Mining Bulletin*, **14**. Industrial Research Centre, Tripoli, 104 pp.
- Mann, A.W. and Horwitz, R.C. (1979) Groundwater calcrete deposits in Australia. Some observations from Western Australia. *Journal of the Geological Society of Australia*, **26**, 293-303.
- Marés, L. (1857) Sur la constitution générale du Sahara dans le S. de la Provence d'Oran. *Bulletin de la Société Géologique de France*, **14**, 524-538.
- Massa, D. and Collomb, G.R. (1960) Observations nouvelles sur la région d'Aouinet Ouenine et du Djebel Fezzan (Libye). 21st Intern. Geol. Cong., Copenhagen, Proc. pt. **12**, 65-73.
- Mrazek, P. (1984) Geological Map of Libya 1:250.000, Sheet: Tanahmù, (NG 33-6), Explanatory Booklet. Industrial Research Centre, Tripoli, p 72.
- Muller-Feuga, R. (1954) Contribution à l'étude de la géologie, de la petrographie, et des ressources hydrauliques et minérales du Fezzan. Ann. Mines. Géol., Tunis, **12**, 354.

- Pachur, H.J. and Altmann, N. (2006) Die Ostsahara im Spätquartär. Ökosystemwände im größten hyperariden Raum der Erde (German Edition) Springer Verlag, 662 pp.
- Pagni, A. (1938) Sull' eta dei 'Calcari di Murzuch' (Fezzan). *Atti Soc. Ital. Sci. Nat.*, 73-78.
- Plaziat, J.C. (1991) Paleogeographic significant of the Cardium, Potamids and Foraminifera living in intra-continental salt lakes of North Africa (Sahara Quaternary, Egypt present Lakes). *Journal of African Earth Science*, **12**, 383-389.
- Plaziat, J.C. (1993) Modern and fossils Potamids (Gastropoda) in Saline lakes. *Journal of Palaeolimnology*, **8**, 163-169.
- Panerjee, S. (1980) Stratigraphic lexicon of Libya. *Department of geological Researches and Mining Bulletin*, **13**. Industrial Research Centre, Tripoli, 300 pp.
- Parizek, A., Klein, L. and Röhlich, P. (1984) Geological Map of Libya 1:250.000, Sheet: Idri, (NG 32-1), Explanatory Booklet, Industrial Research Centre. Tripoli, 62-63.
- Petit-Maire, N., Casta, L., Delibrias, G., and Gaven, C., with appendix by Testud, A.M. (1980) Preliminary data on Quaternary palaeolacustrine deposits in the Wadi ash Shati Area, Libya. In: *The Geology of Libya* (Eds. M.J. Salem and M.T. Busrewil), Academic Press, London, **III**, 797-807.
- Petit-Maire, N. (1982) Le Shati Lac Pléistocène du Fezzan (Libye). Edition du centre de la Recherche Scientifique (C. N.R. S), Paris, 118 pp.
- Petit-Maire, N. (1991) Recent Quaternary climatic change and Man in the Sahara. *Journal of African Earth Sciences*, **12**, 125-132.
- Petit-Maire, N., Sanlaville, P., Abed, A., Yasin, S., Bourrouilh, R., Carbonel, P., Fontugne, M. and Reyss, J.L. (2002) New data for an Eemian Lacustrine phases in southern Jordan, *Episodes*, **25**, 279-280.

- Picard, M.D. and High, Jr., L.R. (1973) Sedimentary structures of ephemeral streams. Amsterdam, Elsevier, 223 pp.
- Reineck, H.E., Singh, I.B. (1980) Depositional Sedimentary Environments. Springer Verlag, Berlin. Heidelberg. New York, 217 pp.
- Rončević, G. (1984) Geological Map of Libya 1: 250 000 scale, Sheet: Hasi Anjiwal, (NG 32-4), Explanatory Booklet, Industrial Research Centre, Tripoli, 43-46.
- Rose, K.D. (1972) A mollusk new to lake Birket Qarun, Egypt. *Nautilus*, **85**, 141-143.
- Scholz, D. and Hoffmann, D. (2008) $^{230}\text{Th}/\text{U}$ -dating of fossil corals and speleothems. *Quaternary Science Journal*, **57**, 52-76.
- Schulz, E., Abichou, A., Hachicha, T., Pomel, S., Salzmann, U. and Zouari, K. (2002) Sebkhas as ecological archives and the vegetation and landscape history of southeastern Tunisia during the last two millennia. *Journal of African Earth Sciences*, **34**, 223-229.
- Schwarcz, H.P. and Latham, A.G. (1989) Dirty calcites: 1. uranium series dating of contaminated calcite using leachates alone. *Chemical Geology (Isotope Geoscience Letters)*, **80**, 35-43.
- Seidl, J.K. and Röhlich, P. (1984) Geological Map of Libya 1:250.000, Sheet: Sabha, (NG 32-2), Explanatory Booklet. Industrial Research Centre, Tripoli-Libya, 89-93.
- Sierralta, M., Kele, S., Melcher, F., Hambach, U., Reinders, J., van Geldern, R. and Frechen, M. (in press) Uranium-Series Dating of Travertine from Süttő: Implications for Reconstruction of Environmental Change in Hungary. *Quaternary International*.
- Solle, G. (1966) Rezente und fossile Wüste. *Notizblatt des Hessischen Landesamtes für Bodenforschung*, **94**, 54-121.
- Soulie'-Märsche, I. (1993a) Diversity of Quaternary aquatic environments in NE Africa as shown by fossil Charophytes. In: *Geoscientific Research in Northeast*

- Africa (Eds. U. Thorweihe and H. Schandelmeier), Balkema, Rotterdam, 575-579.
- Soulie'-Märsche, I. (1993b) Apport des Charophytes fossiles à la recherché de phénomènes climatiques abrupts. *Bulletin de la Société géologique de France* **164**, 123-130.
- Soulie'-Märsche, I. (2008) Charophytes, indicators for low salinity phases in North African Sebkhet. *Journal of African Earth Sciences*, **51**, 69-76.
- Spötl, C. and Mangini, A. (2006) U/Th age constraints on the absence of ice in the central Inn Valley (eastern Alps, Austria) during Marine Isotope Stages 5c to 5a. *Quaternary Research*, **66**, 167-175.
- Štefek, V.K., Röhlich, P. (1984) Geological Map of Libya 1:250.000, Sheet: Awbari, (NG 33-5), Explanatory Booklet, Industrial Research Centre, Tripoli, 69.
- Talbot, M.R. and Allen, P.A. (1996) Lakes. In: *Sedimentary Environments: Processes, Facies and Stratigraphy* (Ed. H.G. Reading), Blackwell, Oxford, 83-124.
- Thiedig, F.M., Oezen, D., El-Chair, M. and Geyh, M.A. (2000) The absolute age of the Quaternary lacustrine limestone of the Al Mahrúqah Formation-Murzuq Basin, Libya. In: *Geological Exploration in Murzuq Basin* (Eds. M.A. Sola, and D. Worsley), Elsevier Science, Amsterdam, 89-16.
- Thiedig, F.M. and Geyh, M.A. (2004) Zyklische lacustrine Kalke im abflusslosen Murzuq-Becken (Libyen) als Zeugnisse interglazialer Feuchtphasen in Nordafrika während der letzten 500 ka. *Die Erde*, **135**, 31-52.
- Tournouér, R. (1878) Sur quelques coquilles marines recueillies par divers explorateurs dans la région des chotts sahariens. *Bull. Ass. Franc. Avanc. Sc.*, Paris: 608-622
- Twidale, C.R. and Hutton, J.T (1986) Silcrete as a climatic indicator: Discussion: *Palaeogeography, Palaeoclimatology, Palaeoecology*, **52**, 351-360.

- Valero Garces, B.L. (1993) Lacustrine deposition and related volcanism in a transitional tectonic setting: Upper Stephanian-Lower Autunian in the Aragon-Beam basin, Western Pyrenees (Spain-France). *Journal of Sedimentary Geology*, **83**, 133-160.
- Van Damme, D. (1984) The fresh water mollusca of Northern Africa Distribution, biogeography and palaeoecology-Developments in Hydrobiology, 25, Dr Junk publ., The Hague, 164 pp.
- Völker, J. (1990) To the problem of dune formation and dune weathering during the Late Pleistocene and Holocene in the southern Sahara and the Sahel. *Zeitschrift für Geomorphology*. N. F., **34**, 1-17.
- Von der Borch, C.C. (1976) Stratigraphy and formation of Holocene dolomite deposits of the Cooring area. South Australia. *Journal of Sedimentary Petrology*, **46**, 952-966.
- Watts, N.L. (1980) Quaternary Pedogenic calcretes from the Kalahari (southern Africa): mineralogy, genesis and diagenesis. *Sedimentology*, **27**, 661-686.
- White, K., McLaren, S., Black, S. and Parker, A. (2001) Evaporite minerals and organic horizons in sedimentary sequences in the Libyan Fezzan: implications for palaeoenvironmental reconstruction. In: *Linking Climate Change to Land Surface Change* (Eds. S.J. McLaren and D.R. Kniveton), Kluwer Academic Press, Amsterdam, 193-208.
- William, G.E. (1971) Flood deposits of the sand beds ephemeral streams of central Australia. *Sedimentology*, **17**, 1-40.
- Woller, F. (1978) Geological Map of Libya 1:250.000, Sheet: Al Washkah, (NG 33-15), Explanatory Booklet, Industrial Research Centre, Tripoli, 104 pp.
- Woller, F. (1984) Geological Map of Libya 1:250.000, Sheet: Al Fuqaha, (NG 33-3), Explanatory Booklet, Industrial Research Centre, Tripoli, 123 pp.
- Wright, V.P., Tucker, M.E. (1991) Calcrete: an Introduction. In *Calcretes* (Eds. V.P. Wright and M.E. Tucker), Oxford: Blackwell Scientific, 1-22.

- Wright, V.P. and Tucker, M.E. (1990) Carbonate Sedimentology. Wiley-Blackwell, 496 pp.
- Zalat, A.A. (1996) Charophyte gyrogonites from Holocene lacustrine sediment of the Fayoum Depression, Egypt. *Neues Jahrbuch für Geologie und Paläontologie, Monatshefte*, 502-516.